



ALMA MATER STUDIORUM
UNIVERSITÀ DI BOLOGNA

DOTTORATO DI RICERCA IN
SALUTE, SICUREZZA E SISTEMI DEL VERDE

Ciclo 37

Settore Concorsuale: 05/G1 - FARMACOLOGIA, FARMACOLOGIA CLINICA E
FARMACOGNOSIA

Settore Scientifico Disciplinare: BIO/14 - FARMACOLOGIA

EPIGENETIC EFFECTS OF LIFESTYLE IN PATIENTS AFFECTED BY
GYNECOLOGICAL TUMORS

Presentata da: Francesca Gorini

Coordinatore Dottorato

Daniele Torreggiani

Supervisore

Sabrina Angelini

Co-Supervisor

Gloria Ravegnini

Paolo Pillastrini

Esame finale anno 2025

ABSTRACT.....	1
1. INTRODUCTION	2
1.1 Gynecological tumors	2
1.1.1 Endometrial cancer	2
1.1.2. Ovarian cancer	7
1.2 Epigenetics	13
1.2.1 MicroRNA	15
1.2.2 Obesity	16
1.2.3 Physical activity	18
1.3 Liquid biopsy	19
2. GENERAL AIM	21
3. TASK 1: Epigenetic effects of obesity in Endometrial Cancer patients.....	22
3.1 AIM.....	22
3.2 MATERIALS AND METHODS.....	22
3.3 RESULTS	31
3.4 DISCUSSION AND CONCLUSION.....	52
4. TASK 2: Epigenetic effects of physical activity in Ovarian Cancer patients.....	55
4.1 AIM.....	55
4.2 MATERIALS AND METHODS.....	55
4.3 RESULTS	57
4.4 DISCUSSION AND CONCLUSION.....	66
5. TASK 3: Drug resistance mechanisms in Ovarian Cancer organoids	67
5.1 AIM.....	67
5.2 MATERIALS AND METHODS.....	67
5.3 RESULTS	73
5.4 DISCUSSION AND CONCLUSION.....	77
6. CONCLUSIONS.....	79
7. REFERENCES.....	80

ABSTRACT

Gynecological cancers are among the most frequent malignancies in women, with over 3.5 million women affected globally. This thesis focuses on endometrial (EC) and ovarian cancers (OC). EC is the sixth most common cancer in women, with obesity being a significant risk factor. Although less common, OC is the most lethal gynecological cancer due to the lack of specific symptoms and early detection biomarkers. Epigenetics investigates gene expression changes that occur without DNA sequence alterations but arise from environmental factors. microRNAs (miRNAs) are non-coding RNA molecules involved in the development of several diseases, including cancer. The aim of the present thesis was to clarify the epigenetic role of lifestyle in gynecological cancers. To achieve this goal, three tasks were planned: Task 1 addressed obesity-related EC, Task 2 explored physical activity's role in OC, and Task 3 focused on OC organoid models.

In Task 1, tissue and plasma samples from obese and non-obese EC patients, as well as from obese non-cancer women, were analysed to investigate the potential link between obesity and miRNA expression in EC. Results revealed a significant miRNA deregulation in obese EC patients, suggesting that obesity-induced epigenetic changes may contribute to EC development and progression. These findings could help identify new biomarkers for managing obese EC patients.

Task 2 analysed miRNA expression in OC patients who were either enrolled in or not enrolled in a structured physical activity program. Results revealed significant variations in miRNA expression, suggesting that regular exercise may influence the molecular mechanisms underlying tumor biology.

Lastly, Task 3 focused on developing a 3D OC organoid model to support future functional studies based on the previous findings.

This study provides new insights into the epigenetic role of lifestyle in gynecological cancers, with potential implications for the development of personalized therapies based on miRNAs.

1. INTRODUCTION

1.1 Gynecological tumors

The term “gynecological cancers” refers to malignancies of the female reproductive system, including cancers of vulva, vagina, cervix uteri, corpus uteri and unspecified uterus parts, ovaries, Fallopian tubes, and placenta, shown in Figure 1.¹ Gynecological tumors are among the most common cancers in women, significantly impacting their quality of life.^{2,3} It is estimated that more than 3.5 million women worldwide suffer from gynecological cancers, while in Italy, around 18000 new diagnoses are recorded each year. In Italy, the most diagnosed among gynecological cancers is represented by endometrial carcinoma, as is the case in all developed countries around the world.⁴ Conversely, cervical cancer is more prevalent in low-resource countries, where prevention and screening programs are insufficient.⁵

The present thesis is specifically focused on endometrial and ovarian cancers.

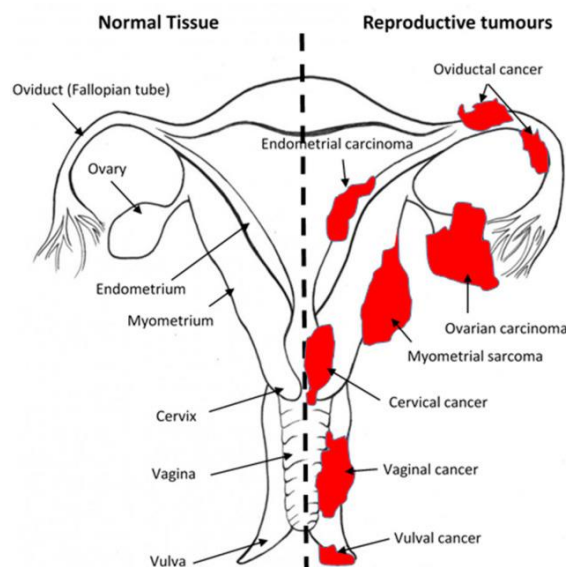


Figure 1: Components of the female reproductive system and their respective potential tumors sites (in red).⁶

1.1.1 Endometrial cancer

Endometrial cancer (EC) is a malignant tumor that affects endometrium, the inner epithelial lining of the uterus, which undergoes structural changes in response to fluctuations in oestrogen and progesterone during menstrual cycle.^{7,8} It is the 6th most common cancer in women worldwide, with almost 400000 new diagnoses in 2022. The highest disease burden is observed in North America and Western Europe, largely due to a high prevalence of EC risk factors in these regions.⁹ According to GLOBOCAN 2022 data, EC ranks as the 13th leading cause of cancer mortality in women worldwide,

but it is the 9th leading cause when considering European women alone.¹⁰ Most cases arise in women aged 65 to 75 years. Factors such as racial disparities, socioeconomic status, and geographical location significantly influence both EC incidence and mortality rates. When EC is diagnosed at an early stage, which occurs in 67% of the cases, the 5-year overall survival (OS) rate is 81%. Conversely, when it is diagnosed in advanced stages, the 5-year OS rate drops to around 15%.⁷

Histopathological and molecular classifications

Historically, EC was typically dichotomized into i) type I and ii) type II tumors, based on histological characteristics.^{7,8,11}

- i) Type I cancers are more common, and they include endometrioid or low-grade tumors associated with obesity and oestrogen exposure, that usually have a favourable prognosis.
- ii) Type II include high-grade endometrioid, serous clear cell tumors and carcinosarcomas with unfavourable prognosis, and usually not caused by oestrogen exposure.

Today, EC is classified according to the 5th edition of “World Health Organization (WHO) Classification of Tumors, Female Genital Tumors” in:

- Low-grade or High-grade Endometrioid carcinomas (EEC), which account for 80% of all ECs;
- Serous carcinoma: the most aggressive of non-EEC subtypes;
- Clear cell carcinoma;
- Mixed carcinoma;
- Undifferentiated carcinoma;
- Carcinosarcoma, which, unlike other histological types, is not exclusively of epithelial origin but also contains mesenchymal components;
- Other unusual types (e.g. mesonephric-like);
- Gastrointestinal mucinous type carcinoma.

These different types of EC exhibit distinct molecular features, microscopic appearance, precursor lesions, and natural history. Histological grading from the International Federation of Gynecology and Obstetrics (FIGO) is used exclusively for EECs, while all the other subtypes are classified as “aggressive”.^{8,12} EEC is classified as high-grade if it meets at least two of the following three criteria: more than 50% solid growth, a diffusely infiltrative growth pattern (characterized by tumor cells irregularly invading adjacent tissues, which can facilitate distant spread) rather than an expansive one

(which generally maintains a boundary between the tumor and healthy tissues, resulting in more defined and less invasive growth), and the presence of tumor cell necrosis.⁸

However, increasing evidence suggests that this dualistic model fails to capture the biological and genetic diversity of EC and from recent studies it has been classified according to the molecular classification^{8,11}. One of the most influential molecular classifications is that proposed in 2013 by The Cancer Genome Atlas (TCGA), which divides ECs into four categories, as shown in Figure 2¹³:

1. POLE/ultramutated (7%), characterized by somatic inactivating hotspot mutations in the POLE exonuclease domain. These tumors, regardless of grade, have an excellent prognosis, with 5-year relapse-free survival (RFS) rate of 98%.
2. Microsatellite instability-high (MSI-H)/hypermutated (28%), characterized by mismatch repair deficiency (MMRd) and microsatellite instability, have an intermediate prognosis (RFS 77.1%). The most commonly mutated genes include PTEN, ARID1A, PIK3CA, PIK3R1 and RPL22; moreover, mutations or epigenetic silencing of MLH1, MSH2, MSH6, PMS2 and EPCAM are often responsible for MSI.⁷
3. Somatic copy-number alteration high (26%), which have a low mutation rate, almost universally TP53 mutations (p53abn), with a highly unfavourable prognosis (RFS = 46.6%). This group includes most of the aggressive subtypes, especially serous carcinomas, and almost 25% of EECs.
4. Somatic copy-number alteration low (39%), also known as No Specific Molecular Profile (NSMP), with low copy-number alterations and low mutational burden. Tumors in this group have an intermediate prognosis, depending on oestrogen receptor expression and histological grade (RFS = 74,4%).^{7,12}

The TCGA molecular classification has improved management, classification, and personalized treatment of patients affected by EC; however, the translation of this classification into the clinical practice is still complex.¹⁴

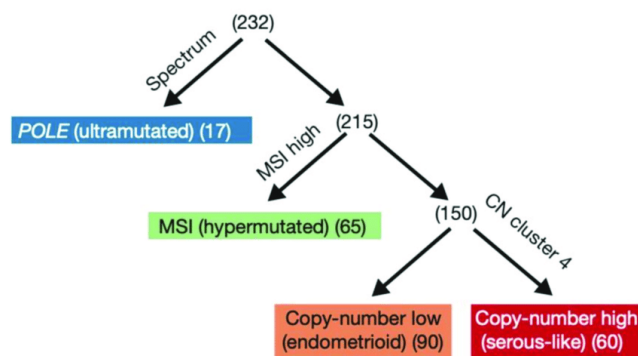


Figure 2: EC classification in four molecular subgroups by TCGA.¹³

Pathophysiology

Prolonged exposure to oestrogens, unopposed by progesterone, during menstrual cycle can cause endometrial hyperplasia, which increases the chance of EC development; however, the molecular basis of this process is still unknown.⁸ The initial identifiable atypical premalignant lesion is referred to as endometrial intraepithelial neoplasia (EIN), which can subsequently lead to invasive EC involving the endometrial stroma and penetrating the myometrium. EIN and EC usually express oestrogen and progesterone receptor, and they are often characterized by PTEN or KRAS2 mutations.¹¹ EC primarily spreads through the lymphatic and vascular systems to the Fallopian tubes and ovaries and, to a lesser extent, to the peritoneum and other pelvic organs. Lymphovascular invasion (LVI) is defined as the presence of tumor cells within lymphatic or blood vessels, and it is considered as one of the first step of metastatic spread in EC; the presence of a significant number of tumoral cells within the lymphatic or blood vessels is typical of the substantial (SUB) LVI while the absence or sporadic occurrences of tumor cells is defined as absent/focal (A/F) LVI.

Other suspected EC etiologic factors, such as insulin resistance and hyperandrogenaemia, are under investigation; however, the mechanisms by which they contribute to EC are not completely understood.¹¹

Risk factors

The risk of developing EC increases with age (≥ 55) and is higher for Black women. The most significant risk factors for EC development are those that lead to prolonged and unopposed exposure to oestrogens, such as obesity (Body Mass Index – BMI $> 30 \text{ kg/m}^2$) and use of exogenous oestrogens (e.g. oestrogen replacement therapy and tamoxifen treatment).^{7,11} Several studies demonstrated that a BMI $> 25 \text{ kg/m}^2$ (which indicates overweight condition) doubles a woman's risk of developing EC, while a BMI over 30 kg/m^2 increases the risk threefold. Obesity contributes to the development of EC primarily by increasing oestrogens production. This happens because adipocytes convert androgens into oestrogen, which then stimulates endometrium growth, potentially leading to hyperplasia and cancer. Additionally, obesity can lead to hyperglycaemia and insulin resistance, which may result in abnormalities in IGF-1 signaling and mTOR pathways, further promoting cell proliferation.⁷ As consequence, risk factors associated with obesity - such as physical inactivity, excessive energy intake, high blood pressure (above 140/90 mmHg), elevated serum glucose levels, and the presence of polycystic ovaries - can also be considered risk factors for EC. Although alcohol consumption is associated with increased oestrogens concentrations, epidemiological studies do not

show a positive correlation between alcohol intake and EC risk, unlike what has been observed for other cancer types (e.g. breast cancer).⁸

Some pathological conditions can increase the risk of EC, such as Hereditary Non-Polyposis Colon Cancer (HNPCC) syndrome (resulted from germline mutations in mismatch repair genes), Lynch and Cowden syndromes.^{7,8} Considering other cancer subtypes, women who have been diagnosed with breast cancer have an increased risk of developing EC. While breast tumors rarely metastasize to the endometrium, EC is more frequently diagnosed in breast cancer survivors due to shared risk factors.⁸ Concerning protective factors against EC, these include: i) smoking, due to its effect on oestrogens production and metabolism; ii) pregnancy, which involves high levels of progestogens, and breastfeeding; iii) use of intrauterine device and tubal ligation; iv) use of combined oestrogen-progestin oral contraceptives (with increased risk reduction as the duration of use increases, and persisting for more than 30 years after discontinuation); v) coffee and tea consumption.^{8,11}

Symptoms and diagnosis

The most common symptom of EC is abnormal uterine bleeding, which may be accompanied by vaginal discharge or pyometra; in some cases, symptoms can also include abdominal pain, constipation or diarrhoea and uterine enlargement.^{7,11}

EC is usually diagnosed through transvaginal ultrasound and confirmed histologically via endometrial tissue biopsies. Although EC is staged surgically, preoperative imaging techniques can help to identify women with advanced stage tumors, allowing for the selection of the most appropriate surgical approach. Magnetic Resonance Imaging (MRI) is particularly useful due to its excellent soft tissue contrast resolution. CA125 can serve as potential tumor marker with higher levels often associated with type II or advanced stage cancers compared to early-stage tumors; however, a normal value cannot exclude tumor presence.^{7,11}

Recurrence of EC can happen locally in vagina, pelvic lymph nodes, or in paraaortic lymph nodes and peritoneum. Distant metastases are most frequently found in lungs and lymph nodes, though less commonly, they can also occur in bones, brain, and intra-abdominal organs.⁷

Treatment

Management of EC typically involves surgical staging. If EC is confined to endometrium and myometrium, hysterectomy with bilateral salpingo-oophorectomy is usually performed, and further treatments are generally not necessary. The prognosis in such cases is typically favourable, with a 5-year OS of 96%. However, in patients with advanced-stage or metastatic EC, surgery must be followed by radiotherapy and/or platinum and paclitaxel-based chemotherapy.^{7,11,15} Radiotherapy or

brachytherapy (internal radiation) is often recommended in adjuvant setting to target residual microscopic disease and reduce the risk of local recurrence. Nonetheless, 1-10% of women who undergo surgery followed by radiotherapy may experience adverse reactions.^{7,8,11}

Hormone therapy (including megestrol or medroxyprogesterone, aromatase inhibitors, fulvestrant and tamoxifen) may be considered as therapies for early-stage EC patients who wish to preserve fertility or are not suitable candidates for surgical treatment. However, recurrence rate is high and also several adverse reactions can occur, including weight gain, edema, thrombophlebitis, depression and hypertension.¹¹

Following the publication of the TCGA molecular classification, increasingly targeted therapies are being sought for cancers with specific molecular abnormalities. In this context, the effect of immune checkpoint inhibitors (ICIs) is monitored in MSI-H tumors due to their high mutational burden; these inhibitors are approved for advanced or recurrent EC following systemic therapy. Among these, pembrolizumab is a monoclonal antibody directed against programmed cell death protein 1 (PD-1) and is used to prevent tumor cells from escaping immune surveillance in MSI-H tumors. Pembrolizumab was approved by the Food and Drug Administration (FDA) in 2021 for MMRd EC and is used as a second-line treatment for MMR-proficient tumors in combination with lenvatinib, a multikinase inhibitor targeting the vascular endothelial growth factor (VEGF) receptor. However, other combinations are under investigation to overcome resistance to ICIs.¹⁴ ICIs are also being studied in association with polyadenosine diphosphate-ribose polymerase inhibitors (PARPi) in POLE mutated EC.^{7,11,14}

Since overexpression of HER2 is a negative prognostic biomarker in p53abn EC, a recent phase II clinical trial found that combining standard chemotherapy with trastuzumab, an anti-HER2 antibody, in advanced/recurrent HER2-positive serous EC improved Progression Free Survival (PFS) compared to chemotherapy alone. Additionally, the PARPi olaparib is under investigation for p53abn EC patients. For NSMP tumors, instead, hormone therapy represents a good option.^{7,11,14}

1.1.2. Ovarian cancer

Ovarian cancer (OC) is a neoplasm characterized by uncontrolled proliferation of cells in the ovaries, two organs located on either side of uterus, to which they are connected via the Fallopian tubes. According to GLOBOCAN data, 324603 new cases of OC were diagnosed and 206956 deaths worldwide were registered in 2022, making it the 7th most common form of cancer and the 8th leading cause of cancer-related death among women, globally.^{10,16}

OCs are more frequently diagnosed in women after menopause (ages 50-70), and in the coming years, the incidence of this neoplasm is expected to increase further due to life expectancy rising. Incidence

rates are higher in high-income and very high-income countries compared to middle-income and low-income countries.^{17,18} According to the National Cancer Institute (NCI), the 5-year survival rate is 92.4% when OC is diagnosed at stage I, but it drops to 31.5% when diagnosis occurs at stages III and IV.¹⁹

Histological classification

OC represents a complex and heterogeneous group of diseases. They are classified into two main subtypes based on the cells of origin: epithelial (EOC) and non-epithelial tumors (germ cell and sex cord-stromal tumors), as shown in Figure 3.²⁰

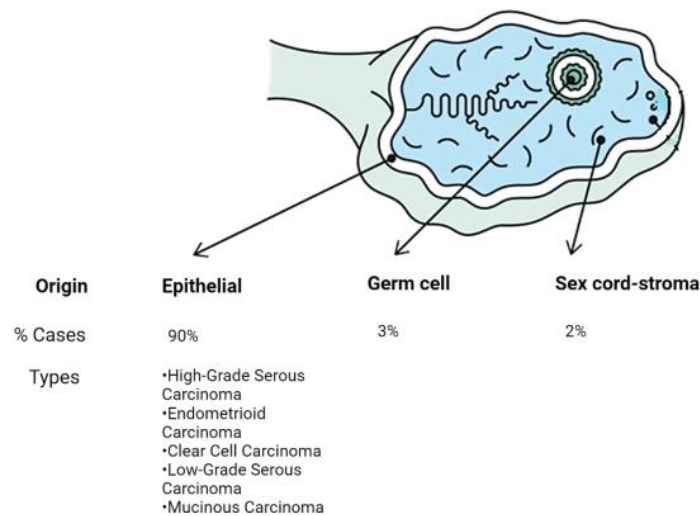


Figure 3: OC classification based on cell type of origin.²⁰

EOCs are the most common type of OC, accounting for 90% of all diagnosed cases. They arise from uncontrolled proliferation of epithelial cells in the outer lining of the ovaries and are histologically classified into five main subtypes. Each subtype has distinct pathological and genetic characteristics, as well as different etiologies and prognosis.²¹

- low-grade serous carcinoma (LGSOC) accounts for less than 5% of all EOCs. It typically originates in the ovaries and is associated with a relatively good prognosis and longer life expectancy. In 60-80% of cases, LGSOCs are serous borderline tumors, which exhibit uncontrolled cellular proliferation without having yet acquired ability to invade or metastasize. These tumors often harbor mutations in KRAS and BRAF genes, while mutations in TP53, BRCA, ERBB2 and NRAS are less common.²¹⁻²³
- high-grade serous carcinoma (HGSOC) represents the 70-80% of all EOCs. HGSOCs originate from epithelial cells of Fallopian tubes, from which they subsequently spread to ovaries. These tumors are associated with a poor prognosis, with a 10-year mortality rate of 70%. They are mostly characterized by TP53 mutations and BRCA abnormalities.²¹⁻²³

- endometrioid carcinoma (EnOC) represents the 10% of all EOCs and is associated with endometriosis in 42% of cases. Among the different OC subtypes, it has the most favourable prognosis because, in most cases, is diagnosed in an early stage. From a molecular perspective, KRAS mutations and PTEN inactivation play a significant role in the malignant transformation of endometriosis into EnOC. Additionally, CTNNB1 mutations are common in EnOCs, along with mutations in PIK3CA, PIK3R1, ARID1A, MSI, and PPP2R1A.^{22,23}
- mucinous carcinoma (MUC) is named after the mucin-rich cytoplasm of the tumor cells. This subtype represents the 3% of all EOCs. KRAS mutations are the most frequent genetic alterations, although HER2 overexpression has also been observed. Cases without HER2 amplification or KRAS mutations are associated with a higher likelihood of recurrence and death compared to tumors that exhibit both alterations.²¹⁻²³
- clear cell carcinoma (CCC) accounts for 10% of all EOCs. It is rarely bilateral and tends to exhibit local growth with frequent resistance to chemotherapy. The name is derived from its histological characteristics: cells with clear cytoplasm due to glycogen accumulation, along with eccentric, rounded, and bulbous nuclei. PIK3CA and ARID1A mutations are frequent, while BRCA and TP53 mutations are generally absent.^{17,21-23}

Other rare subtypes include undifferentiated, mixed, and Brenner tumors.

Non-epithelial tumors represent the 10% of all OCs and are classified into:

- Germ cell tumors (3-5%). These are rare tumors often diagnosed at a young age, particularly between 10 and 30. These tumors originate from germ cells, which are responsible for oocyte formation.
- Sex-cord stromal tumors (< 2%). These are the least common OCs, are rarely malignant and originate from the stroma, where female sex hormones are produced.

Other rare non-epithelial tumors include small cell carcinomas and ovarian sarcomas.¹⁷

Pathophysiology

According to the dualistic model proposed by Kurman, EOCs can be classified into type I and type II carcinomas, which develop through distinct molecular pathways:

- Type I cancers account for 25% of cases and are often clinically indolent, with slow growth. Their precursors are typically borderline tumors or endometriosis. Type I tumors frequently originate from inclusion cysts composed of Müllerian epithelium, which are formed after the

implantation of epithelial cells from the tubal fimbria onto the ovarian surface. LGSOCs, EnOCs, CCCs, MUCs and Brenner tumors are generally classified as type I.^{24,25}

- Type II cancers account for 75% of EOCs and include HGSOCS, as well as other rare carcinomas. They are highly aggressive and rapidly growing tumors that arise directly from epithelial tissue without progressing through a precancerous phase. More recently, the Fallopian tubes have been recognized as playing a more central role in the process of carcinogenesis. The tubal fimbria can be exposed to chronic oxidative stress due to endogenous oxidants, causing the occurrence of TP53 mutations in the secretory cells of the Fallopian tube, and the induction of DNA damage, even before proliferation has taken place. These cells may degenerate into serous tubal intraepithelial carcinoma (STIC), characterized by nuclear pleomorphism, increased mitosis, and loss of polarity. Proliferating STIC cells can shed and implant on the ovarian surface, leading to the development of HGSOCS.²⁴⁻²⁶

Risk factors

OC risk factors can be classified in non-modifiable and modifiable. Non-modifiable risk factors primarily include genetic and hormonal factors while modifiable risk factors are mainly environmental, such as lifestyle, dietary habits, and physical activity.²⁷

Increasing age is the primary risk factor for OC development.²⁸ The genetic risk factor is predominantly manifested as an autosomal dominant mutation in the BRCA1 and BRCA2 genes, located on chromosomes 17q and 13q respectively, which encode proteins involved in double-strand DNA breaks repair, cell cycle checkpoint control, and chromosome segregation. Risk of developing OC in women with BRCA1 mutations ranges from 30% to 44%, whereas it is lower in women with BRCA2 mutations, who have a 27% risk.^{27,29,30} Aside from BRCA 1/2 mutations, approximately 20% of EOCs are associated with hereditary breast and ovarian cancer syndrome (HBOC) or Lynch syndrome.³¹

Hormone release during ovulatory period seems to influence risk of OC development. Over time, three hypotheses have been proposed to correlate OC epidemiology with reproductive physiology:

1. Persistent ovulation hypothesis. In 1971, *M.F. Fathalla* proposed that ovulation (resulting in follicle rupture) could damage the ovarian surface. This trauma could lead to increased proliferation over time in an attempt to repair the damaged epithelium. If this damage is not adequately repaired, it may trigger malignant transformation of ovarian cells.³² This hypothesis is supported by the observation that multiple pregnancies, breastfeeding and use of oral contraceptives (all factors that inhibit ovulation) decrease risk of developing OC.^{33,34} However, EC risk reduction associated with use of the progestin-only pill - which does not

suppress ovulation - is comparable to that provided by the combined oestrogen-progestin oral contraceptive pill, casting doubt on this hypothesis.³⁵

2. Gonadotropin hypothesis. This hypothesis is based on the evidence that elevated serum levels of gonadotropins (luteinizing hormone - LH and follicle-stimulating hormone - FSH) may directly damage the ovarian epithelium or, indirectly, stimulate increased oestrogens production. These hormones act by stimulating the ovarian surface, which can lead to malignant transformations of the epithelium. This hypothesis is supported by the fact that serum levels of gonadotropins increase with age and are particularly high during menopause, a period in which most of OCs occur. However, this hypothesis also seems to falter considering that during breastfeeding, there is an increase in circulating FSH, which, according to this hypothesis, should increase the risk. Yet, the literature classifies breastfeeding as a protective factor against OC.³⁶
3. Hormonal hypothesis. The most recent hypothesis aims to address the conflicts left unresolved by the other two hypotheses and proposes that hormones play a key role in triggering the carcinogenic process in the ovaries. Excessive stimulation by androgens appears to promote cancer development, while progesterone seems to have a protective effect. The fact that women with polycystic ovary syndrome, a history of acne or hirsutism (conditions in which androgens level is elevated) have an increased risk of developing OC, supports this hypothesis. According to this, the protective effect of pregnancy appears to be due to the elevated concentration of progesterone during pregnancy rather than ovulation suppression.³⁵

Among the environmental factors, an improper diet stands out. Indeed, a case-control study carried out in Italy on 1031 cases demonstrated that the risk of developing OC is increased by high consumption of fats and meat, while consumption of fruits and vegetables appears to be a protective factor.²⁹ At the same time, a study by *Cottreau* et al., involving 767 EOC women demonstrated a 27% reduced risk of EOC development in women who regularly engage in physical activity compared to less active women. However, currently available data do not allow for definitive conclusions.³⁷ Regarding cigarette smoking, an association has been identified with MUC, while no association has been found for other histological subtypes.²⁷ Finally, due to increase of available data on the potential carcinogenic effects of talc in experimental animals, in July 2024, the International Agency for Research on Cancer (IARC) classified talc as probably carcinogenic to humans (Group 2A), with particular attention to OC.³⁸

Symptoms and diagnosis

Early-stage OC is frequently asymptomatic or characterized by non-specific symptoms like flatulence, difficulty in digestion, abdominal pain, and bloating. In the advanced stage, symptoms often include abdominal distension, ascites, cachexia, vaginal bleeding, and disturbances in bowel movements and urination.²⁸ Currently, there are no scientifically reliable screening tests for early detection of OC, and this is the main reason OC has the lowest survival rate among female cancers. The initial diagnosis is typically performed through pelvic examination and abdominal palpation, transvaginal ultrasound, and, in some cases, abdominal Computed Tomography (CT) scan and Magnetic Resonance Imaging (MRI). If OC is suspected, a diagnostic laparoscopy is conducted to obtain an accurate assessment of the disease extent and to determine operability. Imaging techniques are often accompanied by evaluation of CA125 serum levels, which is elevated in 80% of OC cases, although it can also be high in cases of endometriosis.³⁹ At the time of diagnosis, based on surgical evaluation, OC is classified according to the FIGO staging system released in 2018.⁴⁰

Treatment

The primary treatment for OC is cytoreductive surgery, aimed at removing all tumor cells; the residual tumor volume after surgery is, indeed, one of the major determinants of survival for OC patients.⁴¹ To reduce the likelihood of recurrence, adjuvant chemotherapy is administered following surgical treatment. It consists of a combination of platinum compounds and paclitaxel, given intravenously over 3 hours every 21 days for 6 cycles. In cases where initial surgery is not feasible due to extended tumor mass or patient's clinical condition, neoadjuvant platinum- and paclitaxel-based chemotherapy (NACT) is applied, followed by interval debulking surgery (IDS). The Italian SCORPION study, a phase III randomized trial comparing outcomes with NACT followed by IDS to primary surgery in patients with advanced OC, showed better results with NACT in terms of perioperative complications and quality of life, but no superiority in survival rate was observed. For this reason, primary surgery remains the preferred treatment for OC, with the exception of cases with extensive extraperitoneal spread, high anaesthetic risk, or when disease dissemination is so extensive that complete surgical resection is not feasible.⁴² In recent years, chemotherapy has been complemented by targeted therapies that have improved patients' survival. Among these, bevacizumab, a monoclonal antibody against VEGF (which is overexpressed in OC), is administered to patients diagnosed with stage III-IV OC, in combination with standard chemotherapy, to block angiogenesis reducing the blood supply to the tumor, and thereby limit its growth.⁴³ Since PARP-1 and PARP-2 enzymes play a crucial role in the single-strand DNA breaks repair, PARPi, such as olaparib, niraparib and rucaparib, currently represent an effective strategy in combating OC, as maintenance therapy following treatment with standard chemotherapy. In particular, BRCA1/2 mutated tumors are particularly sensitive to these

drugs due to the accumulation of single-strand DNA breaks. This phenomenon leads to synthetic lethality, where the combined defects in DNA repair pathways - caused by BRCA1/2 mutations and PARP inhibition - render the tumor cells unable to survive.⁴⁴

1.2 Epigenetics

The term “epigenetics” was first used by Conrad Waddington in 1942, who described this field as “the branch of biology that studies the causal interactions between genes and their products which bring the phenotype into being”.⁴⁵ It examines changes in gene expression that do not result from alterations in the DNA sequence.⁴⁶ As shown in Figure 4, humans are constantly exposed to, and live in, a dynamic environment that triggers chemical changes capable of activating or silencing genes. For example, exposure to drugs and toxic substances, diet, physical exercise, stress, and other environmental factors - whether of natural or social origin, including daily habits and lifestyle - can induce epigenetic modifications with lasting effects on health.⁴⁷

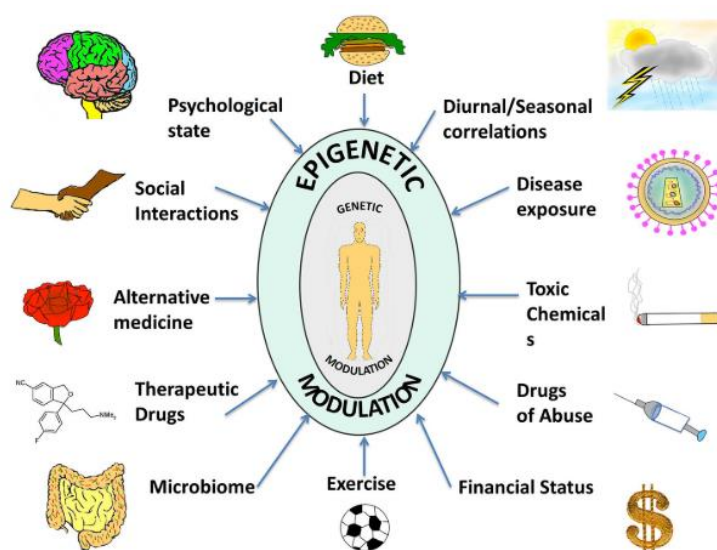


Figure 4: Epigenetic variables that can influence human life.⁴⁷

For many years, chronic and degenerative human diseases, including cancer, were considered the direct consequence of DNA mutations. However, it is now well understood that these conditions are also characterized by alterations in the epigenetic profile. Therefore, the onset of a disease is not solely dependent on genetic variability, which determines the individual's predisposition, but also on epigenetic factors.⁴⁸ Despite extensive knowledge about role and consequences of genomic alterations in cancer, understanding how epigenetic deregulations trigger and promote tumorigenesis is still in its early stages. In the future, integration of genomic and epigenomic data could pave the

way for new diagnostic and prognostic methods, as well as for revealing new potential targets for therapeutic interventions.⁴⁹

Epigenetic mechanisms are classified into three main groups, shown in Figure 5:

- DNA methylation, a stable mechanism of transcriptional repression that is difficult to reverse. In pathological conditions, both hypermethylation and hypomethylation can occur. CpG islands hypermethylation is the most frequent epigenetic change in cancer and it is associated with the inappropriate transcriptional silencing of tumor suppressor genes. Conversely, DNA hypomethylation can lead to activation of proto-oncogenes.⁵⁰
- Histone modifications, post-translational modifications occurring on the amino acids of histones N-terminal tails. These modifications include acetylation of lysine residues (mediated by enzymes called histone acetyltransferases - HATs), methylation of lysine and arginine residues, phosphorylation of serine and threonine residues, and ubiquitination of lysine residues. Generally, acetylation of lysine residues on histone tails leads to chromatin relaxation, allowing transcription to occur. In contrast, deacetylation, carried out by histone deacetylases (HDACs), makes the chromatin more compact, resulting in transcriptional inactivation.⁵⁰
- Post-transcriptional modifications by non-coding RNAs (ncRNAs). ncRNAs are RNA sequences of variable length that do not code for proteins but mediate expression regulation of specific target genes. When their length is approximately 18-24 nucleotides, they are referred to as microRNAs (miRNAs or miRs). If they are longer, reaching up to 200 nucleotides, they are known as long non-coding RNAs (lncRNAs).⁵⁰

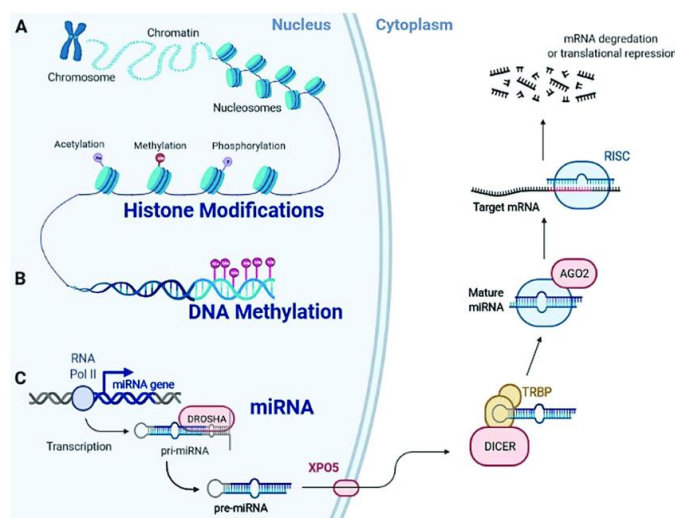


Figure 5: Epigenetic mechanisms comprising (A) histone post-translational modifications (HPTMs); (B) DNA methylation, and (C) non-coding RNAs (miRNAs) regulation. Gene expression can be controlled prior to the initiation of transcription through HPTMs and DNA methylation while miRNAs regulate the expression of genes at the post-transcriptional level.⁵¹

1.2.1 MicroRNA

miRNAs are small non-coding RNA fragments, that play a crucial role in gene regulation and have been extensively studied in recent years.⁴⁸ The first miRNA to be discovered, in 1993, was *lin-4*, which inhibits the translation of the LIN-14 gene in *Caenorhabditis elegans*. To date, according to the miRBase database, over 2500 functional miRNAs have been identified, regulating expression of approximately 60% of protein-coding genes.⁵²

Biogenesis

The process of miRNA biogenesis is relatively complex. MiRNAs are transcribed in the nucleus primarily by RNA polymerase II, resulting in primary miRNAs (pri-miRNAs) with variable lengths ranging from 100 bp to 10 kb.⁵³ The pri-miRNA is then cleaved by the Drosha protein complex, which includes two RNA polymerase III domains, into a precursor known as pre-miRNA, consisting of approximately 70 nucleotides. This pre-miRNA is then transported to the cytoplasm by the transport protein EXPORTIN-5. Here the pre-miRNA is processed by the Dicer complex, which also contains RNA polymerase III domains, to form the mature miRNA, a double-stranded RNA of approximately 22 nucleotides.⁵⁴ The Dicer complex interacts with the Transactivation Responsive RNA Binding Protein (TRBP), which recruits the Argonaute (Ago) protein, forming a trimolecular complex that gives rise to the RNA-induced silencing complex (RISC). At this point, one of the two strands of the mature miRNA, known as the "guide" or active strand, is loaded into the RISC complex, where it performs its function, while the inactive or "passenger" strand, is degraded.⁵⁵ miRNA biogenesis is described in Figure 5 above.

Mechanism of action

MiRNAs regulate gene expression by binding a complementary sequence in a target messenger RNA (mRNA). This binding typically occurs between the miRNA seed region (located between nucleotides 2 and 8 at the 5' end), and the 3' UTR of the mRNA.⁵⁴ Depending on the degree of complementarity between miRNA and mRNA strands, a miRNA can inhibit its target in two different ways: mRNA degradation or translation repression. Perfect complementarity leads to mRNA degradation catalysed by Ago, whereas imperfect complementarity results in translation repression. The exact mechanism of translation repression by miRNAs is still not fully understood. However, in both cases, a reduction in protein amount will be the final effect.⁵⁶ It is important to emphasize that a single miRNA can regulate expression of hundreds of mRNAs, and conversely, a single mRNA can contain multiple sequences that allow interaction with several miRNAs. Additionally, after interacting with its initial

target, miRNA is not immediately degraded, with possibility for further interactions with other mRNAs.⁵⁷

MiRNA in cancer

Given that miRNAs are involved in the modulation of gene expression, their dysregulation is associated with the onset of various diseases, including cancer, particularly when it affects genes involved in several biological processes such as apoptosis, cell division, aging, and hematopoietic differentiation.⁵³ miRNAs play a role in regulating tumor suppressor genes and oncogenes. It is now well established that chromosomal regions containing miRNAs involved in down-regulation of tumor suppressor genes (known as onco-miRNAs) can be amplified during cancer development, leading to increased miRNA expression and subsequent silencing of the tumor suppressor gene, thereby preventing its translation. Conversely, miRNAs that repress oncogenes (known as tumor suppressor miRNAs) are often located in fragile sites, where deletions or mutations are more likely to occur, leading to reduced miRNA levels and overexpression of the target oncogene. Dysregulation of miRNA expression profiles in cancer can be attributed to various mechanisms, including genetic alterations, epigenetic changes, Single Nucleotide Polymorphisms in miRNA-coding genes, or defects in the miRNA biogenesis process.⁵⁸ An aberrant miRNA profile is associated with tumor development, progression, metastasis, and chemotherapy resistance, suggesting their potential use not only as diagnostic but also as predictive biomarkers of therapeutic efficacy, potentially guiding the selection of alternative therapeutic approaches.⁵⁹

1.2.2 Obesity

Obesity is a condition caused by an abnormal accumulation of body fat, which can negatively affect overall well-being. According to the WHO, overweight and obesity are defined as “*abnormal or excessive fat accumulation that presents a risk to health*”. BMI, calculated as $[(\text{weight in kg})/(\text{height in m})^2]$, is widely used to classify individuals' weight according to the table shown in Figure 6.⁶⁰

BMI	Category
< 16.0	Severely Underweight
16.0 - 18.4	Underweight
18.5 - 24.9	Normal
25.0 - 29.9	Overweight
30.0 - 34.9	Moderately Obese
35.0 - 39.9	Severely Obese
≥ 40.0	Morbidly Obese

Figure 6: WHO adult classification based on BMI.⁶⁰

Obesity is an escalating global issue, with prevalence rising in both industrialized and developing countries.⁶⁰ In 2024, the Non-Communicable Diseases Risk Factor Collaboration (NCD-RisC) estimated that over one billion people worldwide are obese, including approximately 880 million adults and 159 million children and adolescents aged 5-19. When overweight individuals are also considered, this number rises to nearly 3 billion. Considering these numbers, obesity is now acknowledged as a major global public health issue.⁶¹ Although obesity is primarily driven by an imbalance between energy intake (dietary consumption) and energy expenditure (through metabolic and physical activities), its underlying causes are highly complex. In fact, obesity development is influenced by a wide range of factors, including genetic, physiological, environmental, psychological, social, economic, and even political elements, all of which interact in various ways to contribute to its onset.⁶² Obesity can have consequences for all organ systems. Most notably, it affects cardiovascular system, increasing the likelihood of developing hypertension, dyslipidaemia, type-2 diabetes mellitus, coronary heart disease (CHD), and heart failure. Obesity is also defined by the WHO as a contributing factor to metabolic syndrome, a pathological condition characterized by abdominal obesity, insulin resistance, hypertension, and hyperlipidaemia. Additionally, obesity can impact endocrine system, as well as gastrointestinal and nervous systems.^{63,64} Keaver et al. predicted that by 2030, rates of overweight and obesity will rise to 89% in males and 85% in females. This surge is expected to lead to a 97% increase in CHD, a 61% rise in cancer cases, and a 21% increase in type-2 diabetes. Consequently, healthcare costs related to obesity will be affected by a significant increase.⁶⁵

According to IARC, there is strong evidence that excess body weight is linked to an increased risk of cancer development at least in 13 different anatomical sites. These include cancers of the endometrium, oesophagus, kidney, pancreas, hepatocellular carcinoma, gastric cancer, meningioma,

multiple myeloma, as well as colorectal, postmenopausal breast, ovarian, gallbladder, and thyroid cancers. The association between obesity and gynecological cancers, including endometrial, postmenopausal breast, and ovarian cancers, is of particular interest and highlights involvement of female sex hormones in the development of these tumors.⁶⁶ Even if the mechanisms by which obesity can contribute to cancer etiopathogenesis is not totally clear, the main pathways involved in this process are: 1) hyperinsulinemia and abnormalities of the IGF-1 system and signaling; 2) sex hormones biosynthesis and pathway; 3) subclinical chronic low-grade inflammation and oxidative stress; 4) alterations in adipocytokine pathophysiology; 5) factors deriving from ectopic fat deposition; 6) microenvironment and cellular perturbations; 7) factors causing obesity and cancer such as disruption of circadian rhythms and dietary nutrients; 8) altered intestinal microbiome; and 9) mechanic factors in obesity.⁶⁶ Moreover, in recent years, the Akt/PI3K/mTOR signaling pathway has gained attention as a common player shared by obesity and cancer. In this context, leptin, which is produced by adipose tissue, is positively associated with fat stores, and it promotes cancer progression by activating PI3K/Akt, MAPK, mTOR, and STAT3 signaling pathways, potentially serving as a mediator in obesity-related cancer.⁶⁷

1.2.3 Physical activity

WHO defines physical activity as “*any bodily movement produced by skeletal muscles that requires energy expenditure*”.⁶⁸ Physical activity includes all forms of movement, whether during leisure time, commuting, or as part of work or household tasks. Common activities include walking, cycling, wheeling, sports, recreational activities. It is well known that physical activity promotes health and well-being, while a lack of physical activity increases the risk of several negative health outcomes. In view of these considerations, physical activity is recommended both in childhood and adults. According to the WHO guidelines on physical activity and sedentary behaviour published in 2020, 150–300 minutes/week of moderate-intensity aerobic physical activity is recommended for adults, or at least 75–150 minutes/week of vigorous-intensity aerobic physical activity; or an equivalent combination of moderate- and vigorous-intensity activity throughout the week, for substantial health benefits.⁶⁹ According to a recent study, almost 1/3 of the world population is physically inactive, and women are less active than men. Several factors are known to influence how active individuals are; these factors may be linked to individual characteristics or broader social, cultural, environmental, and economic conditions that affect access to and opportunities for engaging in safe and enjoyable physical activity.^{68,70}

In recent years, researchers have focused their attention on physical activity due to its protective effects on human health, particularly in relation to cardiovascular diseases, injuries and cancer.

Indeed, physical inactivity is one of the major risk factors for mortality from non-communicable diseases. According to WHO statistics, individuals who are not enough physically active have a 20% to 30% higher risk of death compared to those who are engaged in sufficient physical activity. In particular, it is shown that physical activity can reduce the risk of all causes mortality, as well as the risk of hypertension and other cardiovascular diseases, different site-specific cancers, type-2 diabetes and may also improve mental health.⁶⁸ A recent systematic review showed that people engaging in higher levels of physical activity have 10-20% lower risk of developing bladder, breast, colon, endometrial, oesophageal adenocarcinoma, renal and gastric cancers.⁷¹ Moreover, guidelines for cancer survivors recommend physical activity and exercise as a fundamental and continuous condition of care for all cancer patients, as physical inactivity is known to be associated with reduced functional independence, decreased tolerance to anti-cancer treatments, and increased overall mortality. Numerous reviews and meta-analyses provide evidence that physical activity and exercise, at an intensity and duration appropriate for the patient's physical condition, are safe and well-tolerated before, during, and after cancer treatment, for all cancer types, including patients in advanced stages of the disease undergoing palliative care.⁷²

1.3 Liquid biopsy

Currently, the gold standard approach for oncological diagnosis is tissue biopsy, a technique that involves the surgical resection of a pathological tissue for analysis. This methodology presents several limitations: i) it is highly invasive, ii) it is costly, iii) it is time-consuming and can delay the start of therapies, iv) in some cases, the removed tissue may be insufficient to perform all the required tests, and v) it is impractical if the tumor is located in anatomically inaccessible areas. Furthermore, it is a procedure that cannot be repeated over time due to these weaknesses, limiting dynamic and real-time monitoring of disease progression.⁷³

A promising alternative to overcome these limitations is liquid biopsy, which involves detection and analysis of specific biomarkers in biological fluids, primarily blood, but also saliva, ascitic fluid, breast milk, urine, and cerebrospinal fluid. Liquid biopsy is emerging as a potentially useful technique for early tumor diagnosis and population screening, as well as for determining prognosis and monitoring the response to therapy. It offers several advantages: i) it is a minimally invasive procedure that allows real-time monitoring of the disease, ii) it is painless and poses no risk to the patient, iii) it requires minimal reagent consumption, and iv) it significantly reduces both diagnostic costs and time.⁷⁴

The main components released by tumor in body fluids are circulating tumor cells (CTCs), circulating tumor nucleic acids, and extracellular vesicles, including exosomes.⁷³

The first liquid biopsy-based test approved by the FDA in 2016 was Cobas® EGFR Mutation Test v2 (Roche), able to detect a specific alteration in the circulating tumor DNA (ctDNA). In particular, it identifies a mutation on EGFR, which is common in non-small cell lung cancer (NSCLC), and it is useful to determine the most appropriate treatment. Since then, several additional tests have been approved and are now used in clinical practice.⁷⁵ At present, there are no liquid biopsy tests approved by the FDA specifically for gynecological cancers. However, some FDA-approved tests for solid tumors, although not originally approved for gynecological cancers, may also be used for ovarian or endometrial tumors. Of particular relevance is FoundationOne®Liquid CDx, designed to detect genetic mutations in ctDNA, including BRCA 1 and BRCA 2 mutations. In OC, BRCA mutations are important for determining eligibility for targeted therapies, such as PARPi.^{76,77}

2. GENERAL AIM

The global impact of gynecological cancer is growing rapidly, with projections indicating a continuous rise over the next two decades. In 2020, it was estimated that 1.4 million women worldwide were newly diagnosed with gynecological cancers, leading to 680000 deaths. Approximately 1 in 20 women develop gynecological cancer in their lifetime, and 1 in 33 women die from it.¹ In recent years, increasing attention has been paid towards maintaining a healthy lifestyle, as the latter has been identified as a protective factor in the majority of cancers.⁷⁸ In particular, obesity is considered one of the major risk factors for EC and a BMI exceeding 30 kg/m² triples the risk of EC development. On the other side, guidelines for cancer survivors recommend physical activity and exercise as a fundamental part of care for all cancer patients, as physical inactivity is known to be associated with reduced functional independence, decreased tolerance to anti-cancer treatments, and increased overall mortality.^{7,72}

Given these premises, epigenetics, that studies gene expression variations resulting from environmental conditions, may play a key role in determining the effect of lifestyle on human cancer. For the above-mentioned reasons, to better clarify the epigenetic role of lifestyle in gynecological cancers, the present study aimed to:

- i) Identify deregulated expression in miRNA related to obesity, in EC patients.
- ii) Identify variations in miRNA expression in OC patients who were enrolled in, or not enrolled, in a specific physical activity program.

Lastly, in the final part of the project, the research activity was focused on learning how to establish a specific 3D OC model, with the goal of using it for further *in vitro* validations and analysis of the previously obtained results.

To better present the main topics, the thesis is divided in three parts; the first part focus on obesity-related EC (Task 1), the second one on physical activity in OC (Task 2) and the last one is dedicated to 3D OC models (Task 3).

3. TASK 1: Epigenetic effects of obesity in Endometrial Cancer patients

3.1 AIM

As previously mentioned, obesity is one of the major risk factors for EC development; however, it is not well known how epigenetic modifications induced by obesity may influence EC development or prognosis. The aim of this study was to investigate the role of miRNAs in EC within the context of obesity, exploring miRNAs expression in relation to BMI across various groups of women, including EC patients who were either obese or non-obese, as well as obese non-cancer women. Initially, the study assessed the miRNA profile in endometrial tissues of obese women with and without an EC diagnosis, to identify any potential links between miRNAs, EC, and obesity. Subsequently, miRNA levels were analysed specifically in EC patients tissue samples, categorizing them according to their BMI, to understand if miRNAs expression is different between the two subgroups. The second part of the study aimed to analyse miRNA expression in the same groups of patients, but within the context of liquid biopsy, which is gaining momentum due to its non-invasiveness.

3.2 MATERIALS AND METHODS

Study population

The study included a first part focused on tumor and normal tissue while the second part was focused on plasma samples. For more clarity, the first part will be rereferred as “Tumor Epigenetics” and the second one as “Liquid Biopsy Epigenetics”. A complete workflow of the project is shown in Figure 7.

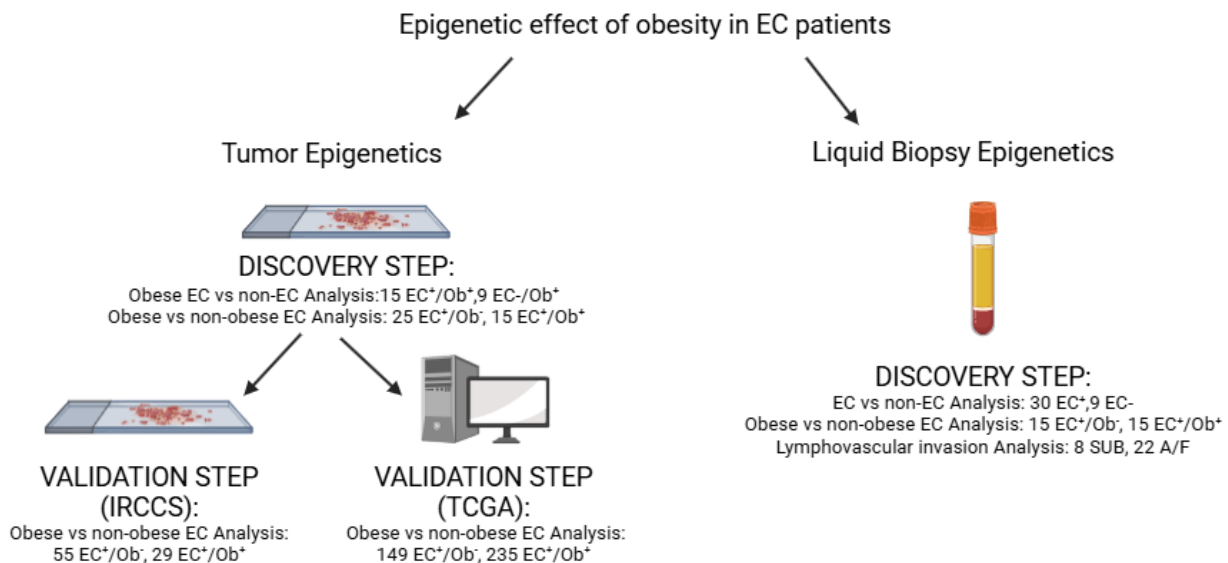


Figure 7: "Epigenetic effects of obesity in Endometrial Cancer patients" project workflow. Created with BioRender.

This study was approved by the Institutional Review Board 189/2021/Oss/AOUBo, ClinicalTrials.gov Identifier NCT04845425. Patients were included in the study after signing an informed consent form. The inclusion criteria were: i) being at least 18 years old; ii) having a diagnosis of EC with no prior treatment; iii) alternatively, having a diagnosis of obesity (BMI \geq 30) without any additional complications. Patients enrolled in the present study were treated at the Division of Oncologic Gynecology and in the Division of Endocrinology and Diabetes Prevention and Care, Istituto di Ricovero e Cura a Carattere Scientifico (IRCCS), Azienda Ospedaliero-Universitaria of Bologna.

Tumor Epigenetics

The “Tumor Epigenetic” study was conducted through a discovery and a validation phases. A total of 84 early-stage EC patients (EC⁺) were enrolled in the study, 29 of which obese, with a BMI \geq 30 (EC⁺/Ob⁺), and 55 non-obese, with a BMI < 30 (EC⁺/Ob⁻); moreover, 9 non-cancer obese patients (EC⁻/Ob⁺) were recruited. Formalin-fixed, paraffin-embedded (FFPE) primary tumors from 84 EC patients and uterine tissue from 9 non-cancer obese women were retrieved from the archives of the Department of Pathology, IRCCS Azienda Ospedaliero-Universitaria of Bologna between 2014 and 2023. Tumor tissue samples were collected for EC patients during surgical operations for tumor staging, while for obese individuals, biopsies were collected during surgery for weight control (sleeve gastrectomy or Roux-en-Y gastric bypass).

Sample processing

FFPE tissue slides were examined by two expert pathologists who confirmed the EC diagnosis and ensured the inclusion of more than 70% of cancer cells in EC samples. When fewer than 70% of the cells on a slide were cancerous, it was macro-dissected to remove non-tumoral cell contamination, following the pathologist’s guide.

RNA extraction from FFPE tissue samples

RNA was isolated from FFPE (three to six sections >10 μ m per sample) using the RecoverAll™ Total Nucleic Acid Isolation Kit (Invitrogen™) following the manufacturer’s instructions. Paraffine was removed from the FFPE tissue samples by submerging the slides in xylene (3 x 10 minutes) and absolute ethanol (2 x 5 minutes). Subsequently, the slides were incubated at room temperature overnight to allow for complete drying. Tumor material was scraped and collected in a tube together with Digestion buffer and Protease. After incubation at 50°C and 80°C, Isolation Additive and 100% ethanol were added, and the material was loaded into a Filter Cartridge. Following several washes of the filter with different buffers, a DNase solution was added to the filter and incubated at room

temperature for 30 minutes. After additional washes, the samples were eluted in 20 μL of nuclease-free water.

miRNA reverse transcription

1 ng of RNA extracted from FFPE tissue samples was reverse transcribed using the TaqMan™ Advanced miRNA cDNA Synthesis Kit (Applied Biosystems™), following the manufacturer’s instructions. This kit consists of four reactions:

1. Poly (A) tailing reaction: addition of a poly(A) tail to the 3' end of miRNAs. The reaction was prepared as follows:

Component	1 Reaction
10X Poly (A) Buffer	0,5 μL
ATP	0,5 μL
Poly (A) Enzyme	0,3 μL
RNase-free water	1,7 μL
Total Volume	3,0 μL

Each PCR tube containing 3 μL of the previously prepared mix and 2 μL of the sample was incubated in a thermal cycler under the following conditions:

Step	Temperature	Time
Polyadenylation	37°C	45 minutes
Stop reaction	65°C	10 minutes
Hold	4°C	∞

2. Ligation reaction: addition of an adaptor to the 5' end. The reaction was prepared as follows:

Component	1 Reaction
5X DNA Ligase Buffer	3 μL
50% PEG 8000	4,5 μL
25X Ligation Adaptor	0,6 μL
RNA Ligase	1,5 μL
RNase-free water	0,4 μL
Total volume	10 μL

10 μL of the mix was added to the tube already containing 5 μL of the previous reaction and incubated in a thermal cycler under the following conditions:

Step	Temperature	Time
Ligation	16°C	60 minutes
Hold	4°C	∞

3. Reverse Transcription (RT) reaction: the universal RT primer binds to the poly(A) tail located at the 3' end of the miRNA and converts the RNA into cDNA. The reaction was prepared as follows:

Component	1 Reaction
5X RT Buffer	6 μ L
dNTP Mix (25 mM each)	1,2 μ L
20X Universal RT Primer	1,5 μ L
10X RT Enzyme Mix	3 μ L
RNase-free water	3,3 μ L
Total Volume	15 μL

15 μ L of the mix was added to the tube already containing 15 μ L of the previous reaction and incubated in a thermal cycler under the following conditions:

Step	Temperature	Time
Reverse Transcription	42°C	15 minutes
Stop reaction	85°C	5 minutes
Hold	4°C	∞

4. miR-Amp reaction: the universal miR-Amp forward primer and miR-Amp reverse primer amplify the number of cDNA molecules. The reaction was prepared as follows:

Component	1 Reaction
2X miR-Amp Master Mix	12,5 μ L
20X miR-Amp Primer Mix	1,25 μ L
RNase-free water	8,75 μ L
Total Volume	22,5 μL

In a new tube, 22,5 μ L of the mix were added, together with 2,5 μ L of the RT reaction product.

The tubes were then incubated in a thermal cycler under the following conditions:

Step	Temperature	Time	Cycles
Enzyme activation	95°C	5 minutes	1
Denature	95°C	3 seconds	16
Anneal/Extend	60°C	30 seconds	
Stop reaction	99°C	10 minutes	1
Hold	4°C	∞	

Discovery step: miRNA expression profiling

The discovery step was performed on 49 samples (25 EC⁺/Ob⁻, 15 EC⁺/Ob⁺, and 9 EC⁻/Ob⁺) using the TaqMan™ Advanced miRNA Human A Card (Applied Biosystems™), an array consisting of 384 pre-loaded wells, which simultaneously analyse the expression of 377 common human miRNAs, along with endogenous hsa-miR-16-5p (5 replicates) and exogenous ath-159a (2 replicates) controls.

cDNA from each sample obtained in the previous reaction was diluted 1:10, loaded into the array together with TaqMan® Fast Advanced Master Mix (2X) (Applied Biosystems™), as follows:

Component	1 card
1:10 diluted cDNA template	212,5 µL
TaqMan® Fast Advanced Master Mix (2X)	425 µL
RNase-free water	212,5 µL
Total Volume	850 µL

The arrays were run on a 7900HT Fast PCR system (Applied Biosystems™), following the parameters:

Step	Temperature	Time	Cycles
Enzyme activation	92°C	10 minutes	1
Denature	95°C	1 seconds	40
Anneal/Extend	60°C	20 seconds	

Validation step: miRNA analysis by qRT-PCR

Hsa-miR-2210 (assay ID #477971_mir), hsa-miR-449a (assay ID #478561_mir), and hsa-miR-199a-5p (assay ID #478231_mir) were validated in 84 EC patients (55 EC⁺/Ob⁻ and 29 EC⁺/Ob⁺) treated at the Oncologic Gynecology Unit, IRCCS Azienda Ospedaliero-Universitaria of Bologna. Expression levels of selected miRNAs were evaluated by qRT-PCR using the TaqMan™ Advanced miRNA Assay (Applied Biosystems™). Hsa-miR-16-5p (assay ID #477860_mir) was used as internal reference based on a literature review and an assessment of its stability in our study cohort. Each reaction was run in triplicate in a 96-well plate and the mix was prepared as follows:

Component	1 Reaction
Taqman® Fast Advanced Master Mix (2X)	5 µL
Taqman® Advanced miRNA Assay (20X)	0,5 µL
RNase-free water	2 µL
Total Volume	7,5 µL

7,5 µL of the mix were added in each well, together with 2,5 µL of 1:10 diluted cDNA template. The plate was sealed with an adhesive cover and loaded on a 7900HT Fast PCR system (Applied Biosystems™), under the following conditions:

Step	Temperature	Time	Cycles
Enzyme activation	95°C	20 seconds	1
Denature	95°C	3 seconds	40
Anneal/Extend	60°C	30 seconds	

Validation of the results in the TCGA cohort

miRNAs resulted significantly deregulated between EC⁺/Ob⁻ and EC⁺/Ob⁺, were tested in The Cancer Genome Atlas—Uterine Corpus Endometrial Carcinoma (TCGA-UCEC) cohort. The molecular subtypes of patients included in the TCGA-UCEC cohort were retrieved through *TCGA biolinks*, while sample-level log₂ miRSeq, mRNASeq expression data, and clinical data were retrieved using the FireBrowser R package.^{79–81}

Statistical analysis

For the IRCCS validation, miRNA amplification data were analysed using the ThermoFisher Cloud app (Applied Biosystems™). miRNAs with C_t values ≥ 35 were considered not expressed and excluded from further analysis. Relative expression levels were calculated through the 2^{-ΔΔC_t} method using hsa-miR-16-5p as reference. Statistical significance was assessed using the nonparametric Mann–Whitney–Wilcoxon test, with a P-value (p) < 0.05 considered statistically significant. Principal Component Analysis (PCA), heatmap and volcano plot were created through SRplot⁸² while validations graphs were created with GrapPad Prism 8.0.2 for Windows, GraphPad Software, Boston, Massachusetts USA, www.graphpad.com. For the TCGA validations, statistical analysis was conducted using GraphPad Prism 8.0.2 and SPSS v20 software.⁸³ P value < 0.05 was considered statistically significant. The median miRNA expression was used as a cutoff to create Kaplan–Meier curves representing OS.

Target prediction

For miRNA-target prediction analysis, a list of experimentally validated mRNA targets for the relevant miRNAs was downloaded from Targetscan Human 8.0 database. Expression data of these targets were retrieved from the TCGA-UCEC tumor samples and were used to compare obese and non-obese EC patients. ToppGene tool was used to analyse the molecular functions of the predicted target genes.

Liquid Biopsy Epigenetics

In the second part of the study, which focused on liquid biopsy, blood samples were collected from 30 EC patients (15 EC⁺/Ob⁺ and 15 EC⁺/Ob⁻) and 10 EC⁻/Ob⁺. Blood samples were collected for EC patients during surgical operations for tumor staging, while for obese individuals were collected during surgery for weight control (sleeve gastrectomy or Roux-en-Y gastric bypass).

Sample processing

Blood was collected in a BD Vacutainer® K2 (EDTA) tube. Within 2 hours from blood draw, it was centrifuged at 3000 rpm for 10 minutes in a refrigerated centrifuge (4°C). Supernatant was then

transferred into a new tube and centrifuged at maximum speed for 15 minutes at 4°C. The final supernatant was stored in 500 µL aliquots at -80°C until use.

miRNA extraction from plasma samples

miRNAs were isolated from 200 µL of plasma using the miRNeasy Serum/Plasma kit (Qiagen), following the manufacturer's instructions. In particular, 1 mL of QIAzol Lysis Reagent was added to the sample, together with 2 µL of ath-159a spike-in control. After the addition of chloroform, three different phases were visible; the upper aqueous phase was transferred to a new tube and supplemented with 100% ethanol. The mixture was transferred to a RNeasy MinElute spin column, and, after several washes, final RNA elution was performed in 35 µL of nuclease-free water.

miRNome profiling

To analyse the global miRNA profile, cDNA libraries were prepared from 5 µL of RNA using QIAseq miRNA Library Kit (Qiagen), following the manufacturer's instructions. In particular, the protocol was made up of 6 steps, described below:

1. 3' ligation reaction: a pre-adenylated DNA adapter is ligated to the 3' ends of all miRNAs.

On ice, the mix was prepared as follows, maintaining the described order of addition:

Component	1 Reaction
QIAseq miRNA NGS 3' Buffer	2 µL
QIAseq miRNA NGS 3' Adapter (diluted 1:5)	1 µL
QIAseq miRNA NGS RI	1 µL
QIAseq miRNA NGS 3' Ligase	1 µL
2x miRNA Ligation Activator	10 µL
Template RNA	5 µL
Total volume	20 µL

The tubes were incubated in a thermal cycler under the following conditions:

Temperature	Time
28°C	60 minutes
65°C	20 minutes
4°C	∞ (at least 5 minutes)

2. 5' ligation reaction: a RNA adapter is ligated to the 5' end of mature miRNAs.

On ice, the mix was prepared according to the following table:

Component	1 Reaction
Nuclease-free water	15 µL
QIAseq miRNA NGS 5' Buffer	2 µL
QIAseq miRNA NGS RI	1 µL
QIAseq miRNA NGS 5' Ligase	1 µL

QIAseq miRNA NGS 5' Adapter (diluted 1:2,5)	1 μ L
Total volume	20 μL

20 μ L of this mix were added to the 20 μ L of the previous reaction, for a total volume of 40 μ L. The tubes were then incubated as follows:

Temperature	Time
28°C	30 minutes
65°C	20 minutes
4°C	∞ (at least 5 minutes)

3. Reverse Transcription (RT): the RT primer binds to a region of the 3' adapter and facilitates conversion of the miRNAs into cDNA.

First of all, 2 μ L of QIAseq miRNA NGS RT Initiator were added to each tube and incubated as follows:

Temperature	Time
75°C	2 minutes
70°C	2 minutes
65°C	2 minutes
60°C	2 minutes
55°C	2 minutes
37°C	5 minutes
25°C	5 minutes
4°C	∞

Meanwhile, on ice the mix for the reaction was prepared, according to protocol's instructions:

Component	1 Reaction
QIAseq miRNA NGS RT Primer (diluted 1:5)	2 μ L
Nuclease-free water	2 μ L
QIAseq miRNA NGS RT Buffer	12 μ L
QIAseq miRNA NGS RI	1 μ L
QIAseq miRNA NGS RT Enzyme	1 μ L
Total volume	18 μL

18 μ L of this mix were added to the 42 μ L of the previous reaction, for a total volume of 60 μ L. The tubes were then incubated as follows:

Temperature	Time
50°C	60 minutes
70°C	15 minutes
4°C	∞ (at least 5 minutes)

4. Preparation of QIAseq miRNA NGS Beads (QMN Beads).

For each sample, 400 μL of QIA Beads were transferred to a microcentrifuge tube to allow for the separation of the beads on a magnet stand. Once the beads had fully migrated, the supernatant was discarded; subsequently, 150 μL of QIAseq miRNA NGS Bead Binding Buffer were added to the beads. The tube was placed on a magnet stand to facilitate the separation of the beads. After migration was complete, the supernatant was discarded, and the beads were resuspended in 400 μL of QIAseq miRNA NGS Bead Binding Buffer.

5. cDNA cleanup reaction.

143 μL of QMN Beads, already vortexed, were added to the 60 μL of the previous reaction product. After a 5-minutes incubation, the tubes were placed on a magnet stand until the beads had fully migrated. The supernatant was discarded, and two washes with 80% ethanol were performed. After completely removing any residual ethanol and air-drying the beads, the DNA was eluted from the beads by adding 17 μL of nuclease-free water, which was then transferred to a new tube.

6. Library amplification using HT Plate Indices (331565): this reaction allows to barcode each sample with a unique 8-base indexing primer.

On ice, the reaction mix was prepared as follow:

Component	1 Reaction
QIAseq miRNA NGS Library Buffer	8 μL
HotStarTaq DNA Polymerase	1,5 μL
Nuclease-free water	15,5 μL
Total volume	25 μL

25 μL of the prepared mix were used to solubilize the lyophilized index and then added to 15 μL of the cDNA cleanup reaction product, for a total of 40 μL . The tubes were incubated in the thermal cycler according to the following parameters:

Step	Temperature	Time	Cycles
Hold	95°C	15 minutes	1
3-step cycling	Denaturation	95°C	15 seconds
	Annealing	60°C	30 seconds
	Extension	72°C	15 seconds
Hold	72°C	2 minutes	1
Hold	4°C	∞ (at least 5 minutes)	

37,5 μL of QMN Beads were added to the product of the previous reaction and, after a 5-minutes incubation, placed on a magnet stand. Once the beads had fully migrated, the supernatant was transferred to a new tube, to which 65 μL of QMN Beads were added and

placed on a magnet stand until the beads had fully migrated. The supernatant was discarded, and two washes with 80% ethanol were performed. After completely removing any residual ethanol and air-drying the beads, the DNA was eluted from the beads by adding 17 μL of nuclease-free water, which was then transferred to a new tube.

Libraries concentration was measured with a High Sensitivity DNA Kit on an Agilent TapeStation system by mixing 2 μL of sample with 2 μL of High Sensitivity D1000 Sample Buffer (Agilent). Barcoded cDNA libraries were pooled to a final concentration of 4 nM, and the concentration was verified again using the same Agilent system, through a High Sensitivity D1000 ScreenTape device (Agilent). The samples were sequenced on the NextSeq 500 (Illumina, San Diego, CA) with 75-bp single-end reads. To do that, 5 μL of the combined pool 4 nM were mixed with 5 μL of 0,2 N NaOH. The sample, which was at this time point diluted to 2 nM, was incubated for 5 minutes at room temperature to allow the denaturation and then was added of 5 μL of 200 mM TrisCl (pH 7). 985 μL of HT1 Hybridization Buffer were added to 15 μL of the previous product to achieve a concentration of 20 pM. The sample was diluted again to 1,2 pM in HT1 Hybridization Buffer and loaded onto the NextSeq reagent cartridge in sample position #10.

Statistical analysis

Analysis was conducted in R version 4.4.0 (2024-04-24 ucrt) – “Puppy Cup”. Clustering of samples was assessed through Principal Component Analysis (PCA). Differentially expressed miRNAs were visualized with Volcano plots created using the EnhancedVolcano package.⁸⁴ The binary classification performance of miRNAs was assessed using Receiver Operating Characteristic (ROC) curves from the pROC package.⁸⁵ A p-value of 0.05 was deemed statistically significant for individual comparisons, while the Benjamini-Hochberg (FDR) adjusted p-value was applied for multiple comparisons.⁸⁶

3.3 RESULTS

Tumor Epigenetics

Discovery phase: obese EC vs obese non-cancer patients

miRNA expression profile was initially assessed between obese women, comparing 15 patients from the cohort of EC patients and 9 from the cohort of non-cancer patients, for a total of 24 samples. Both groups had comparable BMI values (BMI = 36.1 in EC patients and 38.2 in non-cancer patients), as well as similar rates of hypertension and type-2 diabetes; on the other hand, they differed for mean age at diagnosis and menopausal status. Demographic and clinical characteristics of the obese women included in the Discovery phase of the “Tumor Epigenetics” study are shown in Table 1.

Table 1. Demographic and clinical characteristics of the obese women included in the Discovery phase of the “Tumor Epigenetics” study.

Variable	Ob ⁺ patients (N=24)		P-value
	EC ⁺ /Ob ⁺ N=15 (62.5%)	EC ⁻ /Ob ⁺ N=9 (37.5%)	
Age at diagnosis mean (±sd)	61.4 (±10.73)	49.22 (±6.70)	0.006
Age Group N (%)	<50 y	2 (13.3)	5 (55.6)
	≥50 y	13 (86.7)	4 (44.4)
BMI mean (±sd)	36.1 (±7.6)	38.2 (±5.1)	0.47
Menopause N (%)	13 (86.7)	4 (44)	0.03
Hypertension N (%)	11 (73.3)	7 (77.8)	0.81
Type-2 diabetes (%)	4 (26.7)	2 (22)	0.81

EC: Endometrial Cancer; Ob: obesity; sd: standard deviation; N: number of patients; y: years; BMI: body mass index.

Figure 8 illustrates the miRNAs expression in the cohort of samples through PCA, volcano plot and unsupervised heatmap. As shown in the PCA (Figure 8A), miRNA expression differed between samples derived from tumor tissue and those from healthy tissue, forming two distinct clusters.

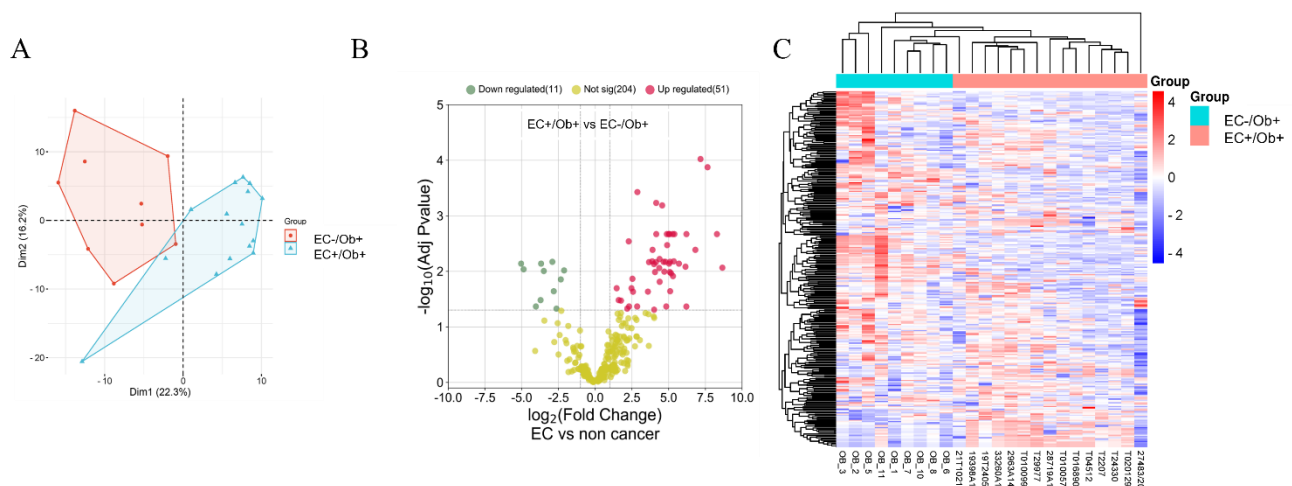


Figure 8: miRNA expression in the 24 samples analysed via the TaqMan Low density array. A) Principal component analysis; (B) Volcano plot showing the relationship between fold change and statistical significance. (C) Heatmap: each row represents a miRNA and each column one sample.

The findings showed a significant deregulation of 91 miRNAs ($p < 0.05$), with 62 maintaining statistical significance after adjusting for multiple comparisons (Adj P-val < 0.05), as shown in Table 2. Among these miRNAs, 51 were up-regulated and 11 were down-regulated in EC⁺/Ob⁺ compared to EC⁻/Ob⁺ samples.

Table 2. Differential miRNA expression in obese EC (EC⁺/Ob⁺) vs obese healthy women (EC⁻/Ob⁺).

miRNA ID	LogFold Change	P-value	Adj P-val	Deregulation in EC ⁺ /Ob ⁺
----------	----------------	---------	-----------	--

hsa-miR-96-5p	7.17	0.000	0.000	↑
hsa-miR-340-5p	7.65	0.000	0.000	↑
hsa-miR-425-5p	2.87	0.000	0.000	↑
hsa-miR-301a-3p	4.15	0.000	0.001	↑
hsa-miR-422a	4.56	0.000	0.001	↑
hsa-miR-335-5p	8.29	0.000	0.002	↑
hsa-miR-106b-5p	5.01	0.000	0.002	↑
hsa-miR-576-5p	5.06	0.000	0.002	↑
hsa-miR-362-3p	6.21	0.000	0.002	↑
hsa-miR-301b-3p	4.16	0.000	0.002	↑
hsa-miR-142-3p	5.27	0.000	0.002	↑
hsa-miR-28-5p	5.39	0.000	0.002	↑
hsa-miR-95-3p	4.88	0.000	0.002	↑
hsa-miR-21-5p	2.28	0.000	0.003	↑
hsa-miR-218-5p	4.90	0.000	0.003	↑
hsa-miR-183-5p	6.82	0.000	0.004	↑
hsa-miR-873-5p	3.91	0.000	0.004	↑
hsa-miR-365a-3p	4.38	0.000	0.006	↑
hsa-miR-136-5p	5.35	0.000	0.007	↑
hsa-miR-103a-2-5p	3.88	0.000	0.007	↑
hsa-miR-451a	-2.91	0.001	0.007	↓
hsa-miR-219a-5p	4.66	0.001	0.007	↑
hsa-miR-106a-p	4.78	0.001	0.007	↑
hsa-miR-140-5p	5.09	0.001	0.007	↑
hsa-miR-545-3p	3.66	0.001	0.007	↑
hsa-miR-193a-3p	4.13	0.001	0.007	↑
hsa-miR-331-3p	5.03	0.001	0.007	↑
hsa-miR-325	-3.68	0.001	0.007	↓
hsa-miR-486-5p	-5.04	0.001	0.007	↓
hsa-miR-551b-3p	5.70	0.001	0.007	↑
hsa-miR-182-5p	4.00	0.001	0.007	↑
hsa-miR-454-3p	6.15	0.001	0.008	↑
hsa-miR-141-3p	8.66	0.001	0.009	↑

hsa-miR-582-5p	4.36	0.001	0.009	↑
hsa-miR-105-5p	-4.87	0.001	0.009	↓
hsa-miR-448	-2.12	0.001	0.010	↓
hsa-miR-516b-5p	-3.50	0.001	0.010	↓
hsa-miR-590-5p	4.71	0.001	0.010	↑
hsa-miR-133a-3p	5.08	0.001	0.010	↑
hsa-miR-135a-5p	4.07	0.001	0.010	↑
hsa-miR-27a-3p	5.16	0.002	0.011	↑
hsa-miR-18a-5p	5.30	0.002	0.012	↑
hsa-miR-200b-3p	2.54	0.002	0.014	↑
hsa-miR-224-5p	-2.34	0.002	0.014	↓
hsa-miR-192-5p	4.39	0.003	0.015	↑
hsa-miR-429	2.47	0.003	0.020	↑
hsa-miR-93-5p	1.46	0.003	0.020	↑
hsa-miR-501-3p	-2.82	0.004	0.023	↓
hsa-miR-9-5p	5.10	0.004	0.023	↑
hsa-miR-32-5p	3.59	0.004	0.023	↑
hsa-miR-331-5p	2.58	0.004	0.023	↑
hsa-miR-654-5p	-3.71	0.006	0.033	↓
hsa-miR-455-5p	1.60	0.006	0.033	↑
hsa-miR-181c-5p	1.76	0.007	0.034	↑
hsa-miR-449a	4.84	0.009	0.043	↑
hsa-miR-500a-5p	2.31	0.009	0.043	↑
hsa-miR-135b-5p	2.86	0.009	0.043	↑
hsa-miR-431-5p	-4.03	0.009	0.043	↓
hsa-miR-197-3p	6.21	0.009	0.043	↑
hsa-miR-338-3p	2.18	0.010	0.047	↑
hsa-miR-129-2-3p	-2.63	0.010	0.047	↓
hsa-miR-133b	4.01	0.011	0.049	↑

EC: endometrial cancer; Ob: obesity; ↑: up-regulated in EC⁺/Ob⁺; ↓ down-regulated in EC⁺/Ob⁺.

Of these deregulated miRNAs, pathway-enriched analysis was performed using the miRNet tool (Reactome database).⁸⁷ Top 25 pathways, with their P-values and Adj P-val are shown in Table 3.

Table 3. Pathway-enriched analysis of deregulated miRNAs in EC⁺/Ob⁺ vs EC⁻/Ob⁺ analysis.

Pathway	P-value	Adj P-val
Loss of Function of SMAD2/3 in Cancer	0.000	0.001
SMAD2/3 MH2 Domain Mutants in Cancer	0.000	0.001
Signaling by TGF-beta Receptor Complex in Cancer	0.000	0.001
TGFBR1 KD Mutants in Cancer	0.001	0.025
Loss of Function of TGFBR1 in Cancer	0.001	0.025
TGF-beta receptor signaling activates SMADs	0.002	0.032
Generic Transcription Pathway	0.003	0.048
Signaling by Activin	0.004	0.048
Signaling by NOTCH	0.004	0.048
Nucleotide-binding domain, leucine rich repeat containing receptor (NLR) signaling pathways	0.005	0.048
Inflammasomes	0.008	0.069
Signaling by NODAL	0.009	0.079
Downregulation of SMAD2/3:SMAD4 transcriptional activity	0.013	0.09
Glucagon-like Peptide-1 (GLP1) regulates insulin secretion	0.013	0.09
Pre-NOTCH Expression and Processing	0.015	0.094
Antigen Presentation: Folding, assembly and peptide loading of class I MHC	0.015	0.094
Syndecan interactions	0.016	0.095
Downregulation of TGF-beta receptor signaling	0.017	0.097
Signaling by TGF-beta Receptor Complex	0.019	0.098
SMAD2/SMAD3:SMAD4 heterotrimer regulates transcription	0.020	0.1
Transcriptional regulation of pluripotent stem cells	0.023	0.109
Gene Expression	0.030	0.129
Peptide chain elongation	0.031	0.129
Transport to the Golgi and subsequent modification	0.032	0.129
MHC class II antigen presentation	0.032	0.129

EC: endometrial cancer; Ob: obesity.

Discovery phase: obese vs non-obese EC

Then, miRNAs expression was evaluated comparing obese and non-obese EC patients, for a total of 40 samples (25 EC⁺/Ob⁻ and 15 EC⁺/Ob⁺). Characteristics were similar between the two groups, except for BMI, as shown in Table 4.

Table 4. Demographic and clinical characteristics of the EC patients included in the Discovery phase of the “Tumor Epigenetics” study.

Variable	EC patients (N=40)		P-value
	EC ⁺ /Ob ⁻ N=25 (62.5%)	EC ⁺ /Ob ⁺ N=15 (37.5%)	
Age at diagnosis mean (±sd)	65.64 (±10.05)	61.4 (±10.73)	0.22
Age Group N (%)	<50 y	3 (12)	0.90
	≥50 y	22 (88)	

BMI mean (\pm sd)		24.9 (\pm 3.0)	36.1 (\pm 7.6)	<0.001
Menopause N (%)		22 (88)	13 (86.7)	0.90
Hypertension N (%)		13 (52)	11 (73.3)	0.18
Type-2 diabetes N (%)		2 (8)	4 (26.7)	0.11
Histotype N (%)	Endometrioid	17 (48)	13 (86.7)	0.29
	De-differentiated	5 (20)	2 (13.3)	
	Serous	3 (12)	0	
ESMO risk N (%)	Low	2 (8)	2 (13.3)	0.11
	Intermediate	4 (16)	0	
	High-intermediate	7 (28)	9 (60)	
	High	12 (48)	4 (26.7)	
Grade N (%)	Low	12 (48)	11 (73.3)	0.12
	High	13 (52)	4 (26.7)	
FIGO stage (2014) N (%)	I	13 (52)	11 (73.3)	0.20
	II	2 (8)	2 (13.3)	
	III	10 (40)	2 (13.3)	
TCGA classification N (%)	POLE	1 (4)	1 (3)	0.31
	NSMP	12 (48)	11 (73.3)	
	MSI	5 (20)	2 (13.3)	
	P53	7 (28)	1 (3)	

EC: endometrial cancer; Ob: obesity; sd: standard deviation; N: number of patients; y: years; BMI: body mass index; ESMO: European Society for Medical Oncology; FIGO: International Federation of Gynecology and Obstetrics; TCGA: The Cancer Genome Atlas.

Figure 9 shows the PCA of the 40 samples analysed via the TaqMan Low density array.

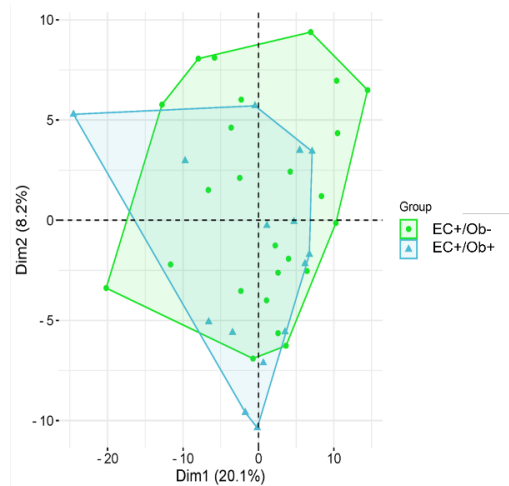


Figure 9: PCA showing miRNAs expression in 40 samples (25 EC⁺/Ob⁻ and 15 EC⁺/Ob⁺).

20 miRNAs resulted deregulated in obese EC compared to non-obese patients, with $p < 0.05$; in particular, all of them resulted up-regulated in obese EC patients. However, none of the identified miRNAs had a Adj P-val < 0.05 , so the analysis was conducted based on the unadjusted P-values. Significantly deregulated miRNAs are summarized in Table 5.

Table 5. Differential miRNA expression in obese (EC⁺/Ob⁺) vs non-obese EC (EC⁺/Ob⁻).

MiRNA ID	LogFold Change	P-value	Deregulation in EC ⁺ /Ob ⁺
hsa-miR-2110	1.40	0.002	↑
hsa-miR-137	4.50	0.004	↑
hsa-miR-449a	4.52	0.004	↑
hsa-miR-422a	2.45	0.006	↑
hsa-miR-136-5p	3.31	0.009	↑
hsa-miR-449b-5p	3.00	0.009	↑
hsa-miR-199a-5p	2.15	0.016	↑
hsa-miR-548b-3p	4.29	0.022	↑
hsa-miR-455-5p	0.98	0.026	↑
hsa-miR-548d-5p	0.93	0.026	↑
hsa-miR-525-3p	1.98	0.027	↑
hsa-miR-488-3p	3.15	0.030	↑
hsa-miR-885-5p	2.09	0.032	↑
hsa-miR-193a-3p	2.70	0.032	↑
hsa-miR-425-5p	0.83	0.033	↑
hsa-miR-551b-3p	3.04	0.041	↑
hsa-miR-155-5p	0.89	0.041	↑
hsa-miR-451a	1.33	0.043	↑
hsa-miR-23a-3p	2.25	0.044	↑
hsa-miR-448	1.04	0.046	↑

EC: endometrial cancer; Ob: obesity ↑: up-regulated in EC⁺/Ob⁺.

Of these deregulated miRNAs, pathway-enriched analysis was performed using the miRNet tool (Reactome database).⁸⁷ Top 25 pathways, with their P-values and Adj P-val are shown in Table 6.

Table 6. Pathway-enriched analysis of deregulated miRNAs in EC⁺/Ob⁻ vs EC⁺/Ob⁺ analysis.

Pathway	P-value	Adj P-val
Signaling by NOTCH	0.000	0.000
Fc epsilon receptor (FCERI) signaling	0.000	0.000
Pre-NOTCH Transcription and Translation	0.000	0.000
Pre-NOTCH Expression and Processing	0.000	0.000
DAP12 signaling	0.000	0.000
Oncogene Induced Senescence	0.000	0.000
Diseases of signal transduction	0.000	0.000
DAP12 interactions	0.000	0.000
Signal Transduction	0.000	0.000
Platelet activation, signaling and aggregation	0.000	0.001
Signaling by SCF-KIT	0.000	0.001
Signaling by NGF	0.000	0.001
Signaling by NOTCH1 PEST Domain Mutants in cancer	0.000	0.001
Signaling by NOTCH in cancer	0.000	0.001
Constitutive Signaling by NOTCH1 PEST Domain Mutants	0.000	0.001

Signaling by NOTCH1 HD+PEST Domain Mutants in cancer	0.000	0.001
Constitutive Signaling by NOTCH HD+PEST Domain Mutants	0.000	0.001
VEGFA-VEGFR2 Pathway	0.000	0.001
Signaling by VEGF	0.000	0.001
Signaling by EGFR	0.000	0.001
VEGFR2 mediated vascular permeability	0.000	0.001
Signaling by Wnt	0.000	0.001
Signaling by NOTCH1	0.000	0.001
Beta-catenin independent WNT signaling	0.000	0.001
Signaling by PDGF	0.000	0.001
EC: endometrial cancer; Ob: obesity.		

9 miRNAs were deregulated in both the analysis (EC⁺/Ob⁺ vs EC⁻/Ob⁺ and EC⁺/Ob⁺ vs EC⁺/Ob⁻). Hsa-miR-449a, hsa-miR-422a, hsa-miR-136-5p, hsa-miR-455-5p, hsa-miR-193a-3p, hsa-miR-425-5p and hsa-miR-551b-3p were up-regulated in obese EC, both when compared to non-obese EC and to obese healthy women. Instead, hsa-miR-451a was down-regulated in obese EC compared to obese controls, while it was up-regulated in obese EC compared to non-obese EC.

Validation phase: obese vs non-obese EC

A total of 84 EC samples (55 EC⁺/Ob⁻ and 29 EC⁺/Ob⁺) enrolled at Azienda Ospedaliero-Universitaria of Bologna were analysed, 40 of which were already analysed in the Discovery phase. Demographic and clinical characteristics of the EC patients included in the Validation phase of the “Tumor Epigenetics” study are shown in Table 7. Except for BMI, EC patients in the two groups also differed in terms of hypertension and type-2 diabetes status.

Variable	EC patients (N=84)		P-value	
	EC ⁺ /Ob ⁻ N=55 (65%)	EC ⁺ /Ob ⁺ N=29 (35%)		
Age at diagnosis mean (±sd)	64.98 (±10.06)	62.62 (±9.68)	0.3	
Age Group N (%)	<50 y	4 (7)	0.62	
	≥50 y	51 (93)		26 (90)
BMI mean (±sd)	24.7 (±2.9)	36.3 (±6.5)	<0.001	
Menopause N (%)	49 (89)	25 (86)	0.69	
Hypertension N (%)	24 (44)	22 (76)	0.005	
Type-2 diabetes N (%)	4 (7)	7 (24)	0.04	
Histotype N (%)	Endometrioid	44 (80)	0.09	
	De-differentiated	4 (7)		4 (14)
	Serous	7 (13)		0
ESMO risk N (%)	Low	10 (18.2)	0.11	
	Intermediate	8 (14.5)		1 (3.4)
	High-intermediate	17 (30.9)		16 (55.2)

	High	20 (36.4)	7 (24.1)	
Grade N (%)	Low	35 (64)	21 (72)	0.57
	High	20 (36)	8 (28)	
FIGO stage (2014) N (%)	I	29 (52.7)	22 (75.9)	0.11
	II	11 (20.0)	3 (10.3)	
	III	15 (27.3)	4 (13.8)	
TCGA classification N (%)	POLE	1 (2)	1 (3)	0.24
	NSMP	23 (42)	17 (59)	
	MSI	22 (40)	10 (35)	
	P53	9 (16)	1 (3)	

EC: endometrial cancer; Ob: obesity; sd: standard deviation; N: number of patients; y: years; BMI: body mass index; ESMO: European Society for Medical Oncology; FIGO: International Federation of Gynecology and Obstetrics; TCGA: The Cancer Genome Atlas.

Three of the topmost deregulated miRNAs between obese and non-obese EC patients were validated in a larger cohort made up of 84 patients. Results are shown in Figure 10: in the validation cohort from IRCCS, Azienda Ospedaliero-Universitaria of Bologna, only hsa-miR-449a maintained the statistical significance ($p = 0.012$).

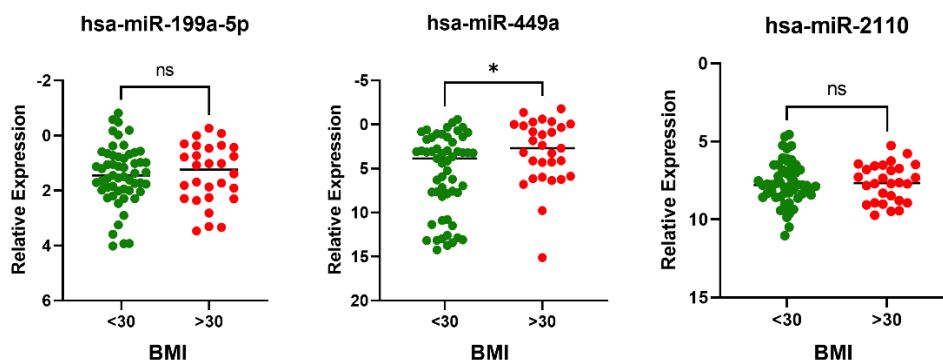


Figure 10: Validation of three of the most deregulated miRNAs in the Discovery phase in 84 patients, stratified according to BMI. *: $p < 0.05$; ns: non-significant.

To increase the statistical power of the analysis, the three miRNAs were validated in a larger and independent cohort from TCGA database, made up of 384 patients (149 EC⁺/Ob⁻ and 235 EC⁺/Ob⁺). Moreover, hsa-miR-449b-5p was also investigated because, together with hsa-miR-449a, it's part of the same cluster and the two miRNAs are co-transcribed. As shown in Figure 11, hsa-miR-199a-5p, hsa-miR-449a and hsa-miR-449b-5p were found to be up-regulated in obese EC patients, respectively with $p = 0.018$, $p = 0.004$ and $p = 0.0008$, while hsa-miR-2110 resulted not significant. For this reason, hsa-miR-2110 was excluded from further analysis.

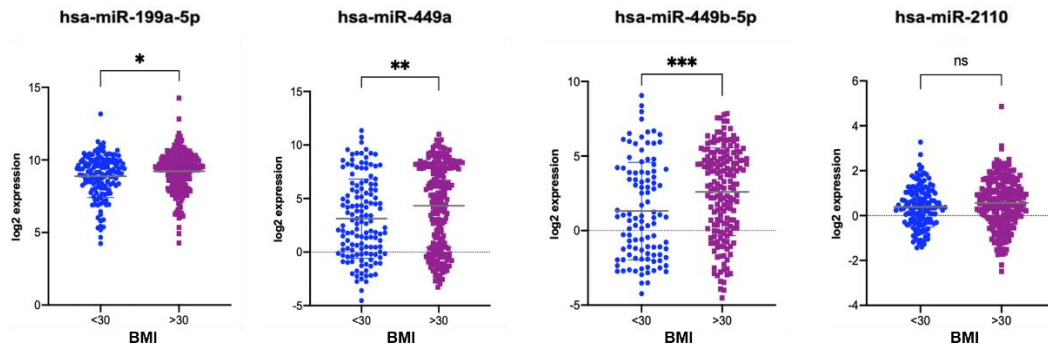


Figure 11: Validation of the three deregulated miRNAs in the TCGA cohort. miRNA levels are expressed as log₂. *: $p < 0.05$; **: $p < 0.01$; ***: $p < 0.001$; ns: non-significant.

Additionally, we further stratified the TCGA patients into normal weight (N; BMI < 25, $n = 83$), overweight (OW; $25 \leq \text{BMI} < 30$, $n = 67$), and obese (OB; BMI ≥ 30 , $n = 234$). We observed a statistically significant increase in hsa-miR-199a-5p, hsa-miR-449a and hsa-miR-449b-5p expression among these three groups. These findings are shown in Figure 12.

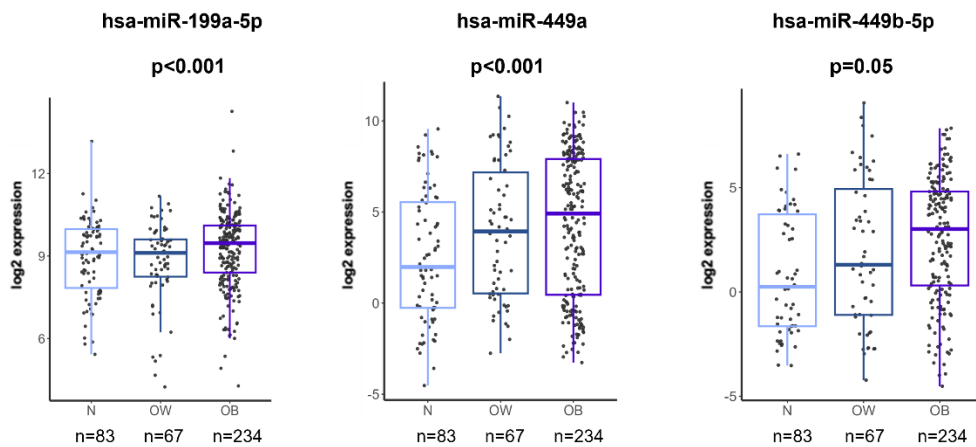


Figure 12: Expression levels of hsa-miR-199a, hsa-miR-449a, and hsa-miR-449b-5p in the TCGA cohort, stratifying the patients as normal weight, overweight and obese. miRNA levels are expressed as log₂.

Target prediction

The potential targets of hsa-miR-449a, hsa-miR-449b-5p and hsa-miR-199a-5p were predicted using TargetScan Human 8.0. A total of 247 genes were retrieved, including 65 mRNA targets for hsa-miR-449a, 182 for hsa-miR-449b, and 478 genes for hsa-miR-199a-5p. These genes were analysed in 514 EC patients in the TCGA cohort (209 EC⁺/Ob⁻ and 305 EC⁺/Ob⁺). This analysis identified 24 and 61 genes, respectively, for hsa-miR-449a/449b and hsa-miR-199a-5p, which were significantly deregulated between the two subgroups, as shown in Table 8.

Table 8. Expression of the predicted target genes for hsa-miR-449a/miR-449b and hsa-miR-199a in the TGCA cohort.		
Gene	P-value	Deregulation in EC ⁺ /Ob ⁺
hsa-miR-499a/miR-499b-5p		

AAGAB	0.021	↓
ADCY5	0.025	↓
ADIPOR2	0.050	↓
COL12A1	0.029	↑
DNAJB1	0.022	↓
EML5	0.042	↑
GPR158	0.013	↓
GRM7	0.021	↑
HECW2	0.019	↓
IQGAP3	0.044	↓
MBD6	0.001	↑
MGAT4A	0.001	↓
MLLT3	0.038	↑
PGM1	0.048	↓
PKP4	0.044	↑
PPP3R1	0.007	↓
RAB11FIP4	0.003	↓
RFX3	0.001	↑
SDK2	0.017	↑
SLC12A2	0.003	↑
SLC7A2	0.013	↓
SLC8A1	0.018	↑
TAF5	0.013	↓
TRAFD1	0.032	↓
hsa-miR-199a-5p		
ABTB2	0.001	↓
ACVR2A	0.044	↓
ADAMTSL3	0.049	↑
AKAP1	0.012	↓
APPB2	0.039	↓
ARHGAP19	0.029	↓
ARHGAP29	0.009	↓
ASRGL1	0.004	↑
CBX5	0.017	↓
CCDC43	0.043	↓
CDKN2AIP	0.035	↓
CEP72	0.040	↓
CHN2	0.044	↑
CLTC	0.021	↓
CTNNA2	0.004	↑
DLC1	0.001	↑
E2F3	0.027	↓
EXOC8	0.014	↓
FBXO9	0.044	↓
FIGN	0.007	↓
FLRT3	0.040	↓
FPGS	0.003	↑
GIT1	0.015	↓

GPR89A	0.049	↓
HSPA4	0.046	↓
KIAA0226	0.029	↓
KLHL6	0.011	↑
KPNA4	0.006	↓
LAMC1	0.019	↓
LASP1	0.040	↓
LRP4	0.039	↓
MAP2	0.049	↓
MCFD2	0.008	↓
MUC21	0.027	↑
NAA40	0.046	↑
NCKAP1	0.031	↓
NFYA	0.022	↓
NUFIP2	0.023	↓
PCYOX1	0.004	↓
POGK	0.003	↓
PREPL	0.047	↓
PRPF40A	0.008	↓
RBM24	0.000	↑
RFFL	0.025	↓
RFX3	0.001	↑
RRP15	0.023	↓
SACS	0.027	↓
SAR1A	0.013	↓
SAT1	0.004	↑
SLC24A2	0.009	↑
SLC36A4	0.015	↓
SRL	0.023	↓
STRADB	0.007	↓
STRN	0.017	↓
TERF2	0.009	↓
UNG	0.034	↓
USP37	0.008	↓
VPS26A	0.043	↓
WBP11	0.046	↓
ZNF516	0.000	↑
ZNF528	0.012	↑

EC: endometrial cancer; Ob: obesity; TCGA: The Cancer Genome Atlas; ↑: up-regulated in EC⁺/Ob⁺; ↓ down-regulated in EC⁺/Ob⁺.

Considering the inverse relationship between miRNA and mRNA expression, where high miRNA levels indicate a downregulation of their target mRNAs and low miRNA levels lead to target upregulation, we identified 60 genes with reduced expression in obese EC patients. Of these, 14 were potentially regulated by hsa-miR-449a/449b, and 46 by hsa-miR-199a-5p.

Functional enrichment analysis was carried out through ToppGene and EnrichR, applying a Benjamini and Hochberg FDR threshold of <0.05. The gene ontology (GO) terms associated with hsa-miR-449a/449b targets are shown in Table 9; notably, most of the key molecular functions identified are involved in obesity regulation. In contrast, no statistically significant GO terms, after FDR correction, were found for hsa-miR-199a-5p.

Table 9. Gene ontology of the hsa-miR-499a/499b targets with lower expression in obese and non-obese EC patients.				
Category	ID	Name	P-value	FDR
GO: MF	GO: 0005516	Calmodulin binding	0.001	0.031
GO: MF	GO: 0070856	Myosin VI light chain binding	0.001	0.031
GO: MF	GO: 0086038	Calcium: sodium antiporter activity involved in regulation of cardiac muscle cell membrane potential	0.001	0.031
GO: MF	GO: 0099580	Ion antiporter activity involved in regulation of postsynaptic membrane potential	0.001	0.031
GO: MF	GO: 0055100	Adiponectin binding	0.002	0.031
GO: MF	GO: 0007453	Alanine-glyoxylate transaminase activity	0.002	0.031
GO: MF	GO: 0070853	Myosin VI binding	0.002	0.031
GO: MF	GO: 1905060	Calcium: cation antiporter activity involved in regulation of postsynaptic cytosolic calcium ion concentration	0.002	0.031
GO: MF	GO: 0097003	Adipokinetic hormone receptor activity	0.003	0.031
GO: MF	GO: 0007454	Alpha-1,3-mannosylglycoprotein 4-beta-N-acetylglucosaminyltransferase activity	.003	0.031
GO: MF	GO: 0008597	Calcium-dependent protein serine/threonine phosphatase regulator activity	0.004	0.031
GO: MF	GO: 0008294	Calcium- and calmodulin- responsive adenylate cyclase activity	0.004	0.031
GO: MF	GO: 0004614	Phosphoglucomutase activity	0.004	0.031
GO: MF	GO: 0032027	Myosin light chain binding	0.006	0.047
GO: CC	GO: 0042383	Sarcolemma	0.000	0.028

EC: endometrial cancer; GO: gene ontology; MF: molecular function, CC: cellular component; FDR: False Discovery Rate.

Association between identified miRNAs and prognostic factors in the TCGA cohort

The association between hsa-miR-199a-5p, hsa-miR-449a and hsa-miR-449b-5p expression and prognostic factors was evaluated in the TCGA cohort. All the miRNAs resulted significantly associated with tumor grade and histological subtype. In particular, for all the three miRNAs, higher levels were detectable in endometrioid endometrial adenocarcinoma tumors (hsa-miR-199a, $p = 0.016$; hsa-miR-449a, $p = 2.5 \times 10^{-8}$; hsa-miR-449b-5p, $p = 4.2 \times 10^{-6}$). Hsa-miR-199a-5p and hsa-miR-449a were found to be higher in low grade (G1) tumors, respectively with $p = 0.032$ and

$p = 3.9 \times 10^{-6}$, while hsa-miR-449b-5p was up-regulated in G2 ($p = 0.0009$). Scatter plots are shown in Figure 13.

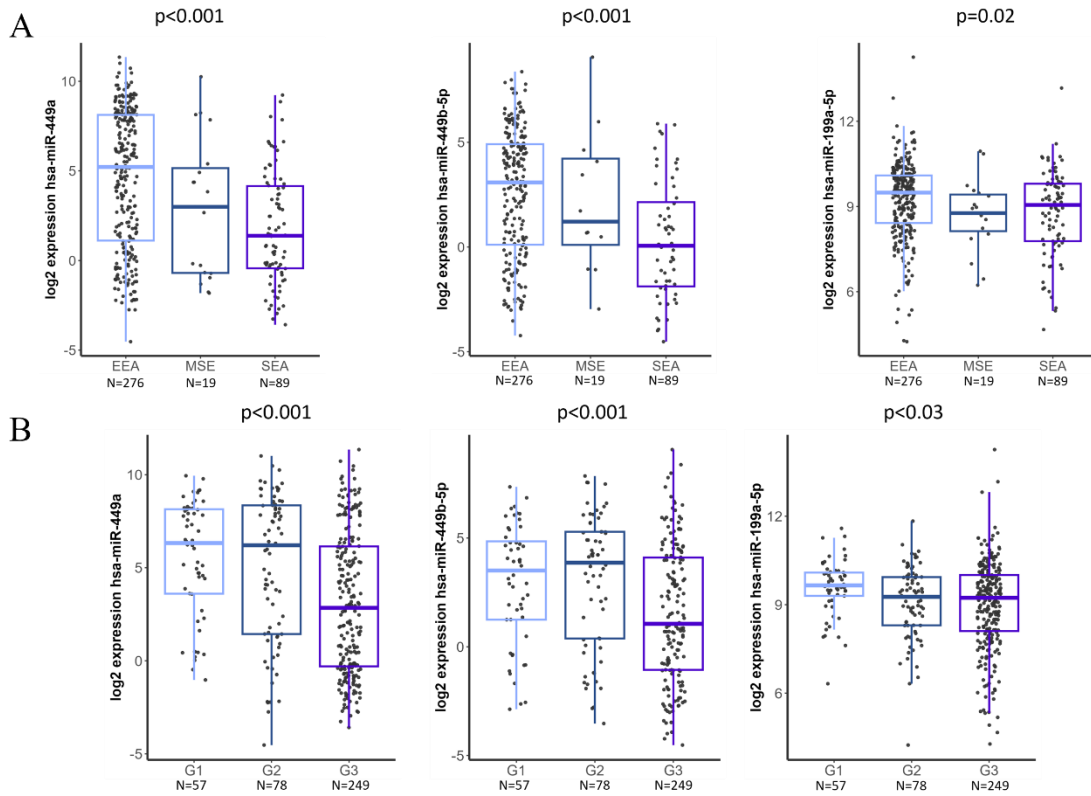


Figure 13: Scatter plot regarding miRNAs expression in A) different histological subtype and B) different tumor grade. EEA: endometrioid endometrial adenocarcinoma; MSE: mixed serous and endometrioid; SEA: serous endometrial adenocarcinoma.

Moreover, correlation between deregulated miRNAs and OS was evaluated through Kaplan-Meier curves (Figure 14). Only hsa-miR-449a showed a significant correlation with OS ($p = 0.0069$), indicating that patients with higher levels of expression experienced longer survival.

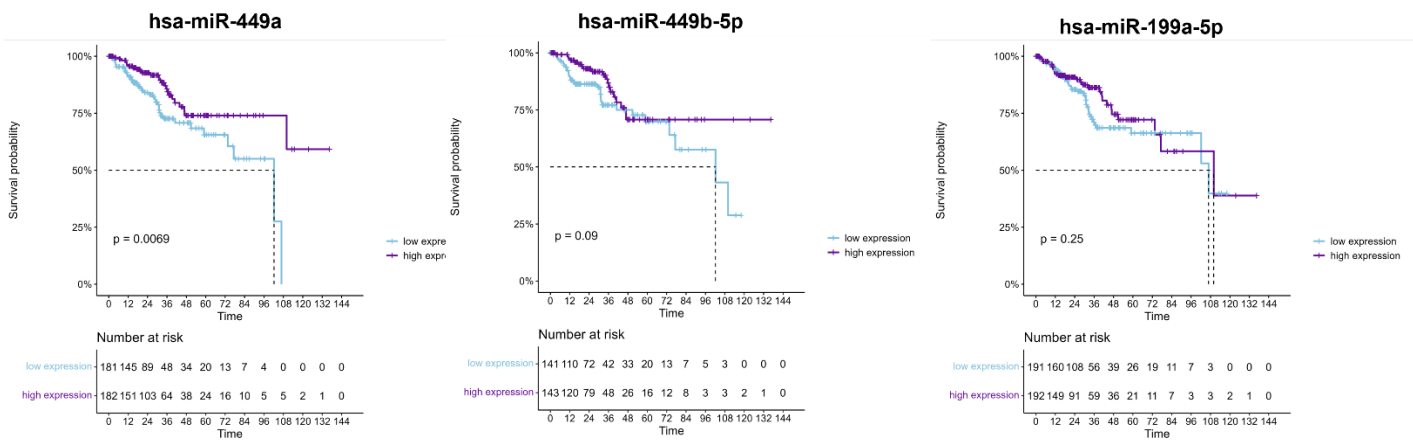


Figure 14: Kaplan-Meier curves showing correlation between miRNAs expression and OS.

Liquid Biopsy Epigenetics

A total of 30 EC samples (15 EC⁺/Ob⁻ and 15 EC⁺/Ob⁺) and 10 EC⁻/Ob⁺ were analysed. For the obese patients, both groups had comparable BMI values (BMI = 41.69 in EC patients and 39.54 in non-cancer patients), as well as similar rates of hypertension and type-2 diabetes; instead, the two subgroups differed for mean age and menopausal status. However, concerning EC, the two patients groups showed significant statistical differences in hypertension, while all other clinical parameters were similar. Characteristics of the patients are shown in Tables 10 and 11.

Table 10. Demographic and clinical characteristics of the obese women included in “Liquid Biopsy Epigenetics” study.

Variable		EC ⁺ /Ob ⁺ (N=15)	EC ⁻ /Ob ⁺ (N=10)	P-value
Age at diagnosis mean (±sd)		64.60 (±9.58)	48.30 (±6.96)	<0.001
Age Group N (%)	<50 y	0	6 (60)	<0.001
	≥50 y	15 (100)	4 (40)	
BMI mean (±sd)		41.69 (±7.7)	39.54 (±6.4)	0.47
Menopause N (%)		15 (100)	5 (50)	0.002
Hypertension N (%)		13 (86.7)	7 (70)	0.31
Type-2 diabetes (%)		1 (10)	2 (20)	0.31

EC: endometrial cancer; Ob: obesity; sd: standard deviation; N: number of patients; y: years; BMI: body mass index.

Table 11. Demographic and clinical characteristics of the EC patients included in “Liquid Biopsy Epigenetics” study.

Variable		EC patients (N=30)		P-value
		EC ⁺ /Ob ⁻ N=15 (50%)	EC ⁺ /Ob ⁺ N=15 (50%)	
Age at diagnosis mean (±sd)		62.60 (±11.59)	64.60 (±9.58)	0.61
Age Group N (%)	<50 y	2 (13.3)	0	0.14
	≥50 y	13 (86.7)	15 (100)	
BMI mean (±sd)		24.4 (±2.7)	41.7 (±7.7)	<0.001
Menopause N (%)		14 (93.3)	15 (100)	0.31
Hypertension N (%)		7 (46.7)	13 (86.7)	0.02
Type-2 diabetes N (%)		1 (6.7)	1 (6.7)	1.0
LVI N (%)	Substantial	4 (26.7)	4 (26.7)	1.0
	Absent/Focal	11 (73.3)	11 (73.3)	
Histotype N (%)	Endometrioid	12 (80)	15 (100)	0.19
	De-differentiated	1 (6.7)	0	
	Serous	2 (13.3)	0	
Grade N (%)	Low	8 (53.3)	12 (80)	0.12
	High	7 (46.7)	3 (20)	
FIGO stage (2014) N (%)	I	13 (86.7)	13 (86.7)	1
	II	1 (6.7)	1 (6.7)	
	III	1 (6.7)	1 (6.7)	
TCGA classification N (%)	POLE	0	1 (6.7)	0.22
	NSMP	4 (26.7)	8 (53.3)	
	MSI	7 (46.7)	5 (33.3)	
	P53	4 (26.7)	1 (6.7)	

EC: endometrial cancer; Ob: obesity; sd: standard deviation; N: number of patients; y: years; BMI: body mass index; LVI: lymphovascular invasion FIGO: International Federation of Gynecology and Obstetrics; TCGA: The Cancer Genome Atlas.

miRNAs expression in the three different categories of samples (EC^+/Ob^+ , EC^+/Ob^- and EC^-/Ob^+) is shown in Figure 15. As visible, PCA highlighted lack of defined clustering, suggesting that miRNA expression was not particularly different among the three groups.

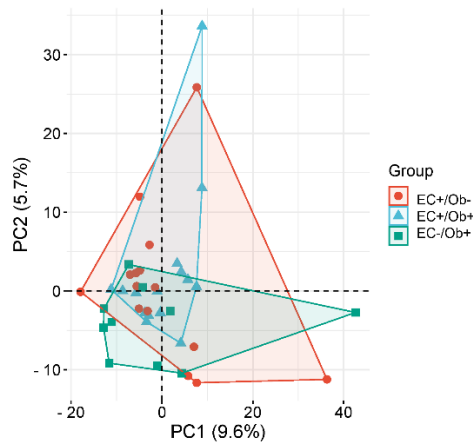


Figure 15: PCA showing miRNAs expression in EC^+/Ob^+ , EC^+/Ob^- and EC^-/Ob^+ .

miRNA analysis: EC vs obese non-cancer patients

miRNA expression profile was firstly assessed between EC (N = 30) and obese non-cancer women (N = 10). 95 miRNAs resulted significantly deregulated ($p < 0.05$) between all EC patients and obese non-cancer individuals, of which 24 showed Adj P-val < 0.05 (Figure 16, Table 12). Of these, 20 were up-regulated and 4 down-regulated in EC group.

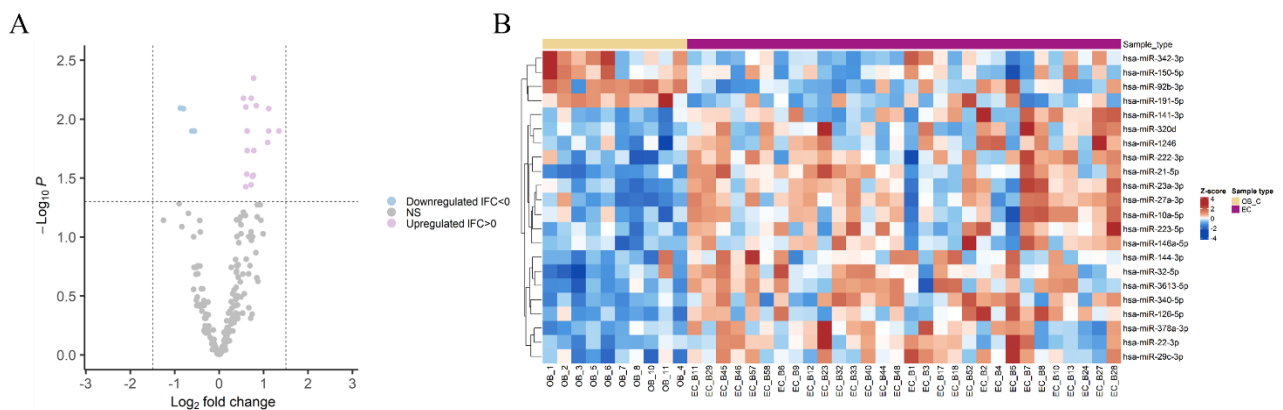


Figure 16: Differentially expressed miRNAs between EC patients and obese non-cancer women in A) Volcano plot showing the relationship between fold change and statistical significance; B) Heatmap: each row represents a miRNA and each column one sample.

Table 12. Differentially expressed miRNAs between EC and obese healthy women.

miRNA ID	LogFold Change	P-value	Adj P-val	Deregulation in EC
hsa-miR-21-5p	0.91	0.000	0.000	↑
hsa-miR-3613-5p	1.15	0.000	0.000	↑
hsa-miR-27a-3p	0.88	0.000	0.001	↑
hsa-miR-23a-3p	0.78	0.000	0.004	↑
hsa-miR-126-5p	0.55	0.000	0.007	↑
hsa-miR-340-5p	0.72	0.000	0.007	↑
hsa-miR-32-5p	0.84	0.000	0.008	↑
hsa-miR-29c-3p	0.60	0.000	0.008	↑
hsa-miR-150-5p	-0.87	0.000	0.008	↓
hsa-miR-191-5p	-0.81	0.000	0.008	↓
hsa-miR-141-3p	1.12	0.000	0.008	↑
hsa-miR-320d	1.12	0.001	0.013	↑
hsa-miR-22-3p	0.63	0.001	0.013	↑
hsa-miR-92b-3p	-0.61	0.001	0.013	↓
hsa-miR-342-3p	-0.56	0.001	0.013	↓
hsa-miR-1290	1.35	0.001	0.013	↑
hsa-miR-1246	1.10	0.001	0.016	↑
hsa-miR-222-3p	0.63	0.001	0.019	↑
hsa-miR-146a-5p	0.78	0.001	0.019	↑
hsa-miR-378a-3p	0.62	0.002	0.029	↑
hsa-miR-223-5p	0.77	0.002	0.030	↑
hsa-miR-10a-5p	0.75	0.002	0.031	↑
hsa-miR-144-3p	0.72	0.003	0.036	↑
hsa-miR-190b-5p	0.60	0.003	0.038	↑

EC: endometrial cancer; ↑: up-regulated in EC; ↓: down-regulated in EC.

miRNAs ability to predict EC

The 20 miRNAs that were found to be up-regulated in cancer patients compared to obese non-cancer controls (Adj P-val < 0.05) were evaluated for their ability to predict EC. Accuracy > 0.7 was considered significant, resulting in 13 out of 20 miRNAs demonstrating a good ability to predict EC (Table 13). ROC curves are shown in Figure 17.

Table 13. miRNAs ability to predict EC.

miRNA	Threshold	Specificity	Sensitivity	Accuracy	NPV	PPV
hsa-miR-21-5p	11.56	0.97	0.90	0.95	0.97	0.90
hsa-miR-3613-5p	6.57	0.93	0.80	0.90	0.93	0.80
hsa-miR-144-3p	8.38	0.90	0.80	0.88	0.93	0.73
hsa-miR-27a-3p	7.23	0.83	0.90	0.85	0.96	0.64
hsa-miR-222-3p	5.70	0.80	0.90	0.83	0.96	0.60
hsa-miR-32-5p	7.07	0.80	0.90	0.83	0.96	0.60
hsa-miR-190b-5p	4.62	0.77	0.90	0.80	0.96	0.56
hsa-miR-340-5p	5.39	0.77	0.90	0.80	0.96	0.56

hsa-miR-29c-3p	9.23	0.83	0.70	0.80	0.89	0.58
hsa-miR-23a-3p	9.10	0.70	1.00	0.78	1.00	0.53
hsa-miR-126-5p	10.88	0.73	0.90	0.78	0.96	0.53
hsa-miR-146a-5p	9.94	0.70	0.90	0.75	0.95	0.50
hsa-miR-10a-5p	7.21	0.70	0.80	0.73	0.91	0.47
EC: endometrial cancer; NPV: negative predictive value; PPV: positive predictive value.						

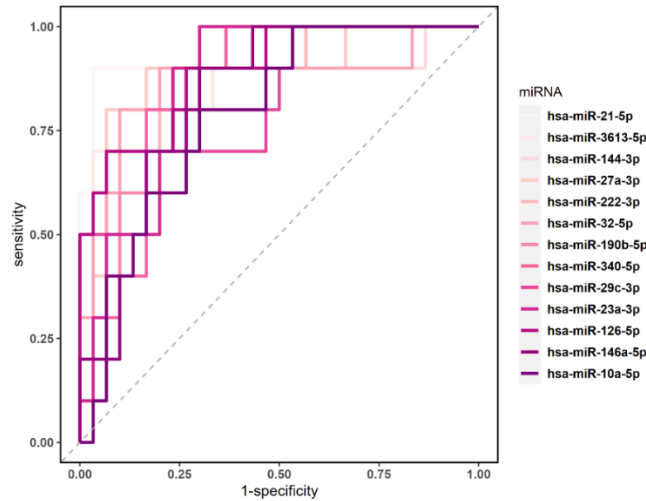


Figure 17: ROC curves indicating the ability of predicting EC.

miRNA analysis: obese EC vs obese non-cancer patients

After that, only obese EC patients (N = 15) were considered for miRNA analysis, and they were compared with obese non-cancer women. 56 miRNAs were found to be significantly deregulated between the two groups, 17 up-regulated and 7 down-regulated in obese EC patients, showing $p < 0.05$; among them, 24 showed a Adj P-val < 0.05 and they are represented in Figure 18 and Table 14.

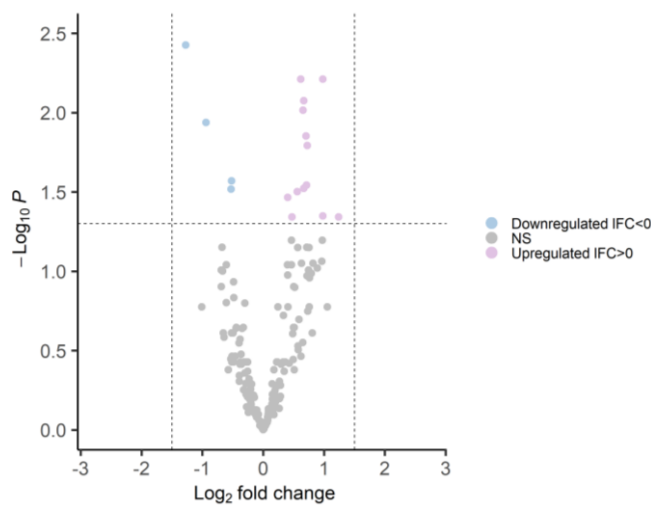


Figure 18: Volcano plot showing miRNAs differentially expressed between EC⁺/Ob⁺ and EC⁻/Ob⁺.

Table 14. Differentially expressed miRNAs between EC⁺/Ob⁺ and EC⁻/Ob⁺.

miRNA ID	LogFold Change	P-value	Adj P-val	Deregulation in EC ⁺ /Ob ⁺
hsa-miR-21-5p	1.05	0.000	0.000	↑
hsa-miR-3613-5p	1.22	0.000	0.000	↑
hsa-miR-92b-3p	-0.86	0.000	0.000	↓
hsa-miR-27a-3p	0.89	0.000	0.000	↑
hsa-miR-23a-3p	0.71	0.000	0.000	↑
hsa-miR-342-3p	-0.75	0.000	0.000	↓
hsa-miR-191-5p	-0.99	0.000	0.001	↓
hsa-miR-93-3p	-1.27	0.000	0.004	↓
hsa-miR-32-5p	0.98	0.000	0.006	↑
hsa-miR-19a-3p	0.62	0.000	0.006	↑
hsa-miR-22-3p	0.67	0.000	0.008	↑
hsa-miR-146a-5p	0.66	0.000	0.010	↑
hsa-miR-150-5p	-0.94	0.000	0.012	↓
hsa-miR-340-5p	0.70	0.001	0.014	↑
hsa-miR-378a-3p	0.73	0.001	0.016	↑
hsa-miR-486-5p	-0.52	0.001	0.027	↓
hsa-miR-223-5p	0.71	0.002	0.029	↑
hsa-miR-10a-5p	0.67	0.002	0.030	↑
hsa-miR-92a-3p	-0.53	0.002	0.030	↓
hsa-miR-222-3p	0.56	0.002	0.031	↑
hsa-miR-126-5p	0.40	0.003	0.034	↑
hsa-miR-320d	0.98	0.004	0.045	↑
hsa-miR-29c-3p	0.47	0.004	0.045	↑
hsa-miR-1290	1.24	0.004	0.045	↑

EC: endometrial cancer; Ob: obesity; ↑: up-regulated in EC⁺/Ob⁺; ↓ down-regulated in EC⁺/Ob⁺.

miRNA analysis: obese vs non-obese EC

Comparing miRNAs expression in EC⁺/Ob⁺ versus EC⁺/Ob⁻, 16 miRNAs resulted deregulated with p < 0.05 (3 up-regulated and 13 down-regulated in obese EC); however, none of them maintained the statistical significance after adjusting for multiple comparisons (Adj P-val < 0.05). Significant miRNAs are shown in Table 15.

Table 15. Differential miRNA expression in EC⁺/Ob⁺ vs EC⁺/Ob⁻ samples.

miRNA ID	LogFold Change	P-value	Deregulation in EC ⁺ /Ob ⁺
hsa-miR-365a-3p	1.22	0.003	↑
hsa-miR-205-5p	-1.00	0.003	↓
hsa-miR-224-5p	0.84	0.008	↑
hsa-miR-92b-3p	-0.44	0.011	↓
hsa-miR-93-3p	-0.64	0.021	↓
hsa-miR-141-3p	-0.70	0.017	↓
hsa-miR-342-3p	-0.33	0.019	↓
hsa-miR-199a-3p	-0.43	0.030	↓
hsa-miR-151a-3p	-0.33	0.043	↓

hsa-miR-145-5p	-0.70	0.044	↓
hsa-miR-423-5p	-0.29	0.028	↓
hsa-miR-194-5p	0.57	0.036	↑
hsa-miR-1294	-0.58	0.039	↓
hsa-miR-361-5p	-0.34	0.041	↓
hsa-miR-584-5p	-0.40	0.033	↓
hsa-miR-182-5p	-0.66	0.031	↓

EC: endometrial cancer; Ob: obesity; ↑: up-regulated in EC⁺/Ob⁺; ↓: down-regulated in EC⁺/Ob⁺.

EC classification for lymphovascular invasion

EC patients were stratified based on LVI: 8 patients showed SUB-LVI, while 22 patients had A/F-LVI. PCA showing miRNA expression in the two subgroups is represented in Figure 19.

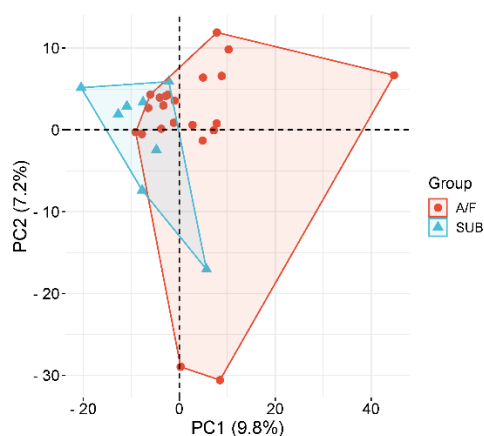


Figure 19: PCA showing miRNA expression in SUB-LVI and A/F-LVI EC samples.

50 miRNAs resulted deregulated between SUB and A/F LVI EC patients and 13 remained significant after FRD adjustment (Adj P-val < 0.05). Of these, 4 were up-regulated and 9 down-regulated in SUB-LVI. Significant deregulated miRNAs are shown in Figure 20 and Table 16.

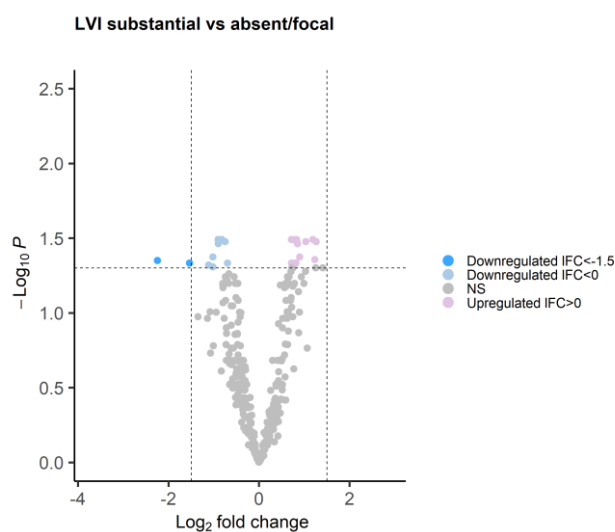


Figure 20: Volcano plot showing miRNAs differentially expressed between SUB- and ABS-LVI EC.

miRNA ID	LogFold Change	P-value	Adj P-val	Deregulation in SUB
hsa-miR-23a-3p	0.72	0.000	0.032	↑
hsa-miR-18a-5p	-0.91	0.000	0.032	↓
hsa-miR-374a-5p	-0.82	0.000	0.032	↓
hsa-miR-17-5p	-0.74	0.001	0.033	↓
hsa-miR-141-3p	1.03	0.001	0.033	↑
hsa-miR-454-3p	-0.90	0.001	0.034	↓
hsa-miR-192-5p	-1.02	0.002	0.042	↓
hsa-miR-10b-5p	0.90	0.002	0.042	↑
hsa-miR-885-3p	-2.24	0.002	0.045	↓
hsa-miR-10a-5p	0.77	0.003	0.046	↑
hsa-miR-122-5p	-1.53	0.003	0.046	↓
hsa-miR-503-5p	-1.11	0.003	0.048	↓
hsa-miR-182-5p	-1.02	0.003	0.049	↓

SUB: substantial; A/F: absent/focal; LVI: lymphovascular invasion; EC: endometrial cancer; ↑: up-regulated in SUB; ↓ down-regulated in SUB.

Up-regulated miRNAs in SUB-LVI patients were tested for their ability to predict the SUB condition in EC patients. Four miRNAs showed an accuracy > 0.7 and they are shown in Table 17, while their ROC curves are shown in Figure 21.

miRNA	Threshold	Specificity	Sensitivity	Accuracy	NPV	PPV
hsa-miR-10b-5p	8.50	0.91	0.63	0.83	0.87	0.71
hsa-miR-23a-3p	9.32	0.77	0.88	0.80	0.94	0.58
hsa-miR-10a-5p	7.48	0.68	1.00	0.77	1.00	0.53
hsa-miR-141-3p	5.67	0.73	0.88	0.77	0.94	0.54

SUB: substantial; LVI: lymphovascular invasion; EC: endometrial cancer; NPV: negative predictive value; PPV: positive predictive value.

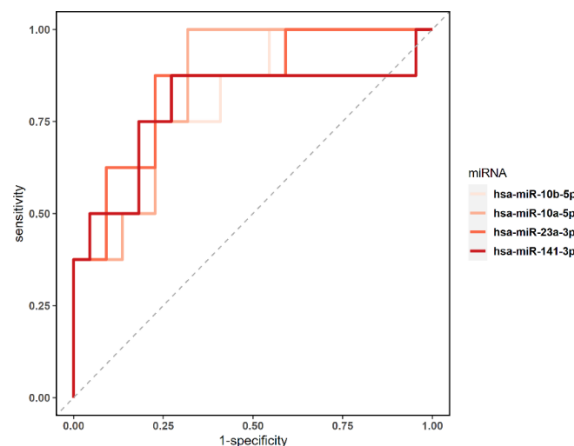


Figure 21: ROC curves indicating the ability of predicting SUB-LVI in EC patients.

3.4 DISCUSSION AND CONCLUSION

Obesity is recognized as the most significant risk factor for EC; however, public awareness of this connection remains limited. To identify miRNAs potentially associated with obesity in EC, we initially evaluated miRNA levels in endometrial tissue from obese women, both with and without EC. As anticipated, this analysis revealed significantly different miRNA profiles, highlighting 62 differentially expressed miRNAs, 51 of which were up-regulated and 11 down-regulated in patients with EC compared to those without cancer. The significant difference was further emphasized by PCA, which identified two distinct clusters. This finding was expected, as it is widely recognized that cancerous tissues exhibit profound molecular alterations, including miRNA deregulation. Subsequently, miRNA levels were assessed in 40 EC patients, stratified considering BMI. Results revealed a notable up-regulation of 11 miRNAs in obese patients compared to non-obese counterparts.

The consistent up-regulation of miRNAs such as hsa-miR-449a, hsa-miR-422a, hsa-miR-136-5p, hsa-miR-455-5p, hsa-miR-193a-3p, hsa-miR-425-5p, and hsa-miR-551b-3p in obese EC patients, compared to both non-obese EC patients and obese healthy women, suggests a potential role for these miRNAs in obesity-associated EC. These miRNAs could be linked to the molecular mechanisms that drive the development or progression of EC in obese individuals, possibly reflecting alterations in pathways related to inflammation, cell proliferation, or metabolism, which are often dysregulated in obesity. On the other hand, the down-regulation of hsa-miR-451a in obese EC compared to obese controls, paired with its up-regulation in obese EC relative to non-obese EC, is particularly interesting. This may indicate a complex role for this miRNA in EC: hsa-miR-451a might be involved in distinguishing between obese and non-obese EC phenotypes, and its dysregulation could be a response to the altered metabolic and inflammatory environment in obese EC. Further studies would be required to understand its exact functional role and whether it could serve as a biomarker or therapeutic target.

Hsa-miR-199a-5p, hsa-miR-449a, hsa-miR-449b-5p and hsa-miR-2110 were further validated in a larger cohort of 84 EC samples from IRCCS of Bologna and in the TCGA independent cohort. Hsa-miR-199a-5p, hsa-miR-449a and hsa-miR-449b-5p remained up-regulated in obese EC patients. Additionally, the three miRNAs were associated to significant prognostic factors, including tumor grade and histological type, suggesting that higher levels of these miRNAs were generally found in low-grade tumors (G1/G2) and in endometrioid endometrial adenocarcinomas. This aligns with existing evidence that ECs associated with obesity are typically low-grade tumors and endometrioid endometrial adenocarcinoma.⁸⁸ Hsa-miR-199a has previously been correlated with obesity, as it is

highly expressed in preadipocytes and plays a key role in the regulation of adipogenesis, indicating its significant regulatory function in obesity.^{89,90}

Hsa-miR-449a and hsa-miR-449b-5p are members of the hsa-miR-34/449 family. Although no studies have reported an association between hsa-miR-449 and obesity, hsa-miR-34 has previously been linked to this condition.^{91,92} Functional enrichment analysis identified several GO molecular functions related to obesity, highlighting the potential role of these miRNAs in obesity-related EC. Moving on to liquid biopsy, 24 miRNAs resulted deregulated between EC patients and non-cancer controls, with a Adj P-val < 0.05. Moreover, 24 miRNAs resulted deregulated comparing obese patients, with and without EC; of these, 7 miRNAs were also deregulated in the same analysis carried out on tissue biopsies, supporting the hypothesis of their involvement in stratifying EC and obese non-cancer women. Moreover, 13 miRNAs (4 of which were also deregulated in “Tumor Epigenetics” analysis) were able to predict EC, with accuracy values > 0.7. Considering obese and non-obese EC patients, 16 miRNAs were significantly deregulated, of which hsa-miR-199a was also shown in the “Tumor Epigenetic” analysis (in particular, hsa-miR-199a-3p in “Liquid Biopsy Epigenetics” while hsa-miR-199a-5p in “Tumor Epigenetics”). This finding highlights the hypothesis that these two miRNAs, which form a cluster, could be used to distinguish obese EC patients through non-invasive methods in plasma samples. Given the emerging importance of LVI in EC risk assessment, cancer patients were stratified based on presence of substantial or absent/focal LVI. 13 miRNAs were found to be deregulated between the two groups after FDR adjustment; of these, 4 miRNAs were identified as being able to predict substantial LVI in EC patients through ROC curves. Further investigations in this study could improve the clinical management of EC patients, enabling earlier detection of lymphovascular invasion status.

The present study has several limitations. Regarding “Tumor Epigenetics”, the entire miRNome was not analysed in the Discovery phase; instead, a pre-cast array that evaluates only 377 miRNAs was used. In addition, the Validation cohort included patients from the Discovery cohort as well. To address this issue, validation was also performed on an independent cohort from TCGA. However, validation in an independent cohort from IRCCS of Bologna, or even through a multicenter study, would be the optimal approach to further validate the obtained results. In contrast, in “Liquid Biopsy Epigenetics” where miRNA sequencing was conducted, the patient’s group was relatively small, and further studies are needed in a larger cohort to confirm these findings. Moreover, in some of the conducted analyses, the populations differed in terms of age or comorbidities, both of which are characteristics that can influence the miRNA expression profile.⁹³ This should be taken into account when observing differentially expressed miRNAs between the two patient groups. It is important to emphasize that the two parts of the study analyse miRNAs in two different contexts

(tumor tissue and plasma). It is well known that miRNA expression profile in the two matrices is only partially overlapping, as circulating miRNAs can also originate from other tissues in the body.⁹⁴

Overall, this study could be considered the first to assess the relationship between miRNA expression in EC and body fat levels through miRNA profiling, revealing that specific miRNAs could play a role in the clinical management of obese EC patients.

4. TASK 2: Epigenetic effects of physical activity in Ovarian Cancer patients

4.1 AIM

As previously mentioned, physical inactivity is known to be associated with reduced functional independence, decreased tolerance to anti-cancer treatments, and increased overall mortality. Furthermore, recent studies have shown a modulation of miRNA expression following acute or chronic physical activity; however, limited information is available regarding miRNA modulation in fluid samples, as well as in OC patients. In this context, Task 2 aimed to identify deregulated miRNAs in plasma samples from OC patients before and after surgery, taking in consideration the effect of physical activity. Moreover, the effects of physical activity on patients' quality of life were evaluated through questionnaires.

To do that, a part of the patients' cohort was enrolled in a specific physical activity program and the remaining patients were not.

4.2 MATERIALS AND METHODS

Study population

This study was approved by the Institutional Review Board 788/2021/Sper/AOUBo, ClinicalTrials.gov Identifier NCT05146505. Patients were included in the study after signing an informed consent form. The inclusion criteria were: i) diagnosis of OC; ii) ownership of a smartphone and of an email address. The exclusion criteria were: i) diagnosis of concomitant tumors; ii) established motor difficulties. Patients enrolled in the present study were treated at the Division of Oncologic Gynecology IRCCS Azienda Ospedaliero-Universitaria of Bologna.

Of the potentially eligible 130 OC patients, a total of 11 patients were enrolled in the study, with a success rate of 8,46%. Patients were randomized 1:1 in an intervention group (INT, N=5) and a control group (CTRL, N=6).

PinkTrainer application

The project was based on the use of the PinkTrainer application, originally developed in the Netherlands for breast cancer patients, which each patient downloaded onto her own smartphone. Through this application, patients were able to connect with medical specialists, including oncologists, gynecologists, personal trainers, and nutritionists, who provided them the necessary information to improve their psychophysical well-being.⁹⁵

Activity program

The INT activity program, provided by a personal trainer specialized in cancer patients, to the patients in this group through the PinkTrainer app, consisted of specific exercises to be performed from enrolment up to two days prior to surgery, and other exercises to be performed for about two months, starting 10 days after surgery. Pre-surgery exercises included three sessions/week of a program aimed at maintaining muscle mass and strength, using bodyweight exercises or small equipment (e.g., mat, 1-liter bottles) and consisting of nine exercises, lasting about 40 minutes. Ten days after surgery, patients were assigned a different, much lighter exercise protocol for three weeks, consisting of 12 bodyweight-only exercises, designed to restore physical function and mobility. After this period, patients returned to the 'light' version of the pre-surgery exercises.

The CTRL program, instead, consisted in daily sessions of breathing exercises, scheduled in PinkTrainer app, lasting about 15 minutes. The protocol consisted in the same breathing exercises before and after surgery, with a 10-days stop immediately after surgery. Moreover, both the INT and CTRL groups of patients received informational materials regarding various healthy and active lifestyle topics. These materials were provided weekly through the PinkTrainer app and included information on preparing for surgery, importance of prehabilitation, international guidelines on the recommended amount of weekly physical activity, and cancer prevention.

Questionnaires

Through PinkTrainer app, at the moment of the enrollment (15 days before surgery) and approximately 2 months after the enrollment, two questionnaires concerning the quality of life were proposed to the patients, both INT and CTRL. In particular, the European Organisation for Research and Treatment of Cancer (EORTC) quality of life questionnaire (QLQ) is an integrated system for measuring the health-related quality of life (QoL) of cancer patients enrolled in international clinical trials. QLQ-C30 was generally about the QoL while EORTC OV28 was specific for OC.⁹⁶ Most of the questions required a response ranging from "Very much", "quite a lot", "a little" to "no", while some involved assigning a score from 1 (very poor) to 7 (excellent).

Plasma collection and processing

Blood was collected in a BD Vacutainer® K2 (EDTA) tube. Within 2 hours of the blood draw, it was processed as previously described in section 3.2: "*Liquid Biopsy Epigenetics, Sample processing*", and aliquots were stored at -80°C until use. Blood samples were taken 15 days before surgery (t-15) and 30 days after surgery (t+30).

RNA extraction from plasma samples

RNA was extracted from plasma samples using the miRNeasy Serum/Plasma kit (Qiagen), following the manufacturer’s instructions, as described in section 3.2: “*Liquid Biopsy Epigenetics, miRNA extraction from plasma samples*”.

miRNA reverse transcription

2 µL of RNA extracted from plasma samples were reverse transcribed using the TaqMan™ Advanced miRNA cDNA Synthesis Kit (Applied Biosystems™), following the manufacturer’s instructions, as described in section 3.2: “*Tumor Epigenetics, miRNA reverse transcription*”.

miRNA analysis

miRNA analysis was conducted on 22 samples from 11 patients, of which 5 belong to the intervention group, whereas 6 to the control group. The analysis was conducted using the TaqMan™ Advanced miRNA Human A Card (Applied Biosystems™), as described in section 3.2: “*Tumor Epigenetics, Discovery step: miRNA expression profiling*”.

Statistical analysis

miRNA amplification data were analysed using the ThermoFisher Cloud app (Applied Biosystems™). MiRNAs with C_t values ≥35 were considered not expressed and excluded from further analysis. Relative expression levels were calculated through the 2^{-ΔΔC_t} method using hsa-miR-16-5p as reference. Statistical significance was assessed using the nonparametric Mann–Whitney–Wilcoxon test, with a p < 0.05 considered statistically significant. PCA was created through SRplot⁸² while validations graphs were created with GrapPad Prism 8.0.2 for Windows, GraphPad Software, Boston, Massachusetts USA, www.graphpad.com.

Target prediction

For miRNA-target prediction analysis, TargetScan Human 8.0, miRTarBase 8.0 and miRDB 6.0 databases were used; miRNA-target interactions resulted in all the three databases, were only considered.

4.3 RESULTS

A total of 11 patients, 5 in INT group and 6 in CTRL group, were enrolled in the project. The two randomized groups were similar with respect to the analysed characteristics regarding OC, as shown in Table 18.

Table 18. Demographic and clinical characteristics of the OC patients included in this study.			
Variable	OC patients (N=11)		P-value
	INT	CTRL	

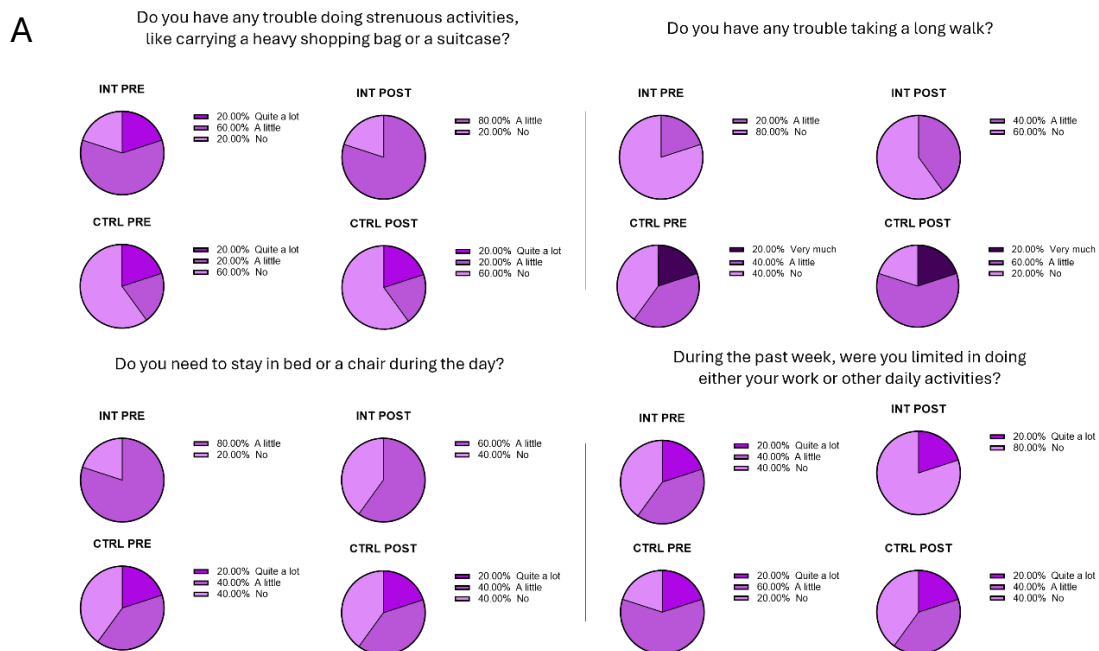
		N= 5 (45,5%)	N= 6 (54,5%)	
Age at diagnosis mean (\pm sd)		59.42 (\pm 10.81)	60.13 (\pm 7.75)	0.9
Age Group N (%)	<50 y	1 (9.1)	1 (9.1)	0.89
	>50 y	4 (36.4)	5 (45.5)	
BMI mean (\pm sd)		21.6 (\pm 3.0)	25.0 (\pm 2.7)	0.08
Histotype N (%)	Endometrioid	2 (18.2)	1 (9.1)	0.39
	Serous	3 (27.3)	5 (45.5)	
Grade N (%)	G1	1 (9.1)	0	0.49
	G2	1 (9.1)	1 (9.1)	
	G3	3 (27.3)	5 (45.5)	
FIGO stage (2014) N (%)	I	0	1 (9.1)	0.32
	II	2 (18.2)	0	
	III	2 (18.2)	3 (27.3)	
	IV	1 (9.1)	2 (18.2)	
BRCA status* N (%)	BRCA WT	2 (18.2)	5 (45.5)	0.07
	BRCA MUT	2 (18.2)	0	

OC: ovarian cancer; INT: intervention group; CTRL: control group; sd: standard deviation; N: number of patients; y: years; BMI: body mass index; FIGO: International Federation of Gynecology and Obstetrics; WT: wild type; MUT: mutated.

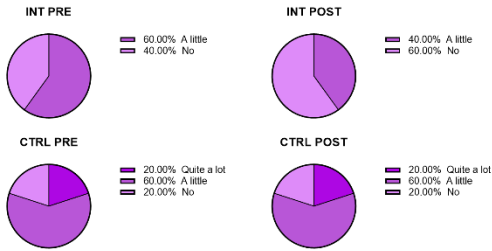
* BRCA status was not available for 2 patients.

Questionnaires

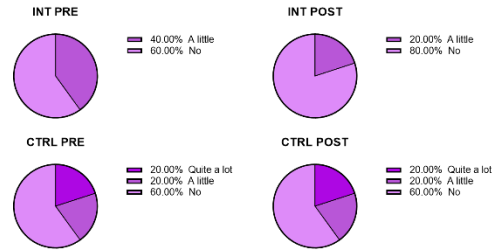
Questionnaires were completed by the participants before and 2 months after surgery. Completed questionnaires were available for only N=5 in the INT group and N=5 in the CTRL group. The number of completed questionnaires was limited, which did not allow for a comprehensive analysis of the results; however, the charts related to the questions that showed differences in responses between the two groups are presented in Figures 22 and 23.



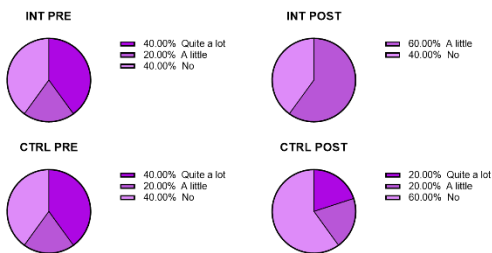
During the past week, were you limited in pursuing your hobbies or other leisure time activities?



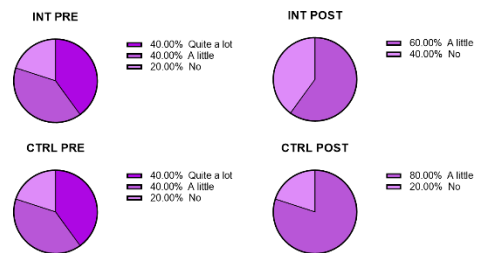
During the past week, were you short of breath?



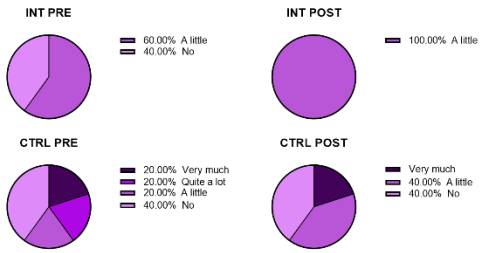
During the past week, have you had pain?



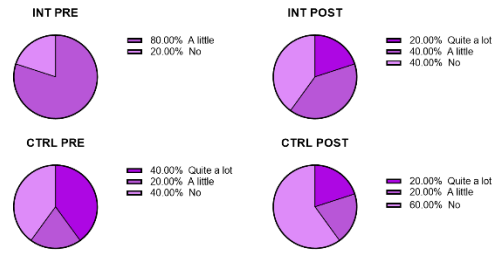
During the past week, did you need to rest?



During the past week, have you had trouble sleeping?



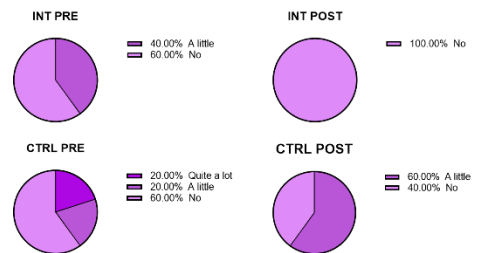
During the past week, have you felt weak?



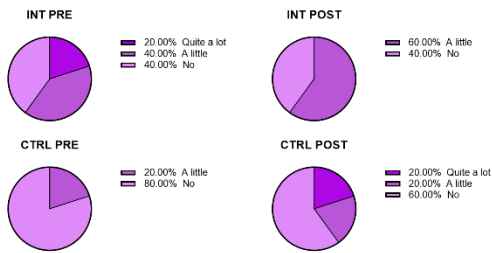
During the past week, have you lacked appetite?



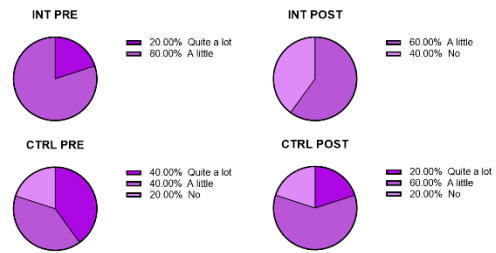
During the past week, have you felt nauseated?



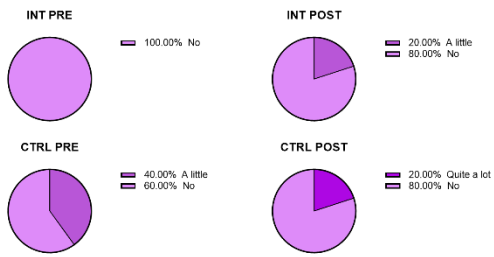
During the past week, have you been constipated?



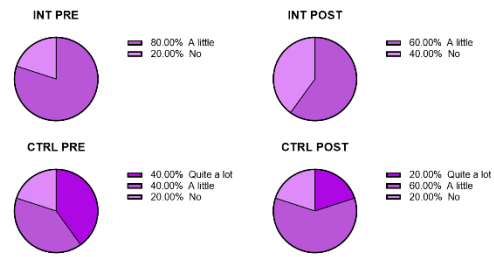
During the past week, were you tired?



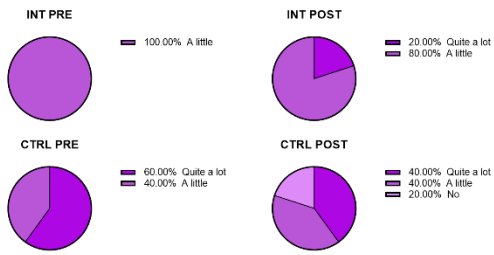
During the past week, have you had difficulty in concentrating on things, like reading a newspaper or watching television?



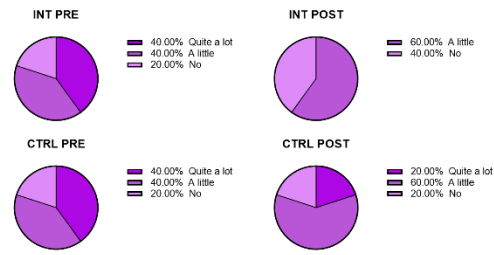
During the past week, did you feel tense?



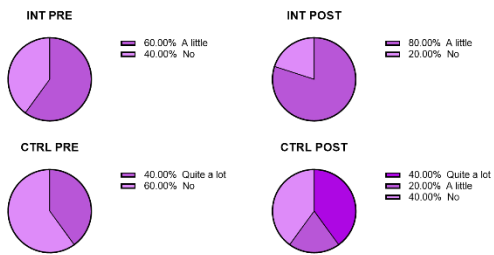
During the past week, did you worry?



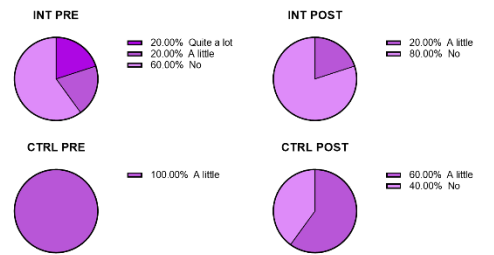
During the past week, did you feel irritable?



During the past week, did you feel depressed?

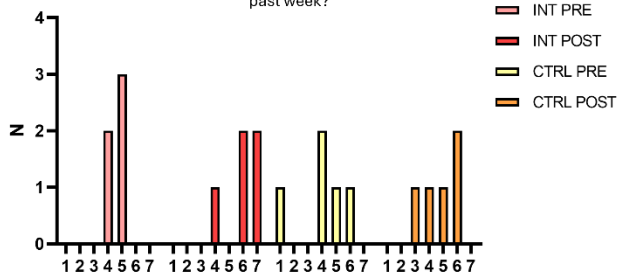


During the past week, has your physical condition or medical treatment interfered with your family life??



B

How would you rate your overall health during the past week?



How would you rate your overall quality of life during the past week?

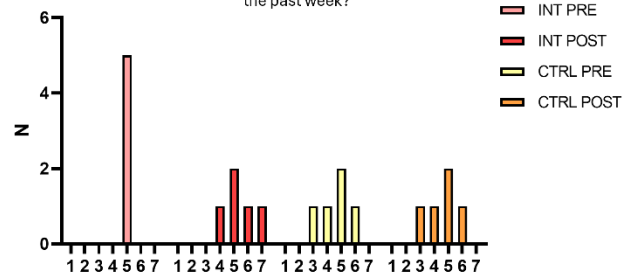


Figure 22: EORTC QLQ-C30 results. A) Pie charts showing the percentage of "Very much", "quite a lot", "a little" to "no" answers in INT and CTRL patients, pre- and post-surgery; B) Separated bar graphs showing quality of life scores from 1 (very poor) to 7 (excellent) in the 2 subgroups before and after surgery.

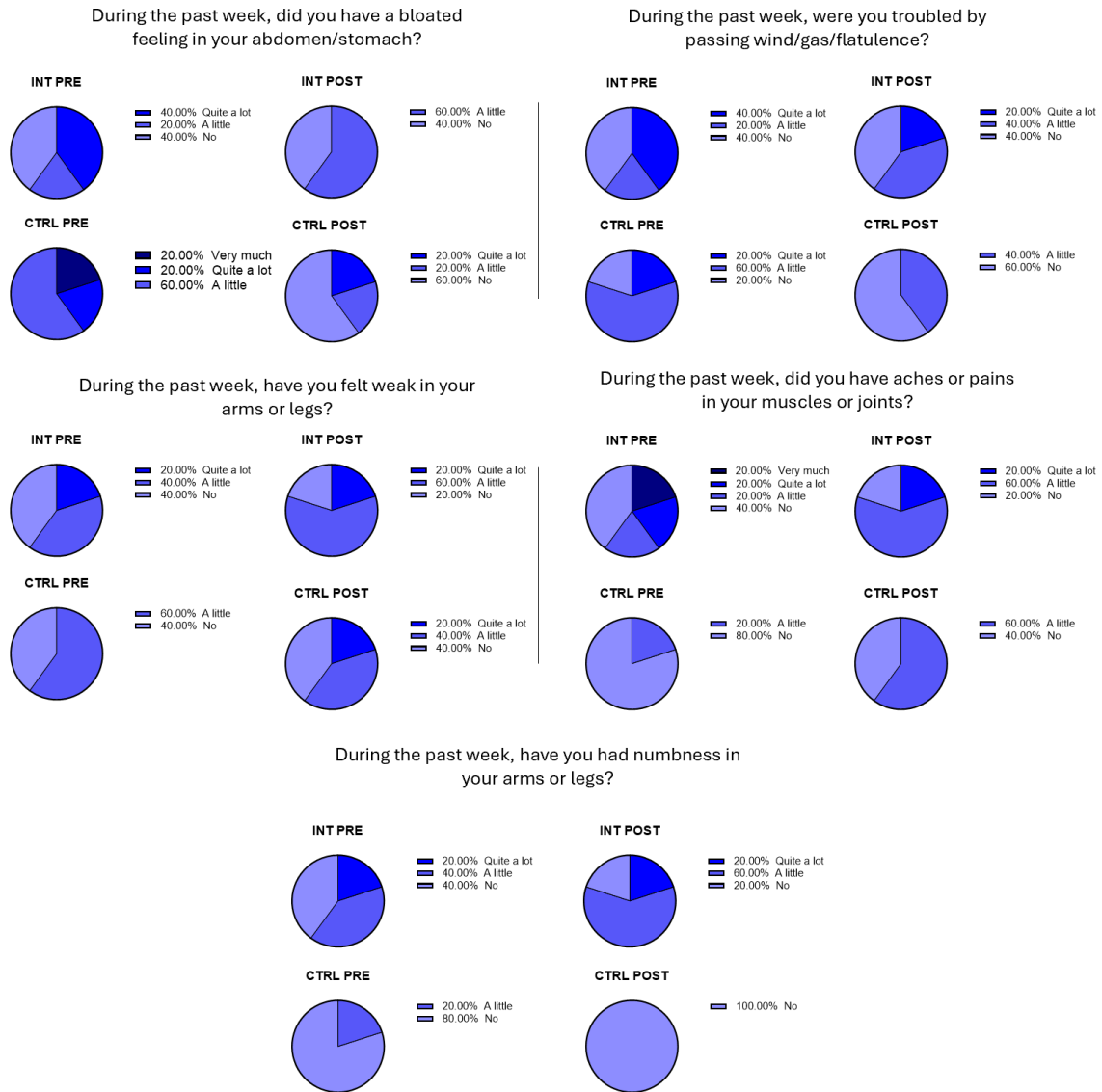


Figure 23: EORTC QLQ-OV28 results. Pie charts showing the percentage of "Very much", "quite a lot", "a little" to "no" answers in INT and CTRL patients, pre- and post-surgery.

In relation to the EORTC QLQ-C30, physical activity appeared to have improved over time certain parameters such as the need for rest, loss of appetite, nausea, constipation, and depression. In contrast, post-intervention questionnaires have demonstrated worse outcomes in patients who were engaged in physical activity concerning sleep issues and fear. Regarding EORTC-OV28 results, physical activity showed benefits for muscle and joint aches and pains, while a worsening effect was observed on numbness in arms and legs.

miRNA analysis: t-15 vs t+30

Firstly, miRNAs levels at t-15 were compared with t+30. PCA in Figure 24 shows the miRNAs expression between the two timepoints; as clearly represented, the PCA did not highlight a separation between the two groups.

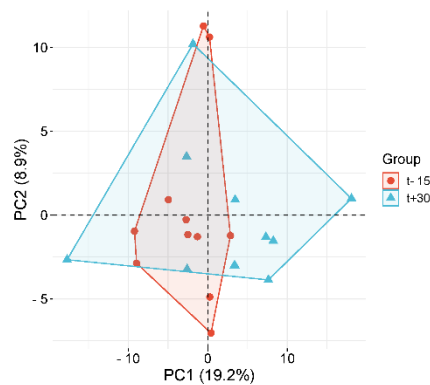


Figure 24: PCA showing miRNAs expression in t-15 and t+30 OC plasma samples.

By this comparison, 12 miRNAs resulted significantly deregulated between the two timepoints, 3 up-regulated and 9 down-regulated in t+30; however, none of them maintained the significance after P-value adjustment. Significantly deregulated miRNAs are shown in Table 19.

MiRNA ID	LogFold Change	P-value	Deregulation in t+30
hsa-miR-27a-3p	3.36	0.009	↑
hsa-miR-125a-3p	-3.55	0.010	↓
hsa-miR-124-3p	-3.07	0.014	↓
hsa-miR-133a-3p	-3.47	0.015	↓
hsa-miR-362-3p	3.16	0.024	↑
hsa-let-7g-5p	-2.03	0.025	↓
hsa-miR-26b-5p	-2.17	0.029	↓
hsa-miR-133b	-1.76	0.032	↓
hsa-miR-146a-5p	-1.21	0.038	↓
hsa-miR-331-3p	2.33	0.040	↑
hsa-miR-191-5p	-1.82	0.040	↓
hsa-miR-423-3p	-1.45	0.049	↓

OC: ovarian cancer; ↑: up-regulated in t+30; ↓: down-regulated in t+30.

Expression of these miRNAs in terms of $\Delta\Delta C_t$ (t+30 – t-15) was then compared between INT and CTRL groups. Only hsa-miR-27a-3p and hsa-miR-133a-3p resulted respectively down-regulated and up-regulated in INT group respect to CTRL (respectively with $p = 0.023$ and $p = 0.025$).

miRNA analysis: INT vs CTRL at t+30

In order to identify miRNAs eventually deregulated after enrolment in a physical activity program, miRNAs expression between INT and CTRL at t+30 was compared. miRNAs expression represented through PCA is shown in Figure 25.

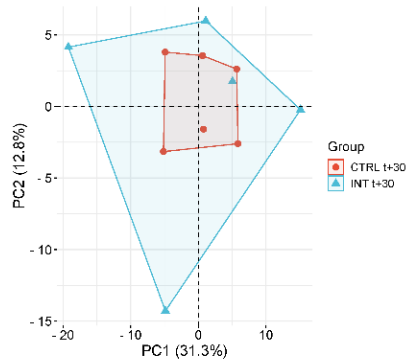


Figure 25: PCA showing miRNAs expression in t+30 samples (N=5 INT and N=6 CTRL).

As shown in Table 20, only 5 miRNAs resulted deregulated between the two groups; however, none of them showed Adj P-val < 0.05. Of the deregulated miRNAs, 3 were up-regulated and 2 down-regulated in INT group.

Table 20. Differential miRNA expression at t+30 in INT vs CTRL.			
MiRNA ID	LogFold Change	P-value	Deregulation in INT
hsa-miR-193a-3p	3.78	0.004	↑
hsa-miR-27a-3p	-3.51	0.036	↓
hsa-miR-365a-3p/ 365b-3p	4.01	0.041	↑
hsa-miR-421	-2.98	0.043	↓
hsa-miR32-5p	5.13	0.048	↑
INT: intervention group; CTRL: control group; ↑: up-regulated in INT; ↓: down-regulated in INT.			

For the differentially expressed miRNAs, $\Delta\Delta C_t$ (t+30 – t-15) was calculated. Of the previously deregulated miRNAs, hsa-miR-193a-3p resulted up-regulated in INT compared to CTRL (p = 0.022), while hsa-miR-27a-3p and hsa-miR-421 resulted down-regulated in INT, respectively with p = 0.023 and p = 0.007). Deregulated miRNAs in the two analyses are represented in Figure 26.

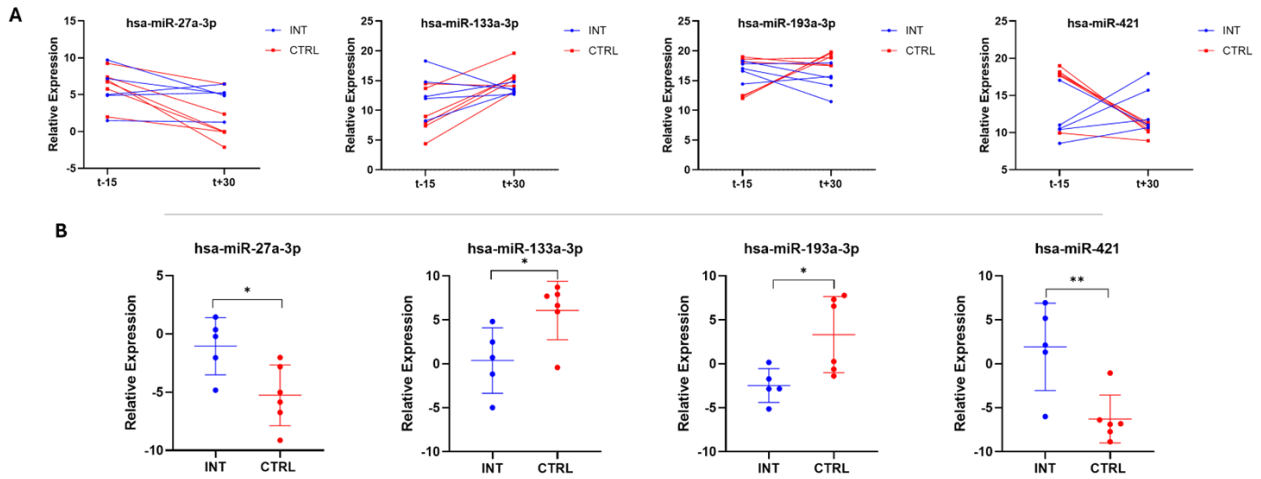


Figure 26: Deregulated miRNAs in the two analyses. A) miRNA expression at t-15 and t+30 in INT and CTRL groups; B) different miRNAs expression in INT and CTRL in terms of $\Delta\Delta Ct$. *: $p < 0.05$; **: $p < 0.01$.

Target prediction

Interactions miRNA-gene were searched for the 4 deregulated miRNAs in the two analyses. Common genes between TargetScan Human 8.0, miRTarBase 8.0 and miRDB 6.0 databases were considered and are shown in Table 21.

Table 21. Target genes of the deregulated miRNAs.	
Gene	Gene name
hsa-miR-27a-3p	
LYSMD3	LysM domain containing 3
LITAF	lipopolysaccharide induced TNF factor
INO80D	INO80 complex subunit D
PPIF	peptidylprolyl isomerase F
EFHD2	EF-hand domain family member D2
AKIRIN1	akirin 1
TAOK1	TAO kinase 1
ZFP36L2	ZFP36 ring finger protein like 2
CNN3	calponin 3
GRB2	growth factor receptor bound protein 2
ZFP36L1	ZFP36 ring finger protein like 1
TGFBR3	transforming growth factor beta receptor 3
SERP1	stress associated endoplasmic reticulum protein 1
NRAS	NRAS proto-oncogene, GTPase
SOS1	SOS Ras/Rac guanine nucleotide exchange factor 1
SGMS1	sphingomyelin synthase 1
SERTAD3	SERTA domain containing 3
E2F7	E2F transcription factor 7
MAPK14	mitogen-activated protein kinase 14
PRKAA2	protein kinase AMP-activated catalytic subunit alpha 2
GFPT2	glutamine-fructose-6-phosphate transaminase 2

hsa-miR-133a-3p	
TAGLN2	transgelin 2
CERS2	ceramide synthase 2
SP1	Sp1 transcription factor
RFFL	ring finger and FYVE like domain containing E3 ubiquitin protein ligase
PTBP1	polypyrimidine tract binding protein 1
hsa-miR-193a-3p	
SLC10A6	solute carrier family 10 member 6
DCAF7	DDB1 and CUL4 associated factor 7
MSANTD2	Myb/SANT DNA binding domain containing 2
KRAS	KRAS proto-oncogene, GTPase
E2F6	E2F transcription factor 6
CCND1	cyclin D1
WDR82	WD repeat domain 82
MCL1	MCL1 apoptosis regulator, BCL2 family member
PLAU	plasminogen activator, urokinase
ALKBH5	alkB homolog 5, RNA demethylase
LAMC1	laminin subunit gamma 1
INO80D	INO80 complex subunit D
YWHAZ	tyrosine 3-monooxygenase/tryptophan 5-monooxygenase activation protein zeta
TMEM30A	transmembrane protein 30A
EBAG9	oestrogen receptor binding site associated antigen 9
TGFB3	transforming growth factor beta receptor 3
ARMC1	armadillo repeat containing 1
IGFBP5	insulin like growth factor binding protein 5
GDF11	growth differentiation factor 11
BAZ2A	bromodomain adjacent to zinc finger domain 2A
ABI2	abl interactor 2
TGFB2	transforming growth factor beta 2
DNAJB9	DnaJ heat shock protein family (Hsp40) member B9
KMT2A	lysine methyltransferase 2A
hsa-miR-421	
PRCC	proline rich mitotic checkpoint control factor
CASP3	caspase 3
JARID2	jumonji and AT-rich interaction domain containing 2
AFF4	ALF transcription elongation factor 4
DNAJC27	DnaJ heat shock protein family (Hsp40) member C27
TXNRD1	thioredoxin reductase 1
SRSF7	serine and arginine rich splicing factor 7
TTC37	SKI3 subunit of superkiller complex
FAM122A	PP2A Aalpha (PPP2R1A) and B55A (PPP2R2A) interacting phosphatase regulator 1
GOSR1	golgi SNAP receptor complex member 1
NIPBL	NIPBL cohesin loading factor
XIAP	X-linked inhibitor of apoptosis
ZNF652	zinc finger protein 652
FAM172A	ARB2 cotranscriptional regulator A

4.4 DISCUSSION AND CONCLUSION

From a literature review, no studies are currently available regarding miRNA expression modulation following physical activity in OC patients. Of the potentially eligible 130 OC patients, a total of 11 were enrolled. The low success rate (8,46%) of this project may have been due to: i) the advanced age of the patients and the consequent lack of smartphone use; ii) lack of willingness to participate in a program that requires physical activity during a particular stage of life; iii) the COVID-19 emergency period, during which it was not possible to attend the hospital for enrollment. This rate does not guarantee the feasibility of conducting a meaningful study; however, a preliminary analysis was carried out on 11 OC patients (5 INT and 6 CTRL). The arrangement of samples in the multidimensional space clearly indicates the overlap of the two sample groups, which do not cluster separately. In fact, by analysing miRNAs differentially expressed at t-15 and t+30, 12 miRNAs resulted significantly deregulated. Of these miRNAs, 2 maintained the statistical significance after analysing the $\Delta\Delta\text{Ct}$ (t+30 – t-15) between INT and CTRL samples. In the second analysis, evaluating the different expressed miRNAs at t+30 between INT and CTRL, 10 miRNAs were significantly deregulated and 3 of them confirmed deregulation considering the $\Delta\Delta\text{Ct}$ (t+30 – t-15). In particular, hsa-miR-27a-3p and hsa-miR-421 were down-regulated while hsa-miR-133a-3p and hsa-miR-193a-3p resulted up-regulated in INT compared to CTRL. Of these miRNAs, only hsa-miR-133a-3p has been previously studied and observed as increased in mice affected by myocardial infarction undergoing aerobic exercise.⁹⁷ Regarding the study of these miRNAs in OC, a reduction in hsa-miR-27a-3p has been associated with decreased cell viability, as well as reduced migration, invasion, and apoptosis in OC cell models.⁹⁸ An increase in hsa-miR-421 (observed in the control group) was found to be associated with enhanced proliferation and invasion capability in OC cells.⁹⁹ Therefore, the effect of physical activity on these two miRNAs appears to be beneficial for their potential role in reducing the malignant behaviour of OC. On the other hand, an increase in hsa-miR-133a-3p, as observed in the CTRL group, was found to be associated with a decrease in tumor proliferation and invasive capacity. Hsa-miR-193a-3p has been found to function as an oncogenic suppressor miRNA in OC; therefore, its increase observed in the control group may suggest an improvement in the condition of these patients.

This study, although carried out on a very limited number of patients, represents the first attempt to understand the role of physical activity in modulating miRNA expression in OC.

5. TASK 3: Drug resistance mechanisms in Ovarian Cancer organoids

5.1 AIM

It is well known that the intricate nature and variability of EOC make it challenging to mimic and replicate it in *in vitro* models, which are unable to sufficiently clarify the molecular processes associated with tumor initiation and disease metastasis. In the recent years, there has been a growing interest in 3-Dimensional (3D) models such as spheroids or organoids, as they offer greater complexity compared to 2-Dimensional (2D) cellular models. In fact, 3D models are more similar to the human environment, and avoid the need to resort to *in vivo* studies, in agreement with the 3R principle (Replacement, Reduction and Refinement). In this scenario, this task aimed to learn how to generate 3D EOC organoids from patients' biopsies, with the future objective of validating the results previously obtained in Task 4 on both 2D and 3D cellular models. In particular, 3D organoids were then used to investigate sensitivity to specific molecules and to set up a platform for arrayed gene editing.

This Task was developed under the supervision of Dr. Wojciech Senkowski within the Wennerberg Group, Biotech Research & Innovation Centre (BRIC), University of Copenhagen (Denmark).

5.2 MATERIALS AND METHODS

Media composition

EOC organoids were cultivated in two different media formulations, optimized by Dr. Senkowski in his previous research.¹⁰⁰ The two different formulations, respectively referred to as M1 and M2, were developed from Advanced DMEM/F12 (1X) (+NEAA; +sodium pyruvate; -L-Glutamine) (Gibco™) and were different for the presence or absence of several factors. Specific media formulations are summarized in Table 22.

M1	
Component	Final Concentration
Advanced DMEM/F12 (1X)	-
Primocin	100 µg/mL
HEPES	10 mM
GlutaMAX	1X
N-Acetyl-L-Cysteine	1 mM
Nicotinamide	5 mM
B-27	1X
β-estradiol	100 nM
SB202190	0.5 µM
A83-01	0.5 µM

FGF-4	10 ng/mL
FGF-10	10 ng/mL
M2	
M1	-
Neuregulin-1	5 nM
EGF	5 ng/mL
Forskolin	5 μ M
Hydrocortisone	500 ng/mL
FGF: Fibroblast Growth Factor; EGF: Endothelial Growth Factor.	

Developing organoid cultures from frozen material

This project used tumor material from patients who participated in the European Union's Horizon 2020-funded HERCULES study (ID: 667403). Collection and storage of the material have been approved by The Ethics Committee of the Hospital District of Southwest Finland (ETMK): ETMK 53/180/2009 § 238. Fresh tumor samples were collected during tumor reduction surgeries, laparoscopic biopsies, or ascites paracentesis at the Department of Gynecology and Obstetrics at Turku University Hospital, Finland. Cryopreserved vials containing enzymatically digested EOC tumor biopsies or ascites, frozen in Stem-CellBanker (Amsbio), were shipped to Wennerberg laboratory and maintained in liquid nitrogen until use. Each culture developed from this material was identified by a distinctive code composed of 'EOC' followed by a unique number, then by 'p' (primary), 'i' (interval), or 'r' (relapse), depending on the stage of the disease from which the sample was obtained, and followed by the initials of the material used to establish the culture (Asc = ascites, Ome = omentum, Per = peritoneum, OvaL or OvaR = left or right ovary, Adn = adnex).

On the day the samples were to be cultured, they were defrosted by placing and swirling the cryovials in a water bath at 37°C for 1-2 minutes. Then, sample was mixed with 10 mL of M1 and centrifuged at 200 g for 5 minutes. Supernatant was discarded taking care not to disturb the pellet; the pellet was then resuspended (maintaining some cell clumps) in 10 mL of M1 supplemented with Y-27632 5 μ M, a Rho Kinase (ROCK) inhibitor that enhances efficiency of primary human organoid formation and improved recovery after thawing and passaging. Cells were counted by mixing them with Trypan Blue reagent through a haemocytometer (Bürker chamber) and then centrifuged at 200 g for 5 minutes. After aspirating the supernatant, cells were resuspended in cold Cultrex Reduced Growth Factor Basement Membrane Extract, Type 2, Pathclear (BME-2, R&D Systems) at a concentration of 7.5 ng/mL (diluted in Phosphate-Buffered Saline - PBS), ensuring a minimum of 10⁶ live cells/mL and seeded into pre-warmed 6-well cell culture plates in 20 μ L droplets (10 droplets/well) using an electronic pipette. Gel droplets were solidified in a humidified cell culture incubator at 37°C for 30-45 minutes and gently covered with 3 mL of medium supplemented with Y-27632 5 μ M. Each culture

was initially maintained in both media formulations until it became clear which one the culture was more stable in. Cultures were kept in a humidified cell culture incubator at 37°C, replacing the culture medium every 2 to 3 days.

Organoids passaging

Once pronounced growth was observed, organoid cultures were washed with PBS, added with 2 mL of TrypLE Express (Gibco™), scraped from the surface of the culture plate and dissociated through vigorous pipetting. The plate was then incubated at 37°C for 15 minutes to allow the complete dissociation of the gel. Cells were then collected in a 15-mL tube rinsing the well with PBS once. Organoids were centrifuged at 300 g for 5 minutes, and the supernatant was removed. Cells were then resuspended in cold 7.5 ng/mL Cultrex and seeded in a pre-warmed 6-well plate as described in the previous section.

Once established, organoids were used for different experiments, that will rereferred as “Imatinib/Mitoxantrone drug testing” and “Gene editing in organoids”.

Imatinib/Mitoxantrone drug testing

Organoids seeding in 384-well plates

Once the cultures were established, they were used for drug screening experiments in 384-well Ultra-Low Attachment black microplates (Corning). Organoid cultures used for these experiments were: EOC677_pAsc, EOC677_rAsc, EOC677_r2Asc, EOC172_rAsc, EOC382_p2Ome, in duplicates. 384-well plates were firstly incubated for 30 minutes at -20°C and then for 15 minutes at +4°C. Organoids were extracted from BME-2 domes as described in the previous section, and resuspended in 7.5 ng/mL Cultrex, according to their split ratio. Cells were then seeded in the 384-well plate, keeping the plate on ice (10 µL/well), using an electronic multichannel pipette and touching the bottom of the plate. The plate was finally tapped against the bench to allow the gel to settle at the bottom, with the ultimate goal of obtaining a monolayer of cells. It was then to incubate on ice for 15 minutes and subsequently at 37°C for 30 minutes. After the incubations, 40 µL/well of the proper medium, supplemented with Y-27632 5 µM, was added to the plate. 30 µL/well of medium was removed every 2-3 days through EL406 microplate washer (BioTek) and replaced with fresh medium.

Drug treatment

On the day of drug treatment, media change was performed using EL406 microplate washer (BioTek). Drugs were diluted to the opportune concentration in a 384-well microplate (defined as “source plate”) and organoids in the “destination plate” were treated using Echo 550 Acoustic Dispenser

(Labcyte), which allows for the rapid and highly precise transfer of liquids by acoustic energy without any physical contact. Cells were treated with increasing concentration of imatinib (0.25 μ M, 0.50 μ M, 1 μ M, 2 μ M, 4 μ M, 8 μ M) and mitoxantrone (0.05 μ M, 0.1 μ M, 0.2 μ M, 0.4 μ M, 0.8 μ M, 1.60 μ M) in combination; DMSO and bortezomib 10 μ M were used respectively as vehicle control and positive control. Microplates were then incubated at 37°C for 96 hours.

CellTiter-Glo® 3D Cell Viability Assay

96 hours after drug treatment, 25 μ L of the culture medium were removed and replaced with 25 μ L of CellTiter-Glo reagent (Promega), which allows the measurement of ATP levels in the sample, proportional to the viability of the cells. Plates were shaken on a vibrating shaker for 5 minutes and then incubated in the dark for 25 minutes to stabilize the luminescent signal. Luminescence was recorded through Luminescence microplate reader GloMax® Discover (Promega). Luminescence signals were normalized on the controls and plotted in SynergyFinder+ in order to identify a possible synergy through Bliss model.^{101,102}

Gene editing in organoids

Cas9 organoids plainfection

Cas9 lentiviral particles were previously produced in HEK293-FT cells using Lenti_PGK-Cas9-P2A-HygR plasmid. Lentiviral particles were used for infecting 4 different organoid cultures, already available in the lab (EOC883_pAsc, EOC883_iAsc, EOC989_iOme and EOC382_p2Ome). For the infection, organoids were digested with 2 mL of TrypLE Express (Gibco™) and incubated at 37°C for 20-25 minutes, to get smaller clumps or, preferably, single cells. Cells were collected in a 15-mL tube and centrifuge at 300 g for 5 minutes. After removing the supernatant, the pellet was resuspended in 2 mL of growth medium supplemented with Y-27632 5 μ M; cells were passed through a 70- μ m cell strainer and counted by mixing with Trypan Blue solution. After that, 500000 cells were seeded in a 70% Cultrex-precoated well of a 6-well plate.

In the GMO-2 lab, cells were infected with lentiviral particles using polybrene at a final concentration of 6-10 μ g/mL. The following day, the infection mixture from each well (cells + viral particles + medium with polybrene) was collected into a 15-mL tube and spun down at 400 g for 5 minutes. Organoids were seeded as previously described in Cultrex and covered with 3 mL of growth medium supplemented with 5 μ M Y-27632 after a 45-minute incubation at 37°C. Selection with hygromycin was started 3 to 4 days after infection, using different antibiotic concentrations for each culture: 400 μ g/mL for EOC883_pAsc and EOC382_p2Ome, 200 μ g/mL for EOC883_iAsc and 300 μ g/mL for EOC989_iOme. Once completed hygromycin selection, infected organoid cultures were passaged as

the other ones; however, after 3 days of recovery following each passage, the cells were cultured in hygromycin for one week. Once they recovered and reached confluence, they were used for further experiments.

Protein extraction and western blotting

After selection with hygromycin and expansion of the cultures, Cas9 expression was tested through Western Blotting. Firstly, organoids were harvested as previously described using TrypLE Express (Gibco™); cells were then centrifuged at 350 g for 5 minutes and the supernatant was discarded. The pellet was resuspended in 1 mL of PBS, and everything was transferred to a 1.5 mL tube. After centrifuging at 2500 rpm for 5 minutes, two additional washes with PBS were performed. Cells were finally resuspended in 120 µL/well of RIPA Buffer, supplemented with protease and phosphatase inhibitor. Tubes were left agitated in the cold room for 1 hour and centrifuged at 4°C for 20 minutes at maximum speed. Supernatant was collected in a new tube and proteins were quantified. Protein quantification was performed through Pierce™ BCA Protein Assay (Thermo Scientific™), following the manufacturer's instructions, after preparing a standard curve with increasing concentrations of Bovine Serum Albumin (BSA).

Samples were diluted to a final concentration of 1.666 µg/µL, in order to load in each well of the gel 25 µg of proteins in 15 µL per sample. Samples were also added with Loading buffer, prepared by mixing LDL sample buffer and β –mercaptoethanol following a ratio of 10:1. Samples were boiled at 97°C for 5 minutes.

15 µL of each sample were loaded in each well of a precast polyacrylamide gel NuPAGE Bis-Tris protein gel (Invitrogen™), assembled in the holding apparatus, which was filled with running buffer 1X MOPS SDS Running Buffer (Invitrogen™). The run was performed at 110 V for at least 1 hour. Proteins were then transferred from the gel to a nitrocellulose membrane preparing a “sandwich” consisted of sponge, filter paper, gel, membrane, filter paper and sponge. The transfer “sandwich” was inserted in the transfer apparatus followed by the addition of Transfer Buffer, prepared using 1X MOPS SDS Running Buffer and 100% ethanol in water. The transferring was carried out in the cold room setting constant amperage of 75mA overnight. After the transfer of the proteins from the gel to the membrane, a blocking solution was used to block the surface of the membrane to prevent nonspecific binding of the detection antibodies during subsequent steps; blocking solution was prepared with 5% BSA in PBS-Tween® (PBST) and added to the membrane for 1 hour in agitation. After that, specific primary antibody solutions were added to the membrane and left overnight at 4°C with gentle shaking. Primary antibodies used were:

- CRISPR-Cas9 antibody (7A9-3A3) – N-Terminus (Novus Biologicals) mouse, diluted 1:500 in 5% non-fat milk in PBST.
- GAPDH (ab9485, abcam) rabbit, diluted 1:10000 in Blocking solution, used as a control.

The day after, the membrane was washed 5 times for 5 minutes with PBST. Secondary antibody solution (specific for anti-rabbit or anti-mouse antibodies) was then added to the membranes and maintained for 2 hours at room temperature with gentle shaking. Finally, membrane was washed for additional 5 times. Super Signal West Pico (Thermo Scientific™) was used to reveal protein expression and signal was detected by the ChemiDoc™ Imaging System #12003153 (Biorad). Pictures were taken for each staining and visualized using ImageLab software (Biorad).

Gene editing

To set up a platform for arrayed gene editing in organoids, experiments were conducted in a black 96-well plate (Greiner 655090). 30000 cells/well were seeded in Opti-MEM™ medium (ThermoFisher), together with 25nM sgRNA and 0.3 μL of Lipofectamine RNAiMAX Transfection Reagent (ThermoFisher), according to the conditions described in Table 23:

Table 23. Gene editing detailed methods.	
Mode A	Precoating of the wells with 70% Cultrex overnight, cell seeding with sgRNA and Lipofectamine and, after 4-hours incubation at 37°C, addition of 90% Cultrex.
Mode B	Cell seeding with sgRNA and Lipofectamine and, after 4-hours incubation at 37°C, addition of 90% Cultrex.
Mode C	Cell seeding with sgRNA and Lipofectamine in 20% Cultrex.
Mode D	sgRNA and Lipofectamine incubation for 4 hours, and subsequent cell seeding in 90% Cultrex.
Mode E	sgRNA and Lipofectamine incubation for 30 minutes, and subsequent cell seeding in 90% Cultrex.
Mode F	Cell seeding in Opti-MEM™ with sgRNA and Lipofectamine and, after 4-hours incubation at 37°C, cells were centrifuged, and the pellet resuspended in 90% Cultrex for seeding.

For all the methods, 45 minutes after Cultrex addition, 100 μL of growth medium without primocin were added. sgRNA used for establishing the gene editing methods were lethal positive Control (LPC) #1 and #2 and non-targeting control (NTC) #1 and #3 (Dharmacon Edit-R™).

Firstly, to understand which method could be the most efficient, organoid culture EOC883_pAsc was used for the pilot experiments. Different seeding methods were tested, using a negative control (cells seeded using the standard procedure, described in section 5.2: “*Imatinib/Mitoxantrone drug testing, Organoids seeding in 384 well*”) and a positive control (cells seeded using the standard procedure and

treated with Bortezomib 10 μ M). Following experiments were conducted in the four transfected organoid cell lines.

CellTox™ Green Cytotoxicity Assay

Viability was assessed after 7 days using CellTox™ Green Cytotoxicity Assay (Promega), following the manufacturer's instructions. 100 μ L of medium were removed through EL406 microplate washer and replaced with 100 μ L of CellTox Green Reagent 2X, supplemented with CellTox™ Green Dye, able to bind DNA in dead cells, and Hoechst 33342 (#B2261, Sigma, final concentration 5 μ g/mL), for nuclear staining. The plate was then incubated in the dark for at least 1.30 hours and the final readout was performed using ImageXpress Confocal HT.ai High-Content Imaging System automated fluorescence microscope (Molecular Devices), available at the High-Content CRISPR Screens (HCCS) core facility, BRIC, University of Copenhagen (Denmark). A single image for each fluorophore was captured per well using a 10X objective lens. Survival indices were calculated through image analysis, utilizing the MetaXpress (Molecular Devices) software. Nuclei were detected as individual objects based on Hoechst 33342 staining and were computationally enlarged. Objects co-localizing with the CellTox™ Green signal were classified as dead cells, while those without overlap were considered viable cells.

CellTiter-Glo® 3D Cell Viability Assay

Viability was also assessed through CellTiter-Glo® 3D Cell Viability Assay (Promega), following the procedure described in the appropriate section in paragraph 5.2.

5.3 RESULTS

Developing organoid culture from frozen material

During my stay at BRIC, University of Copenhagen (Denmark), 4 cultures out of 7 frozen samples were established, 1 of them growing in M1 and 3 in M2, showing a success rate of 57,14%, in line with the results previously achieved in the lab. Figure 27 shows one of the organoid cultures over 14 days.

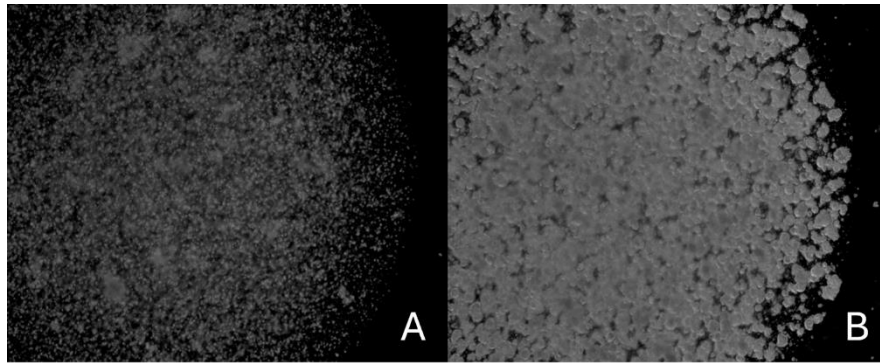


Figure 27: Organoid culture A) immediately after passaging; B)14 days after passaging. Pictures taken with a CCD camera (EC3, Leica) coupled to a phase-contrast microscope at 2.5X magnification.

The establishment of organoid cultures required significantly long periods of time (approximately 2-4 months). Moreover, already established cultures required longer periods than 2D cell cultures to reach confluence; for instance, a typical organoid culture reaches confluence after 12 to 15 days. Therefore, experiments are conducted with extended timelines.

Imatinib/Mitoxantrone drug testing

CellTiter-Glo® 3D Cell Viability Assay results were plotted to predict the Bliss synergy score and are shown in Figure 28. Except for EOC677_r2Asc, Bliss synergy scores were all > 0 , showing a positive synergy, meaning the combined effect is greater than the two drugs alone. However, the drug concentrations used *in vitro* are significantly higher than those typically observed in clinical settings, which could lead to major adverse reactions.

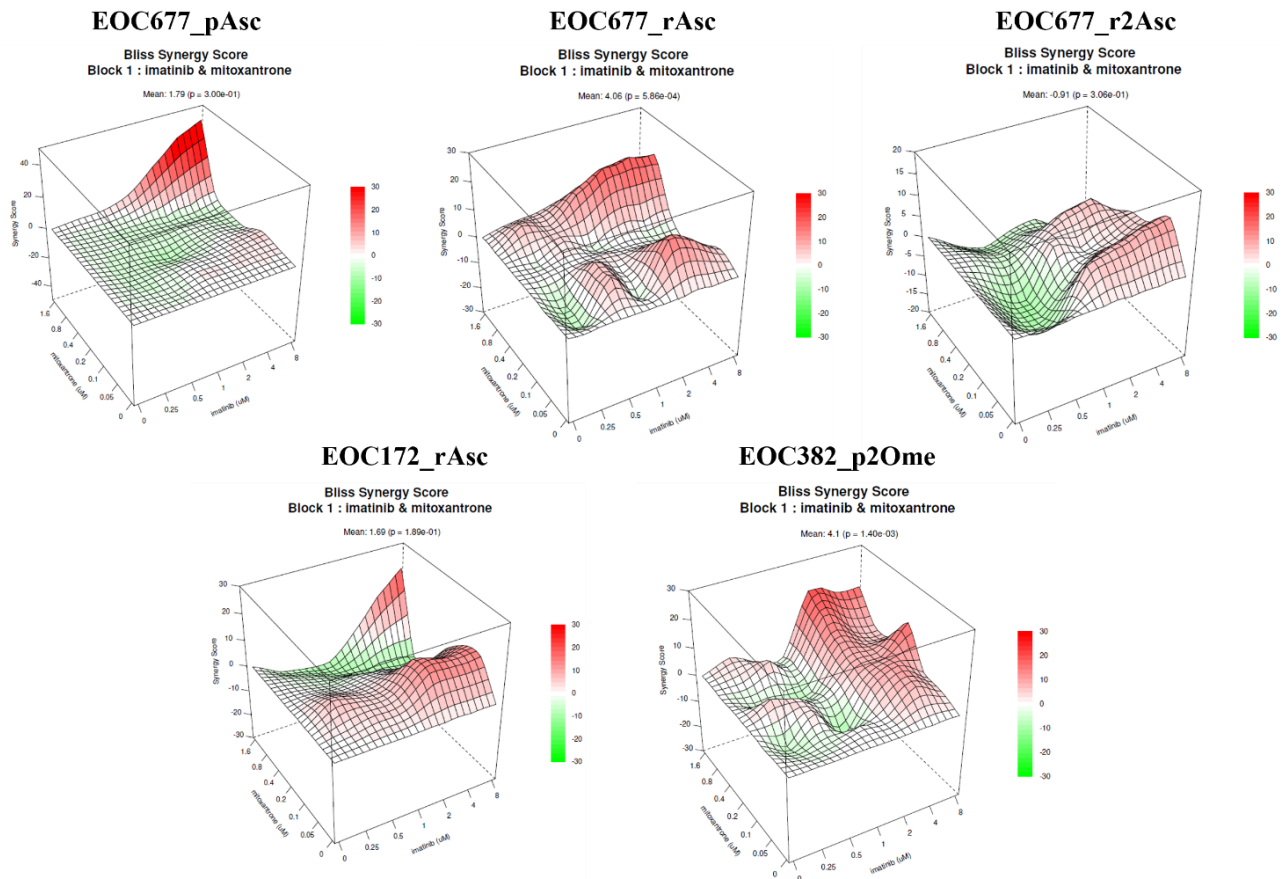


Figure 28: Bliss synergy score of the organoid cultures treated with imatinib/mitoxantrone combinations.

Gene editing in organoids

After lentiviral infection and hygromycin selection, organoids required at least two months for recovery and expansion. Considering the Western Blot results (Figure 29), the infection was successfully for all the cultures compared to the naïve one, even if for EOC883_pAsc the Cas9 expression seems to be weaker.

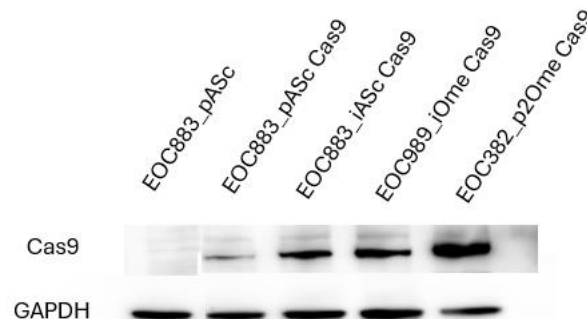


Figure 29: Cas9 expression analysed through Western Blotting, using GAPDH as control.

In the first three experiments carried out on EOC883_pAsc to assess cell viability using different seeding methods, only Modes A, B, C and F was tested, without adding sgRNAs and Lipofectamine. For this reason, Modes D and E which differed from Mode B only for the sgRNAs and Lipofectamine incubation time before cell seeding, were not performed.

The mean results of the CellTiter-Glo® 3D Assay is shown in Figure 30; the same figure also presents a merged image (CellTox Green and Hoechst 33342) for each method.

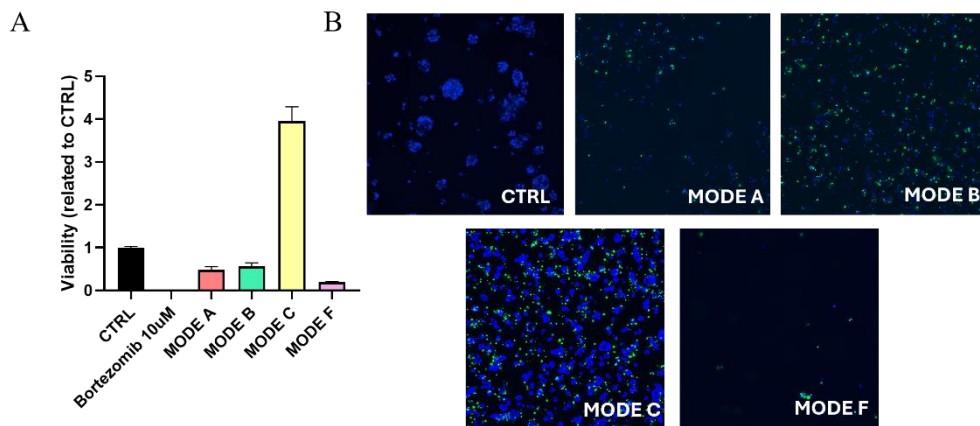


Figure 30: Viability assays for different cells seeding method. A) CellTiter-Glo® 3D Viability Assay; B) CellTox™ Green Cytotoxicity Assay.

The analysis revealed that in Mode C, cells were growing exponentially, faster than in the control well, suggesting a potentially different effect of 20% Cultrex compared to the standard 90% concentration. Although high growth could be considered a positive factor for lab work, such a significant difference in organoid replication may also indicate variations in their characteristics (e.g., metabolism); for this reason, Mode C was excluded from further analysis. Mode F was also excluded from the subsequent experiments because it exhibited very poor viability compared to the control. This may be due to the additional centrifugation performed after 4-hours incubation, which could result in the loss of extra material, as well as the possibility that some cells had already attached to the bottom of the plate after the incubation. As observed, confocal microscope images are not equally representative of the conditions, possibly due to variations in layer volumes created by different percentages of Cultrex and varying seeding methods. For this reason, viability in following experiments was assessed only through CellTiter-Glo® 3D.

The following experiments were conducted on the transfected cell lines (EOC883_pAsc Cas9 and EOC989_iOme Cas9) with sgRNAs analysed in triplicate, while the other two organoid cultures required a longer recovery time after hygromycin selection, which was incompatible with my time spent at BRIC.

CellTiter-Glo® 3D Cell Viability Assay results are shown in Figure 31.

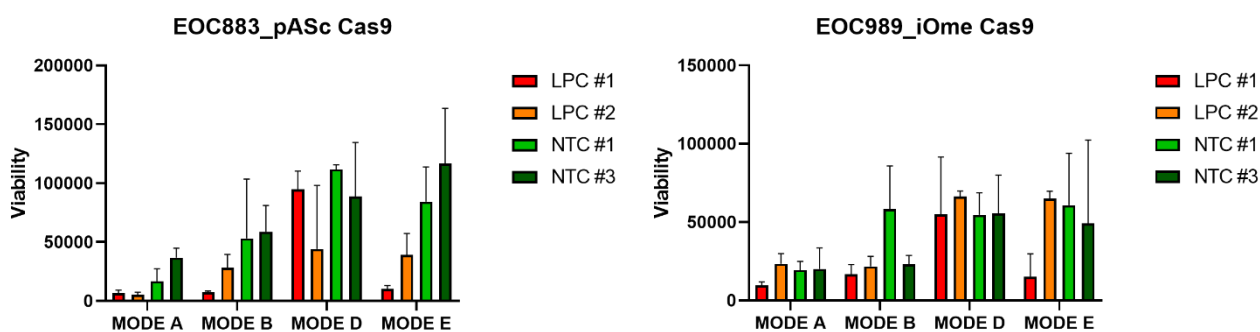


Figure 31: CellTiter-Glo® 3D Cell Viability Assay results in EOC883_pAsc Cas9 and EOC989_iOme Cas9 organoid cultures after transfection with lethal positive control and non-targeting control.

Regarding Mode A, the difference in viability between LPC and NTC was not substantial, but a decrease in signal was observed with both LPCs in EOC833_pAsc Cas9 and with LPC #1 in EOC989_iOme Cas9, indicating a potential successful transfection that allowed the silencing of genes essential for cell viability. The same occurred in Mode B and E, where a greater difference was observed between NTCs and LPCs, except for LPC #2 in EOC989_iOme Cas9. Mode D, instead, showed worst results, as the LPCs did not exhibit the expected decrease in cell viability.

5.4 DISCUSSION AND CONCLUSION

OC cannot be considered a single entity, but rather a complex and heterogeneous group of tumors. For this reason, research studies aiming to optimize patients' clinical benefit should not be conducted using a single model. Moreover, 3D models provide a representation of the clinical condition that more closely resembles real-life scenarios and can help improve our understanding of the tumor microenvironment. In this context, organoids have recently garnered significant interest within the scientific community. In particular, biopsy-derived organoids can reproduce the *in vivo* conditions and studies revealed that they are able to maintain the genetic profile of the original tumor. During my exchange I had the opportunity to learn how to establish organoids from patients' biopsies and how to work with them. Organoid cultures development was a quite long process and, in general, the experiments required longer time than working with 2D cell cultures. Four cultures out of seven samples were finally established with a successful rate of 57,14%.

Regarding imatinib/mitoxantrone synergy hypothesis, five cultures were treated with different drugs combinations, showing in four of them a positive synergy Bliss score. This project originated from previous studies carried out in the lab in 2D cell models, in which a combination of the tyrosine-kinase inhibitor, imatinib, and the topoisomerase II inhibitor, mitoxantrone, showed a positive effect on 2D OC cell lines. Indeed, both drugs have been studied for OC treatment, but their potential

synergy has not been previously investigated.¹⁰³⁻¹⁰⁵ Although this study was conducted on a limited number of organoid cultures, it allowed the observation of a synergy between the two drugs in four out of five cultures. However, the drug concentrations used ranged from 0.25 to 8 μM for imatinib and 0.05 to 1.60 μM for mitoxantrone, which might be too high for a potential *in vivo* translation of the study due to the side effects that could be induced.

Regarding the “Gene editing in organoids” study, one of the main limitations was the time required for organoids growth at each passage. In HGSOc organoid models, the CRISPR-Cas9 technique has not yet been used for drug screening, but it holds great potential for understanding the genes involved in chemotherapy resistance. In this context, establishing a platform for arrayed gene editing in HGSOc organoids, which could be useful for target validation, remains an unmet need for advancing knowledge in HGSOc resistance to chemotherapy.^{106,107} Four different organoid cultures expressing Cas9 were established, and preliminary studies were conducted to determine the most suitable method for organoid transfections. Of the six methods tested, two were excluded due to increased or decreased cell viability compared to the control. The remaining four methods were tested on two HGSOc organoid cultures using a lethal positive control and a non-targeting control, showing a worst effect for Mode D compared with other seeding methods. However, further experiments are needed on additional cultures to optimize the sgRNA and Lipofectamine concentrations, as well as to identify the most suitable method for improving transfection efficiency.

6. CONCLUSIONS

In recent years, the study of epigenetics has gained significant interest, and it is now clear that the onset and progression of diseases such as cancer are not solely dependent on the DNA sequence but also on environmental factors with which individuals routinely interact, such as exposure to substances, smoking, as well as diet, physical inactivity, obesity status, etc. These environmental factors can often constitute risk factors for certain diseases, even though they are modifiable risk factors. In particular, considerable attention is currently focused on maintaining a healthy lifestyle, as this can improve health status, prevent diseases, and/or enhance disease progression.

Endometrial and ovarian cancers are the sixth and seventh most common cancers in terms of incidence among women worldwide, respectively, as well as the thirteenth and eighth leading causes of cancer-related mortality. Many studies have demonstrated that obesity and physical inactivity may promote the onset of these tumors or affect their prognosis.

In this context, the present PhD project aimed to investigate the role of obesity and physical activity in these two gynecological cancers, with a particular focus on miRNAs, whose modulation had not been previously studied in patients affected by EC and OC. In particular, this project aimed at:

- i) Determining the alterations in miRNA expression associated with obesity in EC;
- ii) Examining differences in miRNA expression among OC patients who participated in a specific physical activity program versus those who did not.

With regard to the first goal, specific miRNAs, that could play a role in regulating obesity-related pathways, were found to be associated with BMI and this may offer new insights for the clinical treatment of obese EC patients. With regard to the second aim, the effect of physical activity on a few miRNAs was evident; however, further studies are needed to understand the precise role of physical activity in the epigenetic modulation of miRNAs in OC.

In conclusion, obesity and physical activity have been shown to modulate miRNA expression in gynecological tumors, stimulating increased interest in investigating the role of epigenetics in the onset and prognosis of these diseases.

7. REFERENCES

1. Katakai, A. C., Tiwari, P., Thilagavthi, R. & Krishnatreya, M. Epidemiology of Gynaecological Cancers. *Fundamentals in Gynaecologic Malignancy* 1–8 (2022) doi:10.1007/978-981-19-5860-1_1.
2. Woo, Y. L., Kyrgiou, M., Bryant, A., Everett, T. & Dickinson, H. O. Centralisation of services for gynaecological cancers — A Cochrane systematic review. *Gynecol Oncol* **126**, 286–290 (2012).
3. Keyvani, V., Kheradmand, N., Navaei, Z. N., Mollazadeh, S. & Esmaeili, S. A. Epidemiological trends and risk factors of gynecological cancers: an update. *Medical Oncology* 2023 40:3 **40**, 1–11 (2023).
4. I tumori ginecologici - Home - Acto - Alleanza contro il tumore ovarico. <https://www.acto-italia.org/home/tumori-ginecologici/i-tumori-ginecologici>.
5. Introduzione ai tumori ginecologici - Ginecologia e ostetricia - Manuali MSD Edizione Professionisti. <https://www.msmanuals.com/it-it/professionale/ginecologia-e-ostetricia/tumori-ginecologici/introduzione-ai-tumori-ginecologici>.
6. Taylor, A. H., Tortolani, D., Ayakannu, T., Konje, J. C. & Maccarrone, M. (Endo)Cannabinoids and Gynaecological Cancers. *Cancers (Basel)* **13**, 1–22 (2020).
7. Makker, V. *et al.* Endometrial cancer. *Nat Rev Dis Primers* **7**, (2021).
8. Amant, F. *et al.* Endometrial cancer. *Lancet* **366**, 491–505 (2005).
9. Endometrial cancer statistics | World Cancer Research Fund International. <https://www.wcrf.org/cancer-trends/endometrial-cancer-statistics/>.
10. Cancer Today. https://gco.iarc.fr/today/en/dataviz/bars?mode=cancer&group_populations=1&types=1&sexes=2.
11. Mahdy, H., Casey, M. J., Vadakekut, E. S. & Crotzer, D. Endometrial Cancer. *StatPearls* (2024).
12. Berek, J. S. *et al.* FIGO staging of endometrial cancer: 2023. *International Journal of Gynecology & Obstetrics* **162**, 383–394 (2023).
13. Getz, G. *et al.* Integrated genomic characterization of endometrial carcinoma. *Nature* 2013 497:7447 **497**, 67–73 (2013).
14. Karpel, H. C., Slomovitz, B., Coleman, R. L. & Pothuri, B. Treatment options for molecular subtypes of endometrial cancer in 2023. *Curr Opin Obstet Gynecol* **35**, 270–278 (2023).
15. Latest Data Indicate New Care Standard in Advanced/Recurrent. <https://www.esmo.org/newsroom/press-and-media-hub/esmo-media-releases/latest-data-indicate-new-care-standard-in-advanced-recurrent-endometrial-cancer-results-from-the-ruby-trial>.

16. Nebgen, D. R., Lu, K. H. & Bast, R. C. Novel Approaches to Ovarian Cancer Screening. *Curr Oncol Rep* **21**, (2019).
17. Stewart, C., Ralyea, C. & Lockwood, S. Ovarian Cancer: An Integrated Review. *Semin Oncol Nurs* **35**, 151–156 (2019).
18. Lisio, M. A., Fu, L., Goyeneche, A., Gao, Z. H. & Telleria, C. High-Grade Serous Ovarian Cancer: Basic Sciences, Clinical and Therapeutic Standpoints. *Int J Mol Sci* **20**, (2019).
19. Ovarian Cancer Survival Rates | Ovarian Cancer Prognosis | American Cancer Society. <https://www.cancer.org/cancer/types/ovarian-cancer/detection-diagnosis-staging/survival-rates.html>.
20. Nunes, D. & Ricardo, S. Ovarian Cancer Ascites as a Liquid Tumor Microenvironment. *Ovarian Cancer* 43–55 (2022) doi:10.36255/EXON-PUBLICATIONS-OVARIAN-CANCER-TUMOR-MICROENVIRONMENT.
21. Zamwar, U. M. & Anjankar, A. P. Aetiology, Epidemiology, Histopathology, Classification, Detailed Evaluation, and Treatment of Ovarian Cancer. *Cureus* **14**, (2022).
22. Prat, J., D'Angelo, E. & Espinosa, I. Ovarian carcinomas: at least five different diseases with distinct histological features and molecular genetics. *Hum Pathol* **80**, 11–27 (2018).
23. Hayashi, T. & Konishi, I. Molecular Histopathology for Establishing Diagnostic Method and Clinical Therapy for Ovarian Carcinoma. *J Clin Med Res* **15**, 68–75 (2023).
24. Vercellini, P. *et al.* The 'incessant menstruation' hypothesis: a mechanistic ovarian cancer model with implications for prevention. *Hum Reprod* **26**, 2262–2273 (2011).
25. Kurman, R. J. & Shih, I. M. The Dualistic Model of Ovarian Carcinogenesis: Revisited, Revised, and Expanded. *Am J Pathol* **186**, 733–747 (2016).
26. Kroeger, P. T. & Drapkin, R. Pathogenesis and heterogeneity of ovarian cancer. *Curr Opin Obstet Gynecol* **29**, 26–34 (2017).
27. Hunn, J. & Rodriguez, G. C. Ovarian cancer: etiology, risk factors, and epidemiology. *Clin Obstet Gynecol* **55**, 3–23 (2012).
28. Tumore ovaie: sintomi, prevenzione, cause, diagnosi. <https://www.airc.it/cancro/informazioni-tumori/guida-ai-tumori/tumore-delle-ovaie>.
29. La Vecchia, C. Ovarian cancer: epidemiology and risk factors. *Eur J Cancer Prev* **26**, 55–62 (2017).
30. Russo, A. *et al.* Hereditary ovarian cancer. *Crit Rev Oncol Hematol* **69**, 28–44 (2009).
31. Ghose, A. *et al.* Hereditary Ovarian Cancer: Towards a Cost-Effective Prevention Strategy. *Int J Environ Res Public Health* **19**, (2022).

32. Fathalla, M. F. Non-hormonal interruption of incessant ovulation as a potential approach for ovarian cancer prevention. *International Journal of Gynecology and Obstetrics* **132**, 356–358 (2016).
33. Babic, A. *et al.* Association Between Breastfeeding and Ovarian Cancer Risk. *JAMA Oncol* **6**, (2020).
34. Karlsson, T., Johansson, T., Hoglund, J., Ek, W. E. & Johansson, Å. Time-Dependent Effects of Oral Contraceptive Use on Breast, Ovarian, and Endometrial Cancers. *Cancer Res* **81**, 1153–1162 (2021).
35. Risch, H. A. Hormonal etiology of epithelial ovarian cancer, with a hypothesis concerning the role of androgens and progesterone. *J Natl Cancer Inst* **90**, 1774–1786 (1998).
36. Fleming, J. S., Beaugié, C. R., Haviv, I., Chenevix-Trench, G. & Tan, O. L. Incessant ovulation, inflammation and epithelial ovarian carcinogenesis: revisiting old hypotheses. *Mol Cell Endocrinol* **247**, 4–21 (2006).
37. Cottreau, C. M., Ness, R. B. & Kriska, A. M. Physical activity and reduced risk of ovarian cancer. *Obstetrics and gynecology* **96**, 609–614 (2000).
38. Stayner, L. T. *et al.* Carcinogenicity of talc and acrylonitrile. *Lancet Oncol* (2024) doi:10.1016/S1470-2045(24)00384-X.
39. Doubeni, C. A., Doubeni, A. R. B. & Myers, A. E. Diagnosis and Management of Ovarian Cancer. **93**, (2016).
40. Berek, J. S., Renz, M., Kehoe, S., Kumar, L. & Friedlander, M. Cancer of the ovary, fallopian tube, and peritoneum: 2021 update. *International Journal of Gynecology and Obstetrics* **155**, 61–85 (2021).
41. Jónsdóttir, B., Lomnytska, M., Poromaa, I. S., Silins, I. & Ståhlberg, K. The Peritoneal Cancer Index is a Strong Predictor of Incomplete Cytoreductive Surgery in Ovarian Cancer. *Ann Surg Oncol* **28**, 244–251 (2021).
42. Fagotti, A. *et al.* Phase III randomised clinical trial comparing primary surgery versus neoadjuvant chemotherapy in advanced epithelial ovarian cancer with high tumour load (SCORPION trial): Final analysis of peri-operative outcome. *Eur J Cancer* **59**, 22–33 (2016).
43. Kuroki, L. & Guntupalli, S. R. Treatment of epithelial ovarian cancer. *BMJ* **371**, (2020).
44. Lheureux, S., Braunstein, M. & Oza, A. M. Epithelial ovarian cancer: Evolution of management in the era of precision medicine. *CA Cancer J Clin* **69**, 280–304 (2019).
45. Waddington, C. H. Canalization of Development and Genetic Assimilation of Acquired Characters. *Nature 1959 183:4676* **183**, 1654–1655 (1959).
46. Bradley, C. C., Gordon, A. J. E., Halliday, J. A. & Herman, C. Transcription fidelity: New paradigms in epigenetic inheritance, genome instability and disease. *DNA Repair (Amst)* **81**, (2019).

47. Kanherkar, R. R., Bhatia-Dey, N. & Csoka, A. B. Epigenetics across the human lifespan. *Front Cell Dev Biol* **2**, (2014).
48. Ravegnini, G., Sammarini, G., Hrelia, P. & Angelini, S. Key Genetic and Epigenetic Mechanisms in Chemical Carcinogenesis. *Toxicol Sci* **148**, 2–13 (2015).
49. Khan, S., Ayub, H., Khan, T. & Wahid, F. MicroRNA biogenesis, gene silencing mechanisms and role in breast, ovarian and prostate cancer. *Biochimie* **167**, 12–24 (2019).
50. Cedar, H. & Bergman, Y. Linking DNA methylation and histone modification: patterns and paradigms. *Nat Rev Genet* **10**, 295–304 (2009).
51. Rotondo, J. C., Mazziotta, C., Lanzillotti, C., Tognon, M. & Martini, F. Epigenetic Dysregulations in Merkel Cell Polyomavirus-Driven Merkel Cell Carcinoma. *Int J Mol Sci* **22**, (2021).
52. miRBase. <https://www.mirbase.org/>.
53. Babar, I. A., Slack, F. J. & Weidhaas, J. B. miRNA modulation of the cellular stress response. *Future Oncol* **4**, 289–298 (2008).
54. Baer, C., Claus, R. & Plass, C. Genome-wide epigenetic regulation of miRNAs in cancer. *Cancer Res* **73**, 473–477 (2013).
55. Kala, R., Peek, G. W., Hardy, T. M. & Tollefsbol, T. O. MicroRNAs: an emerging science in cancer epigenetics. *J Clin Bioinforma* **3**, (2013).
56. Simonson, B. & Das, S. MicroRNA Therapeutics: the Next Magic Bullet? *Mini Rev Med Chem* **15**, 467–474 (2015).
57. Pillai, R. S. MicroRNA function: Multiple mechanisms for a tiny RNA? *RNA* **11**, 1753 (2005).
58. Khan, S., Ayub, H., Khan, T. & Wahid, F. MicroRNA biogenesis, gene silencing mechanisms and role in breast, ovarian and prostate cancer. *Biochimie* **167**, 12–24 (2019).
59. Iorio, M. V. & Croce, C. M. MicroRNA dysregulation in cancer: diagnostics, monitoring and therapeutics. A comprehensive review. *EMBO Mol Med* **4**, 143–159 (2012).
60. Obesity. https://www.who.int/health-topics/obesity#tab=tab_1.
61. Prevalence of Obesity | World Obesity Federation. <https://www.worldobesity.org/about/about-obesity/prevalence-of-obesity>.
62. Wright, S. M. & Aronne, L. J. Causes of obesity. *Abdom Imaging* **37**, 730–732 (2012).
63. Safaei, M., Sundararajan, E. A., Driss, M., Boulila, W. & Shapi'i, A. A systematic literature review on obesity: Understanding the causes & consequences of obesity and reviewing various machine learning approaches used to predict obesity. *Comput Biol Med* **136**, 104754 (2021).

64. Saklayen, M. G. The Global Epidemic of the Metabolic Syndrome. *Curr Hypertens Rep* **20**, (2018).
65. Keaver, L. *et al.* Application of the UK Foresight Obesity Model in Ireland: The Health and Economic Consequences of Projected Obesity Trends in Ireland. (2013) doi:10.1371/journal.pone.0079827.
66. Avgerinos, K. I., Spyrou, N., Mantzoros, C. S. & Dalamaga, M. Obesity and cancer risk: Emerging biological mechanisms and perspectives. *Metabolism* **92**, 121–135 (2019).
67. Engin, A. The Definition and Prevalence of Obesity and Metabolic Syndrome. *Adv Exp Med Biol* **960**, 1–17 (2017).
68. Physical activity. <https://www.who.int/news-room/fact-sheets/detail/physical-activity>.
69. WHO guidelines on physical activity and sedentary behaviour. <https://www.who.int/publications/i/item/9789240015128>.
70. Strain, T. *et al.* National, regional, and global trends in insufficient physical activity among adults from 2000 to 2022: a pooled analysis of 507 population-based surveys with 5·7 million participants. *Lancet Glob Health* **12**, e1232–e1243 (2024).
71. Mctiernan, A. *et al.* Physical Activity in Cancer Prevention and Survival: A Systematic Review. *Med Sci Sports Exerc* **51**, 1252 (2019).
72. Maddocks, M. Physical activity and exercise training in cancer patients. *Clin Nutr ESPEN* **40**, 1–6 (2020).
73. Marrugo-Ramírez, J., Mir, M. & Samitier, J. Blood-Based Cancer Biomarkers in Liquid Biopsy: A Promising Non-Invasive Alternative to Tissue Biopsy. *Int J Mol Sci* **19**, (2018).
74. Giannopoulou, L., Zavridou, M., Kasimir-Bauer, S. & Lianidou, E. S. Liquid biopsy in ovarian cancer: the potential of circulating miRNAs and exosomes. *Transl Res* **205**, 77–91 (2019).
75. cobas EGFR Mutation Test v2 | FDA. <https://www.fda.gov/drugs/resources-information-approved-drugs/cobas-egfr-mutation-test-v2>.
76. FoundationOne Liquid CDx | Foundation Medicine. <https://www.foundationmedicine.com/test/foundationone-liquid-cdx>.
77. FDA Expands Approval of Cancer Liquid Biopsy - NCI. <https://www.cancer.gov/news-events/cancer-currents-blog/2020/fda-foundation-one-cancer-liquid-biopsy-expanded-approval>.
78. Byrne, S. *et al.* Lifestyle, genetic risk and incidence of cancer: a prospective cohort study of 13 cancer types. *Int J Epidemiol* **52**, 817 (2023).
79. Colaprico, A. *et al.* TCGAbiolinks: an R/Bioconductor package for integrative analysis of TCGA data. *Nucleic Acids Res* **44**, e71 (2016).

80. Deng, M., Brägelmann, J., Kryukov, I., Saraiva-Agostinho, N. & Perner, S. FirebrowseR: an R client to the Broad Institute's Firehose Pipeline. *Database (Oxford)* **2017**, (2017).
81. Giorgi, F. M., Ceraolo, C. & Mercatelli, D. The R Language: An Engine for Bioinformatics and Data Science. *Life (Basel)* **12**, (2022).
82. Tang, D. *et al.* SRplot: A free online platform for data visualization and graphing. *PLoS One* **18**, e0294236 (2023).
83. Chen, J., Bardes, E. E., Aronow, B. J. & Jegga, A. G. ToppGene Suite for gene list enrichment analysis and candidate gene prioritization. *Nucleic Acids Res* **37**, (2009).
84. Robin, X. *et al.* pROC: An open-source package for R and S+ to analyze and compare ROC curves. *BMC Bioinformatics* **12**, 1–8 (2011).
85. EnhancedVolcano: publication-ready volcano plots with enhanced colouring and labeling.
<https://bioconductor.org/packages/devel/bioc/vignettes/EnhancedVolcano/inst/doc/EnhancedVolcano.html>.
86. Korthauer, K. *et al.* A practical guide to methods controlling false discoveries in computational biology. *Genome Biol* **20**, (2019).
87. Fan, Y. *et al.* miRNet - dissecting miRNA-target interactions and functional associations through network-based visual analysis. *Nucleic Acids Res* **44**, W135 (2016).
88. Anderson, B. *et al.* Obesity and prognosis in endometrial cancer. *Am J Obstet Gynecol* **174**, 1171–1179 (1996).
89. Song, J. *et al.* MiR-199a regulates cell proliferation and survival by targeting FZD7. *PLoS One* **9**, (2014).
90. Gu, N. *et al.* Expression of miR-199a-3p in human adipocytes is regulated by free fatty acids and adipokines. *Mol Med Rep* **14**, 1180–1186 (2016).
91. Jones, P. H. *et al.* Over-expression of miR-34c leads to early-life visceral fat accumulation and insulin resistance. *Sci Rep* **9**, (2019).
92. Ahmadpour, F. *et al.* THE ASSOCIATION OF PLASMA LEVELS OF miR-34a AND miR-149 WITH OBESITY AND INSULIN RESISTANCE IN OBESE CHILDREN AND ADOLESCENTS. *Acta Endocrinol (Buchar)* **14**, 149–154 (2018).
93. Wollborn, L. *et al.* Effects of Clinical Covariates on Serum miRNA Expression among Women without Ovarian Cancer. *Cancer Epidemiology, Biomarkers & Prevention* OF1–OF9 (2024) doi:10.1158/1055-9965.EPI-23-1355.
94. Nagy, Z. B. *et al.* Comparison of Circulating miRNAs Expression Alterations in Matched Tissue and Plasma Samples During Colorectal Cancer Progression. *Pathol Oncol Res* **25**, 97–105 (2019).
95. Pinktrainer | Zorginnovatie. <https://zorginnovatie.nl/innovaties/pinktrainer>.

96. Aaronson, N. K. *et al.* The European Organization for Research and Treatment of Cancer QLQ-C30: a quality-of-life instrument for use in international clinical trials in oncology. *J Natl Cancer Inst* **85**, 365–376 (1993).
97. Liu, N., Zhen, Z., Xiong, X. & Xue, Y. Aerobic exercise protects MI heart through miR-133a-3p downregulation of connective tissue growth factor. *PLoS One* **19**, (2024).
98. Li, E., Han, K. & Zhou, X. microRNA-27a-3p Down-regulation Inhibits Malignant Biological Behaviors of Ovarian Cancer by Targeting BTG1. *Open Med (Wars)* **14**, 577–585 (2019).
99. Q, M. *et al.* MicroRNA 421 induces the formation of high-invasive cell subsets of ovarian cancer from low-invasive cell subsets mediated by exosomes by activating the PI3K/AKT pathway. *Am J Cancer Res* **14**, 2643–2660 (2024).
100. Senkowski, W. *et al.* A platform for efficient establishment and drug-response profiling of high-grade serous ovarian cancer organoids. *Dev Cell* **58**, 1106 (2023).
101. Zheng, S. *et al.* SynergyFinder Plus: Toward Better Interpretation and Annotation of Drug Combination Screening Datasets. *Genomics Proteomics Bioinformatics* **20**, 587–596 (2022).
102. BLISS, C. I. THE TOXICITY OF POISONS APPLIED JOINTLY¹. *Annals of Applied Biology* **26**, 585–615 (1939).
103. Nicoletto, M. O. *et al.* Pharmacokinetics of intraperitoneal hyperthermic perfusion with mitoxantrone in ovarian cancer. *Cancer Chemother Pharmacol* **45**, 457–462 (2000).
104. Matei, D., Chang, D. D. & Jeng, M. H. Imatinib mesylate (Gleevec) inhibits ovarian cancer cell growth through a mechanism dependent on platelet-derived growth factor receptor alpha and Akt inactivation. *Clin Cancer Res* **10**, 681–690 (2004).
105. Mundhenke, C. *et al.* Novel treatment of ovarian cancer cell lines with Imatinib mesylate combined with Paclitaxel and Carboplatin leads to receptor-mediated antiproliferative effects. *J Cancer Res Clin Oncol* **134**, 1397–1405 (2008).
106. Shi, C. X. *et al.* CRISPR Genome-Wide Screening Identifies Dependence on the Proteasome Subunit PSMC6 for Bortezomib Sensitivity in Multiple Myeloma. *Mol Cancer Ther* **16**, 2862–2870 (2017).
107. Wei, L. *et al.* Genome-wide CRISPR/Cas9 library screening identified PHGDH as a critical driver for Sorafenib resistance in HCC. *Nat Commun* **10**, (2019).